

CAPITAL UNIVERSITY OF SCIENCE AND
TECHNOLOGY, ISLAMABAD



Identification of Active
Constituents of *Artemisia*
carvifolia against Breast Cancer

by

Nida Rauf

A thesis submitted in partial fulfillment for the
degree of Master of Science

in the

Faculty of Health and Life Sciences

Department of Bioinformatics and Biosciences

2021

Copyright © 2021 by Nida Rauf

All rights reserved. No part of this thesis may be reproduced, distributed, or transmitted in any form or by any means, including photocopying, recording, or other electronic or mechanical methods, by any information storage and retrieval system without the prior written permission of the author.

I dedicate this thesis to my Parents who prayers day & night for my success.



CERTIFICATE OF APPROVAL

Identification of Active Constituents of *Artemisia carvifolia* against Breast Cancer

by

Nida Rauf

(MBS193011)

THESIS EXAMINING COMMITTEE

S. No.	Examiner	Name	Organization
(a)	External Examiner	Dr. Sumra Wajid Abbasi	NUMS, Islamabad
(b)	Internal Examiner	Dr. Mahboob Alam	CUST, Islamabad
(c)	Supervisor	Dr. Erum Dilshad	CUST, Islamabad

Dr. Erum Dilshad

Thesis Supervisor

December, 2021

Dr. Sahar Fazal

Head

Dept. of Bioinformatics and Biosciences

December, 2021

Dr. M. Abdul Qadir

Dean

Faculty of Health and Life Sciences

December, 2021

Author's Declaration

I, **Nida Rauf** hereby state that my MS thesis titled “**Identification of Active Constituents of *Artemisia carvifolia* against Breast Cancer.**” is my work and has not been submitted previously by me for taking any degree from Capital University of Science and Technology, Islamabad, or anywhere else in the country/abroad.

At any time if my statement is found to be incorrect even after my graduation, the University has the right to withdraw my MS Degree.

(Nida Rauf)

Registration No: MBS193011

Plagiarism Undertaking

I solemnly declare that the research work presented in this thesis “**Identification of Active Constituents of *Artemisia carvifolia* against Breast Cancer.**” is solely my research work with no significant contribution from any other person. Small contribution/help wherever taken has been dully acknowledged and that complete thesis has been written by me.

I understand the zero-tolerance policy of the HEC and Capital University of Science and Technology towards plagiarism. Therefore, I as an author of the above-titled thesis declare that no portion of my thesis has been plagiarized and any material used as reference is properly referred to/cited.

I undertake that if I am found guilty of any formal plagiarism in the above-titled thesis even after awarding of MS Degree, the University reserves the right to withdraw/revoke my MS degree and that HEC and the University have the right to publish my name on the HEC/University website on which names of students are placed who submitted plagiarized work.

(Nida Rauf)

Registration No: MBS193011

Acknowledgement

All the praises are to be for **Almighty ALLAH TALLAH** and then for His Prophet **MUHAMMAD (SAW)**. I would like to express my wholehearted thanks to my family for their generous support throughout pursuing the MS degree. I am heartily grateful to my supervisor **Dr. Erum Dilshad** (Assistant professor, Department of Bioinformatics & Biosciences, CUST) for her kind support, guidelines, and arrangement of tutorial classes. I especially say thanks to Dr. Naeem Mahmood Ashraf (Lecturer Biochemistry & Biotechnology, University of Gujrat) for his assistance in computational approaches.

Thanks to all.

(**Nida Rauf**)

Abstract

Breast cancer is the most common cancer in women worldwide. Advancement in screening methods, treatment strategies, and conventional therapies has increased the survival rate however, the adverse effects are considerable. Globally people have become more concerned to use natural products over synthetic ones. That's why this research is planned to discover potential anticancer agents from *Artemisia carvifolia*. Fifteen bio compounds, representatives of all classes namely kaempferol, luteolin, gallic acid, quercetin, isoquercetin, caffeic acid, rutin, chrysoptanol D, artemisinin, arteannuin B, artesunate, artemether, arteminol, artemisone, and dihydroartemisinin were selected. These ligands were then screened out based on Lipinski Rule and through studying the ADMET properties of the ligands. Virtual screening of these ligands was carried out against drug targets that are estrogen receptor, HER2 and progesterone receptor by CB-Dock. Luteolin showed itself as a lead compound against estrogen receptors, artemisone as a lead compound against HER 2, and kaempferol was shown as a lead compound against progesterone receptors. Tamoxifen, capecitabine, and mifepristone were used as the standard drugs for comparison. Lead compounds selected were far more active and less toxic than the selected standard drugs. All the interaction visualization analysis studies were performed by PyMol molecular visualization tool and LIGPLOT+. Finally, as a result of this study, luteolin, artemisone, and kaempferol have been discovered as the most potent anti-cancer agents which can be considered as drug candidates to treat breast cancer and related cancer types in the future. However further research is necessary to investigate their potential medicinal use.

Keywords: *Artemisia carvifolia*, Virtual screening, CB-Dock, Estrogen receptor, HER2, Progesterone receptor, Lead compound, Luteolin. Artemisone, Kaempferol, Tamoxifen, Capecitabine and Mifepristone

Contents

Author's Declaration	iv
Plagiarism Undertaking	v
Acknowledgement	vi
Abstract	vii
List of Figures	xii
List of Tables	xiv
Abbreviations	xvii
1 Introduction	1
1.0.1 Problem Statement	4
1.0.2 Aims and Objectives	4
2 Literature Review	5
2.1 Cancer	5
2.2 Breast Cancer	5
2.2.1 Brest Cancer Incidence	6
2.2.2 Breast Cancer Symptoms	7
2.2.3 Risk Factors for Breast Cancer	7
2.2.4 Breast Cancer Types	9
2.2.5 Diagnosis of Breast Cancer	9
2.2.6 Breast Cancer Treatments	11
2.3 Medicinal Plant	13
2.4 Natural Compound in Treatment of Breast Cancer	15
2.5 <i>Artemisia carvifolia</i>	15
2.5.1 Taxonomic Hierarchy	16
2.6 Anti-Cancer Mechanism of Action of Bioactive Constituent of <i>Artemisia</i> Species	17
2.7 Targeted Protein	17
2.7.1 Estrogen Receptor	18

2.7.2	HER2	19
2.7.3	Progesterone Receptor	19
2.8	Molecular Docking	20
3	Materials And Methods	21
3.1	Selection of Disease	21
3.2	Selection of Proteins	21
3.3	Primary Sequence Retrieval	22
3.4	Analysis of Physiochemical Properties	22
3.5	Cleaning of the Downloaded Proteins	22
3.6	Functional Domains of Target Proteins	22
3.7	Selection of Active Metabolic Ligands	23
3.8	Ligands Preparation	23
3.9	Molecular Docking	23
3.10	Visualization of Docking Results via PyMol	24
3.11	Analysis of Docked Complexes via LigPlot	24
3.12	Ligands ADMET Properties	24
3.13	Lead Compounds Analysis and Toxicity Measurement	25
3.14	Selection of Standard Drugs against Breast Cancer	25
3.15	Comparison of Standard Drugs and Lead Compounds	25
3.16	Context Diagram	26
4	Results and Discussion	27
4.1	Structure Modeling	27
4.1.1	Primary Sequence Retrieval	27
4.1.2	Physiochemical Characterization of ER, HER2, PR	28
4.1.3	3D Structure Predictions of Proteins	31
4.1.4	Functional Domain Identification of Proteins	32
4.1.5	Templates Selection	35
4.1.6	Structure of Proteins Refined for Docking	36
4.2	Ligands Selection	36
4.3	Applicability of Lipinski's Rule	39
4.3.1	Toxicity Prediction	40
4.3.1.1	Arteannuin-B	42
4.3.1.2	Artemether	42
4.3.1.3	Artemisinin	43
4.3.1.4	Artesunate	44
4.3.1.5	Chrysosplenol D	45
4.3.1.6	Dihydroartemisinin	45
4.3.1.7	Kaempferol	46
4.3.1.8	Luteolin	47
4.3.1.9	Quercetin	48
4.3.1.10	Rutin	48
4.3.1.11	Isoquercetin	49

4.3.1.12	Artenimol	50
4.3.1.13	Artemisone	51
4.3.1.14	Caffeic acid	51
4.3.1.15	Gallic acid	52
4.4	Molecular Docking	53
4.5	Interaction of Ligands and Target Protein	61
4.5.1	Interaction of Ligands with Estrogen Receptor	62
4.5.2	Interaction of Ligands with HER 2	68
4.5.3	Interaction of Ligands with Progesterone Receptor	75
4.6	ADME Properties of Ligands	82
4.6.1	Pharmacodynamics	82
4.6.2	Pharmacokinetics	82
4.6.3	Absorption	82
4.6.3.1	Absorption Properties of Artemisinin, Artemether, Artesunate, Dihydroartemisinin, and Arteannuin B	83
4.6.3.2	Absorption Properties of Artenimol, Artemisone, Quercetin, Isoquercetin, and Rutin	84
4.6.3.3	Absorption Properties of Gallic acid, Kaempferol, Chrysosplenol D, Luteolin and Caffeic acid	86
4.6.4	Distribution	87
4.6.5	Metabolism	90
4.6.6	Excretion	92
4.7	Lead Compound Identification	94
4.8	Selection of Standard Drugs	96
4.9	Drug ADMET Properties	99
4.9.1	Toxicity Prediction of Reference Drugs	100
4.9.2	Absorption Properties	102
4.9.3	Distribution Properties	104
4.9.4	Metabolic Properties	106
4.9.5	Excretion Properties	107
4.10	Mechanism of Actions of Standard drugs	109
4.10.1	Tamoxifen Mechanism of Action	109
4.10.2	Capecitabine Mechanism of Action	110
4.10.3	Mifepristone Mechanism of Action	111
4.11	Effects on Body of Standard drugs	112
4.11.1	Tamoxifen Effects on Body	112
4.11.2	Capecitabine Effects on Body	112
4.11.3	Mifepristone Effects on Body	113
4.12	Docking Results of Standard drugs	113
4.12.1	Tamoxifen Docking	113
4.12.2	Capecitabine Docking	114
4.12.3	Mifepristone Docking	114
4.13	Standard Drugs and Lead Compounds Comparison	115
4.13.1	ADMET Properties Comparison	116

4.13.1.1	Toxicity Comparison	116
4.13.1.2	Absorption Properties Comparison	120
4.13.1.3	Distribution Properties Comparison	122
4.13.1.4	Metabolic Properties Comparison	124
4.13.1.5	Excretion Properties Comparison	126
4.13.2	Physiochemical Properties Comparison	127
4.13.3	Docking Score Comparison	129
4.13.3.1	Docking Analysis Comparison	131
5	Conclusion and Future Prospects	138
5.1	Recommendations	139
	Bibliography	158
	An Appendix	158

List of Figures

2.1	How cancer spreads [25].	6
2.2	The figure represents the <i>Artemisia carvifolia</i> plant [59].	16
3.1	The methodology flow chart	26
4.1	Human estrogen receptor alpha LBD with GW368.	31
4.2	HER2 in complex with Fab MF3958.	32
4.3	Human progesterone receptor LDB in complex with the ligand metribolone	32
4.4a	Functional domain of ER [96].	33
4.4b	Functional domains of ER with residue length [97].	33
4.5a	Functional domains of HER2 [98].	34
4.5b	Functional domains of HER2 with residue length [99].	34
4.6	Functional domains of PR with residue length [99].	34
4.7	Refined 3D Structure of estrogen receptor.	36
4.8	Refined 3D Structure of HER 2.	37
4.9	Refined 3D Structure of progesterone receptor.	37
4.10	Interactions of Artemisinin with ER by Ligplot.	63
4.11	Interactions of Artemether with ER by Ligplot.	63
4.12	Interactions of Dihydroartemisinin with ER by Ligplot.	64
4.13	Interactions of Artesunate with ER by Ligplot.	64
4.14	Interactions of Arteannuin B with ER by Ligplot.	64
4.15	Interactions of Artemisone with ER by Ligplot.	65
4.16	Interactions of Artenimol with ER by Ligplot.	65
4.17	Interactions of Quercetin with ER by Ligplot.	65
4.18	Interactions of Isoquercetin with ER by Ligplot.	66
4.19	Interactions of Rutin with ER by Ligplot.	66
4.20	Interactions of Gallic acid with ER by Ligplot.	66
4.21	Interactions of kaempferol with ER by Ligplot	67
4.22	Interactions of Chrysosplenol D with ER by Ligplot.	67
4.23	Interactions of Luteolin with ER by Ligplot.	67
4.24	Interactions of Caffeic acid with ER by Ligplot.	68
4.25	Interactions of Artemisinin with HER 2 by Ligplot.	70
4.26	Interactions of Artemether with HER 2 by Ligplot.	70
4.27	Interactions of Artesunate with HER 2 by Ligplot.	71
4.28	Interactions of Dihydroartemisinin with HER 2 by Ligplot.	71

4.29	Interactions of Arteannuin B with HER 2 by Ligplot.	71
4.30	Interactions of Artemimol with HER 2 by Ligplot.	72
4.31	Interactions of Artemisone with HER 2 by Ligplot.	72
4.32	Interactions of Quercetin with HER 2 by Ligplot.	72
4.33	Interactions of Isoquercetin with HER 2 by Ligplot.	73
4.34	Interactions of Rutin with HER 2 by Ligplot.	73
4.35	Interactions of Gallic acid with HER 2 by Ligplot.	73
4.36	Interactions of kaempferol with HER 2 by Ligplot.	74
4.37	Interactions of Chrysosplenol D with HER 2 by Ligplot.	74
4.38	Interactions of Luteolin with HER 2 by Ligplot.	74
4.39	Interactions of Caffeic acid with HER 2 by Ligplot.	75
4.40	Interactions of Artemisinin with PR by Ligplot.	77
4.41	Interactions of Artemether with PR by Ligplot.	77
4.42	Interactions of Artesunate with PR by Ligplot.	77
4.43	Interactions of Dihydroartemisinin with PR by Ligplot.	78
4.44	Interactions of Arteannuin B with PR by Ligplot.	78
4.45	Interactions of Artemimol with PR by Ligplot.	78
4.46	Interactions of Artemisone with PR by Ligplot.	79
4.47	Interactions of Quercetin with PR by Ligplot.	79
4.48	Interactions of Isoquercetin with PR by Ligplot.	79
4.49	Interactions of Rutin with PR by Ligplot.	80
4.50	Interactions of Gallic acid with PR by Ligplot.	80
4.51	Interactions of kaempferol with PR by Ligplot.	80
4.52	Interactions of Chrysosplenol D with PR by Ligplot.	81
4.53	Interactions of Luteolin with PR by Ligplot.	81
4.54	Interactions of Caffeic acid with PR by Ligplot.	81
4.55	2D Structure of Tamoxifen Drug- PubChem.	99
4.56	2D Structure of Capecitabine Drug- PubChem.	99
4.57	2D Structure of Mifepristone Drug- PubChem.	99
4.58	Mechanism of Action of Tamoxifen [131].	109
4.59	Capecitabine and its main metabolic pathway [133].	110
4.60	Mechanism of Action of Mifepristone [138].	111
4.61	Best Pose Interaction of Luteolin as Ligand with ER.	129
4.62	Best Pose Interaction of Tamoxifen as Ligand with ER.	130
4.63	Best Pose Interaction of Artemisone as Ligand with HER2.	130
4.64	Best Pose Interaction of Capecitabine as Ligand with HER2.	130
4.65	Best Pose Interaction of Kaempferol as Ligand with PR.	131
4.66	Best Pose Interaction of Mifepristone as Ligand with PR.	131
4.67	Hydrogen Bonds and Interactions of Luteolin (ligand) with ER. . .	132
4.68	Hydrogen Bonds and Interactions of Tamoxifen (ligand) with ER. .	132
4.69	Hydrogen Bonds and Interactions of Artemisone (ligand) with HER2.	134
4.70	Hydrogen Bonds and Interactions of Capecitabine (ligand) with HER2	134
4.71	Hydrogen Bonds and Interactions of Kaempferol (ligand) with PR. .	136
4.72	Hydrogen Bonds and Interactions of Mifepristone (ligand) with PR.	136

List of Tables

2.1	Accuracy of Breast Imaging Modalities [34].	10
2.2	Chemotherapeutic drugs used in breast cancer management [39].	12
2.3	Taxonomic hierarchy of <i>Artemisia carvifolia</i>	17
4.1	Physiochemical Properties of Human Estrogen receptor.	29
4.2	Physiochemical Properties of HER 2.	30
4.3	Physiochemical Properties of progesterone receptor.	30
4.4	Functional domain identification of ER, HER 2, and PR.	35
4.5	Selected PDB Templates Structures	35
4.6	Selected Ligands with Structural Information.	38
4.7	Applicability of Lipinski Rule on Ligands.	40
4.8	The Toxicity Values of Arteannuin B.	42
4.9	The Toxicity Values of Artemether.	43
4.10	Toxicity prediction of Artemisinin.	43
4.11	The Toxicity Values of Artesunate.	44
4.12	The Toxicity Values of Chrysosplenol D.	45
4.13	The Toxicity Values of Dihydroartemisinin	46
4.14	The Toxicity Values of Kaempferol.	46
4.15	The Toxicity Values of Luteolin	47
4.16	The Toxicity Values of Quercetin.	48
4.17	The Toxicity Values of Rutin	49
4.18	The Toxicity Values of Isoquercetin.	49
4.19	The Toxicity Values of Artemimol.	50
4.20	The Toxicity Values of Artemisone.	51
4.21	The Toxicity Values of Caffeic acid.	51
4.22	The Toxicity Values of Gallic acid.	52
4.23a	Ligands with Best Binding Score Values with estrogen receptor.	54
4.23b	Ligands with Best Binding Score Values with estrogen receptor.	55
4.23c	Ligands with Best Binding Score Values with estrogen receptor.	55
4.24a	Ligands with Best Binding Score Values with HER2.	57
4.24b	Ligands with Best Binding Score Values with HER2.	57
4.24c	Ligands with Best Binding Score Values with HER2.	58
4.25a	Ligands with Best Binding Score Values with progesterone receptor.	59
4.25b	Ligands with Best Binding Score Values with progesterone receptor.	60
4.25c	Ligands with Best Binding Score Values with progesterone receptor.	61

4.26	Absorption Properties of Ligands.	84
4.27	Absorption Properties of Ligands	85
4.28	Absorption Properties of Ligands	86
4.29	The Distribution Properties of Ligands.	88
4.30	The Distribution Properties of Ligands.	88
4.31	The Distribution Properties of Ligands.	89
4.32	Metabolic Properties of Ligands.	90
4.33	Metabolic Properties of Ligands.	91
4.34	Metabolic Properties of Ligands	92
4.35	Excretory Properties of Ligands.	93
4.36	Excretory Properties of Ligands.	93
4.37	Excretory Properties of Ligands	94
4.38	Hit Compounds with Binding Scores with ER.	95
4.39	Hit Compounds with Binding Scores with HER2.	95
4.40	Hit Compounds with Binding Scores with PR.	96
4.41	Drugs and Their Mechanism of Action.	97
4.42	Physiochemical Properties of Drugs.	98
4.43	Toxicity Values of Tamoxifen	100
4.44	Toxicity Values of Capecitabine	101
4.45	Toxicity Values of Mifepristone.	101
4.46	Absorption Properties of Tamoxifen.	102
4.47	Absorption Properties of Capecitabine.	103
4.48	Absorption Properties of Mifepristone.	103
4.48	Absorption Properties of Mifepristone.	104
4.49	Distribution Properties of Tamoxifen.	104
4.50	Distribution Properties of Capecitabine.	105
4.51	Distribution Properties of Mifepristone.	105
4.52	Metabolic Properties of Tamoxifen.	106
4.53	Metabolic Properties of Capecitabine.	106
4.54	Metabolic Properties of Mifepristone	107
4.55	The Excretion Properties of Tamoxifen.	108
4.56	The Excretion Properties of Capecitabine.	108
4.57	The Excretion Properties of Mifepristone.	108
4.58	Tamoxifen Docking Score via CB Dock.	113
4.59	Capecitabine Docking Score via CB Dock.	114
4.60	Mifepristone Docking Score via CB Dock.	114
4.61	Luteolin - Tamoxifen Lipinski Rule of Five.	115
4.62	Artemisone- Capecitabine Lipinski Rule of Five.	116
4.63	Kaempferol - Mifepristone Lipinski Rule of Five.	116
4.64	Toxicity Values of Tamoxifen & Luteolin.	117
4.65	Toxicity Values of Capecitabine & Artemisone	118
4.65	Toxicity Values of Capecitabine & Artemisone	119
4.66	Toxicity Values of Mifepristone & Kaempferol.	120
4.67	Absorption Properties of Tamoxifen & Luteolin.	120

4.68	Absorption Properties of Capecitabine & Artemisone.	121
4.69	Absorption Properties of Mifepristone & Kaempferol.	122
4.70	Distribution Properties of Tamoxifen & Luteolin.	122
4.71	Distribution Properties of Capecitabine & Artemisone.	123
4.72	Distribution Properties of Mifepristone & Kaempferol.	124
4.73	Metabolic Properties of Tamoxifen & Luteolin.	124
4.74	Metabolic Properties of Capecitabine & Artemisone	125
4.75	Metabolic Properties of Mifepristone & Kaempferol.	125
4.76	Excretion Properties of Tamoxifen & Luteolin.	126
4.77	Excretion Properties of Capecitabine & Artemisone.	126
4.78	Excretion Properties of Mifepristone & Kaempferol.	127
4.79	Physiochemical Properties of Tamoxifen & Luteolin.	127
4.80	Physiochemical Properties of Capecitabine & Artemisone.	128
4.81	Physiochemical Properties of Mifepristone & Kaempferol.	128
4.82	Hydrogen Bonds and Interactions Comparison of Tamoxifen & Luteolin.	133
4.83	Hydrogen Bonds and Interactions Comparison of Capecitabine & Artemisone	135
4.84	Hydrogen Bonds and Interactions Comparison of Mifepristone & Kaempferol.	137
5.1	Active Ligand Showing Hydrogen and Hydrophobic Interactions with ER	158
5.2	Active Ligand Showing Hydrogen and Hydrophobic Interactions with HER 2.	164
5.3	Active Ligand Showing Hydrogen and Hydrophobic Interactions with PR.	169

Abbreviations

<i>A. annua</i>	<i>Artemisia annua</i>
AC	Adriamycin and Cyclophosphamide
ADMET	Absorption Distribution Metabolism Excretion & Toxicity
BBB	Blood-brain barrier
Bcl 2	B-cell lymphomas 2
BRCA	Breast Cancer gene
CAF	Cyclophosphamide, Doxorubicin, 5-Fluorouracil
CB Dock	Cavity-detection guided Blind Docking
Cdk 2	Cyclin-dependent kinase 2
CMF	Cyclophosphamide, methotrexate, fluorouracil
CNF	Cyclophosphamide, Novantrone- Mitoxantrone, 5-Fluorouracil
CNS	Central Nervous System
CTD	C terminal domain
CYP2D6	Cytochrome P450 2D6
DBD	DNA binding domain
DCIS	Ductal carcinoma in situ
DNA	Deoxyribonucleic acid
ER	Estrogen receptor
FAC	Fluorouracil, doxorubicin, cyclophosphamide
FAK	Focal adhesion kinase
FDA	Food Drug Authority
FdUMP	5-fluoro-2'-deoxyuridine 5'-monophosphate
FUTP	5-fluorouridine triphosphate
GRAVY	Grand average of hydropathicity

HBA	Hydrogen bond acceptor
HBD	Hydrogen bond donor
hERG	Human Ether-a-go-go-Related Gene
II	Instability index
LBD	Ligand binding domain
LCIS	Lobular carcinoma in situ
MAPK	Mitogen-activated protein kinase
MF	Mifepristone
MRTD	Maximum rate tolerated dose
MW	Molecular weight
NcoR	Nuclear receptor co-repressor 2
NFL	Mitoxantrone, 5-fluorouracil, leucovorin
NR	Total number of negatively charged residue (Asp + Glu)
NTD	N terminal domain
OCT	Organic cation transporter
PDB	Protein Data Bank
PI	Theoretical pI
PI3K	Phosphoinositide-3-kinase
PR	Total number of positively charged residue (Asp + Glu)
PR	Progesterone receptor
RNA	Ribonucleic acid
SMRT	Silencing mediator for retinoid
STAT	Signal transducer and activator of transcription
TBL1	Transducin b like protein1
TS	Thymidylate synthase
UTP	Uridine triphosphate
VDss	Volume distribution at steady state

Chapter 1

Introduction

Cancer incidence rates have risen dramatically in recent years as a result of lifestyle changes, eating patterns, and environmental factors. Cancer incidence is higher in developing countries than in developed countries [1]. By 2020, it is estimated that 15 million people would die from cancer, it may be because of aging, increase in population due to which various factors such as changing reproductive trends, tobacco use, overweightness, physical idleness, and, linked with sustainable growth and urbanization, have prevailed [2]. In both developing and developed countries, lung cancer is the common mortality cause in males, while breast carcinoma is common in females. Other causes of cancer death include colorectal cancer and prostate cancer in developed countries and liver, cervical and stomach cancer in less developed countries. Even though the prevalence rates of all cancers are higher in developed countries, mortality rates in developed countries are just 8% to 15% higher [3]. In developed countries such as United State, 12.5% of women are being diagnosed with Breast cancer [4-5]. Although in Asian countries the incidence rate is lower for breast cancer the global burden is rapidly growing in Asia.

Breast cancer was first reported by ancient Egyptians more than 35000 years ago [6]. Breast cancer was described as a humoral disease by Hippocrates who is considered the father of western medicine [7]. The capacity of breast cancer to spread or metastasize is its most lethal feature. Breast cancers are most often caused in the milk-producing cell or the duct present in the lobule. Breast cancer

risk factors have been linked to an increase in its occurrence in epidemiological research studies. Many variables have been studied to determine patients' risk, including age, family background, receptor status, and others [8].

Most patients with breast carcinoma have higher levels of the progesterone receptor, HER2/neu, and estrogen receptor, all of which are considered cancer progression markers [9]. ER α is involved in many signaling pathways which are responsible for growth and proliferation such as MAPK and PI3K pathway [10]. Progesterone stimulates PR, leading it to upregulate numerous essential cellular functions, including proliferation, which aids the development of breast cancer [11]. Increased expression of HER2 tyrosine kinase activity has an anti-apoptotic effect which results in increased malignancy. HER2 protein activates various signal transduction molecules including signal transducer, kinases transcription activator, and activates many pathways such as STAT, MAPK, and PI3K which regulate the cellular process of proliferation and differentiation [12]. Upregulation of HER2 and HER1 is linked to a deprived clinical prognosis in breast carcinoma patients, in addition to a poor response to endocrine therapy.

Tamoxifen has been used as a drug against estrogen in females with more likelihood of disease. Fulvestrant has also been approved for clinical use against estrogen [13]. Aromatase inhibitors such as anastrozole, letrozole inhibit enzyme aromatases which are involved in the synthesis of estrogen [14]. Anti-HER2 antibodies such as trastuzumab and Pertuzumab have been used in the treatment of breast cancer. They target the extracellular domain of protein preventing its dimerization and phosphorylation [15]. Many tyrosine kinase inhibitors such as neratinib, gefitinib, and lapatinib have been used for treatment by binding HER1 and HER2 domains and cause inhibition of signaling pathways [16]. But despite the availability of all these drugs patients develop resistance against them. MAPK and PI3K are involved in developing tamoxifen resistance. A further side effect of these targeted are mild, but sometimes severe which includes congestive heart failure, leg swelling, diarrhea, shortness of breath, severe fatigue, and liver and lung problems. With the advancement in science and medicine, the survival rate of cancer has improved.

Although effective treatments have been developed these treatments have some side effects and patients also develop resistance against drugs. As a result, for more effective cancer treatment there is a need for a plant-based herbal medication having no side effects. *Artemisia* species are widely used in herbal medicine for several well-known medicinal purposes and surely understood therapeutic and helpful applications (stomachache, parasitism, diarrhea, bronchial and intestinal infections, pimples, angina, wounds, coughs, and colds) all over the world [17].

Artemisia species contain a diverse spectrum of physiologically active chemicals that have a variety of pharmacological effects. Phenols and flavonoids are two of the most important families of phytochemicals found in plants. They have been shown to have antitumor, antioxidant, antispasmodic, insecticidal, antimalarial, antimicrobial, anti-inflammatory, and antifungal properties. Diseases caused by fungi, bacteria, and viruses such as cancer, hepatitis, infections can be treated with the use of *Artemisia* species [18]. Glycosides, terpenoids, flavonoids, sterols, coumarin, and polyacetylene are only a few of the secondary metabolites found in the *Artemisia* genus. Sesquiolactones and flavonoids are two of *Artemisia*'s secondary metabolites that have a lot of therapeutic and restorative potential [19].

Significant antioxidant properties are found in the methanolic extract of *Artemisia carvifolia*. That's why this plant was selected to find a natural anticancer compound to target receptor proteins in breast cancer. Docking is an *In silico* method for determining the correct structure of a ligand within the target binding site and estimating the strength of a bond between a ligand and a target protein using a special scoring feature. The input for docking is the 3-Dimensional structures of the target proteins and ligands [20]. This new class of small molecular compounds has been shown to have important properties, such as a high interaction between target binding and target proteins, as well as proper absorption, distribution, metabolism, and excretion (ADME) to aid in target lead selection [21].

It also focuses on achieving the system's minimum independent energy, which includes properly aligned proteins and ligands [22]. Small ligands, protein peptides, protein proteins, and protein nucleotides can all be used in the molecular docking

of proteins mechanism. An algorithm, receptor flexibility, and ligand flexibility are some of the docking mechanisms [23].

1.0.1 Problem Statement

Cancer is the second most leading cause of morbidity and death around the globe. While many treatments and therapies have been in use over the past two decades, they all have their own set of issues, such as toxicity and immunosuppression. An increase in cancer cases has prompted researchers to look for new, more effective drugs made from plants [24]. Plant extracts have been used in ethnomedical treatments that have fewer side effects as compared with synthetic treatments.

1.0.2 Aims and Objectives

The aim is to identify novel inhibitors, harmless and natural anti-cancer compounds from *Artemisia carvifolia*. And therefore, we focus on protein-ligand interactions, which play a significant role in structural drug design. To achieve the goal, we have the following objectives:

1. To identify various bioactive compounds of *Artemisia carvifolia* as potential inhibitors of estrogen, progesterone, and HER2 receptors.
2. To analyze the binding conformation between targeted proteins and ligands by performing molecular docking.
3. To find the best of the interacting molecules that show inhibitory effects against the targeted receptors.

Chapter 2

Literature Review

2.1 Cancer

It is the phrase used to describe a group of illnesses. In all types of carcinomas, the cells of the body begin to divide uncontrollably and extend into nearby tissue. As cells age or become wounded, they die, and a new one replaces them. When cancer strikes, however, this well-organized mechanism is interrupted. Cells that should die such as old or damaged, live ones, and new cells emerge when they are no longer needed as they grow more irregular. As seen in Figure 2.1, these additional cells divide endlessly, resulting in tumor growth [25].

2.2 Breast Cancer

Breast cancer is a form of cancer that develops in the breast cells. It usually develops in the lobules or ducts. Milk-producing glands are known as lobules, and ducts are the channels that bring milk from the glands to the nipple [26]. Breast cancer can also develop in the fatty tissue or fibrous connective tissue of the breast. Around 5–10% of cases are caused by a genetic predisposition inherited by one's parents, such as BRCA1 and BRCA2, among others [27]. Cancer cells that have gotten out of hand might infiltrate healthy breast tissue and spread to

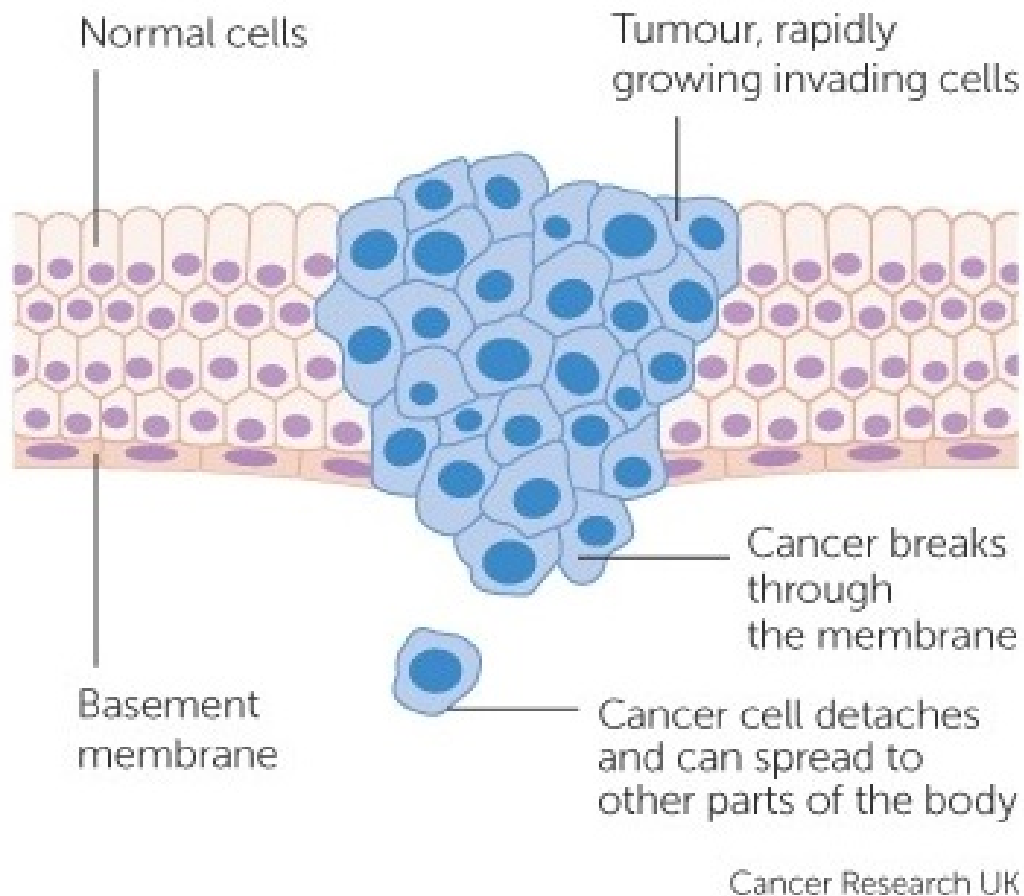


FIGURE 2.1: How cancer spreads [25].

lymph nodes beneath the arms. Cancer cells can travel to other parts of the body through the lymph nodes.

2.2.1 Breast Cancer Incidence

In the United States, breast cancer is the most prevalent cancer in women, accounting for one-fourth of all female cancers. Breast cancer is 100 times less prevalent in men than in women, with a one-in-seven risk of developing it in a woman's lifetime. Breast cancer is the main cause of mortality in women between the ages of 44 to 50, accounting for 15% of all cancer deaths. Breast cancer incidence (number of new cases per 100,000 people) grew by 4% in the 1980s before leveling off in the 1990s at 100.6 cases per 100,000 women. Between 1992 and 1996, the number of women dying of breast cancer declined dramatically, with the younger women

experiencing the greatest reduction. Invasive breast cancer will be detected in almost 211, 240 women in the United States in 2005 according to the American Cancer Society (Stages I-IV). In the Asian population, a peak in breast cancer incidence is observed between the ages of 40 to 59, more specifically age-specific incidence rate in India is 50-59, 40-49 in Korea, 45-54 in Japan, and 60-64 in Sri Lanka [28]. In Pakistan, the risk of breast cancer has increased, whereby 1 in every 9 women has a lifetime risk of being diagnosed with this disease.

2.2.2 Breast Cancer Symptoms

Symptoms in breast malignancies include:

- Tissue thickening or any lump that can be easily felt
- Swelling
- Pitted and reddish skin
- Pain in breast
- Bloody release and discharge from nipple other than milk.
- Scaling or shedding of skin on your nipple
- A rapid, unfamiliar shift in the size and appearance of the breast
- Color variation of the breasts' covering
- Twisted nipple
- Detection of swelling or lump under the arm area [29].

2.2.3 Risk Factors for Breast Cancer

Numerous factors influence the likelihood of acquiring breast cancer. However, showing symptoms does not guarantee that you will inherit the disease. Risk factors are classified into two categories:

1. **Modifiable risk factors** (those that individuals may change themselves, such as alcohol consumption).
2. **Fixed risk factors** (those that cannot be changed) (things that cannot be changed, such as age and biological sex) [30].
 - **Age:** Breast cancer is uncommon in women under the age of 25. The rate of occurrence rises with age, reaching a nadir in women aged 50 to 55.
 - **Genetics:** A person's family background may be a risk factor. The lifetime risk is up to four times higher if both a mother and a sister are affected.
 - People of Ashkenazi Jewish ancestry are at a 2-fold higher risk.
 - When compared to American women, Japanese and Taiwanese women face a fifth of the risk.
 - BRCA1 and BRCA2 mutations are linked to an increased probability of cancer.
 - Four-time increased likelihood of disease in case of Ataxia-telangiectasia heterozygotes.
 - **Other Pathology:** Past breast cancer, ovarian cancer, complex fibroadenoma, endometrial cancer, radial scar, ductal carcinoma in situ. Cervical cancer carries a lower risk.
 - **The number of menstrual cycles:** Factors that raise the menstrual cycles count enhances the danger, most likely due to increased exposure to endogenous estrogen.
 - **Obesity:** In adipose tissue androgens to estrogens conversion is believed to increase risk.
 - **Economic class:** People from a higher socioeconomic class have a higher incidence.
 - **Exogenous factors:** 1-Hormone replacement therapy 2- use of oral contraceptive pills 3- Irradiation 4- Exposure to some viral agents 5- Alcohol consumption [28, 31].

2.2.4 Breast Cancer Types

The two most frequent forms of breast cancer are grouped into two categories:

- **In situ ductal carcinoma**, DCIS (ductal carcinoma in situ) is a malignancy that does not spread. DCIS signifies your breast cancer cells haven't migrated beyond the ducts and haven't spread to the surrounding tissue [32].
- **Lobular carcinoma in situ** LCIS (lobular carcinoma in situ) is a type of breast cancer that starts in the milk glands. Unlike DCIS, the cancer cells haven't penetrated the underlying tissue.

The cancer cells haven't entered the underlying tissue, unlike DCIS.

- **Invasive ductal carcinoma:** It is the most communal type of breast carcinoma. In the breast this type starts in the milk ducts then invades the surrounding tissue.
- **Invasive lobular carcinoma:** It begins in the lobules of mammary glands and spreads to nearby tissue [33].

2.2.5 Diagnosis of Breast Cancer

The doctor will perform a thorough physical examination in addition to a breast exam to determine whether the symptoms are caused by breast cancer or a benign breast ailment.

A **mammogram** is a screening test that may aid in the detection. The best way is to look under your breast surface with a mammogram, which is an imaging examination. Every year, many women over the age of 40 have a mammogram to screen for breast cancer [34]. Table 2.1 represents the accuracy of breast imaging modalities.

- An ultrasound generates a view of the breast tissues presents deep inside using sound waves. An ultrasound will be used to distinguish between a dense mass, such as a minor cyst, and a tumor.

Breast biopsy: During this operation, a tissue sample from the infected area will be collected and evaluated. Breast biopsies come in a variety of shapes and sizes [35].

TABLE 2.1: Accuracy of Breast Imaging Modalities [34].

Modality	Sensitivity	Specificity	Positive Prediction	Indications
Mammo- graphy	63-95% Sensitivity is less than 35% in the case of dense breasts and 92% in women with an age greater than 50.	Palpable (14-90%)	Palpable (10-50%)	In women above 35-year Initial investigation and screening is considered for symptomatic breast.
MRI	(86-100%)	(21-97%)	(52%)	Multifocal and borderline lesions, Scarred breast, implants for breast conservation.
Ultrason- ography	Palpable (68-97%)	Palpable (74-94%)	Palpable (92%)	In females younger than 35-year investigation is considered for lesions.
PET (Positron emission tomogra- phy)	Axillary metastases (96%)	100%	 	Scarred breast Axilla assessment, and multifocal lesions.

	Palpable		Palpable	Drug resistance can
	(76-95%)	Im-	(70- 83%)	be predicted in the
Scintigra-		palpable	Im-	case of axilla asses-
phy	Impalpable	(62-94%)	palpable	sment Lesions
	(52-91%)		(83%-79%)	larger than 1 cm.

Stages of Breast Cancer When cancer is found, it is assigned a grade. A stage is a number that ranges from 0 to IV (with sub-stages represented by letters) that denotes cancer's severity and aggressiveness:

- Breast cancers in situ, such as ductal carcinoma in situ, are stage 0 malignancies. Cancer that has been established in a specific site is referred to as "in situ." That means, cancer has not moved to other regions of the body or affected the tissues around it.
- Stages I through III are used to describe cancer that has spread to tissues inside or close to the breast (localized or regional breast cancer).
- Stage IV breast cancer is defined as cancer that has gone beyond the breast and lymph nodes in the armpit to other parts of the body [36].

2.2.6 Breast Cancer Treatments

Surgery: Surgery entails the physical removal of the tumor, as well as any of the underlying tissue in most cases. During surgery, one or more lymph nodes can be biopsied; increasingly, lymph node sampling is done using a sentinel lymph node biopsy.

Typical procedures include:

- **Mastectomy:** The whole breast is removed.
- **Quadrantectomy:** This procedure involves the removal of a quarter of the breast.

- **Lumpectomy:** It removed a small portion of the breast [37].

Radiation Therapy: Radiation therapy is the use of high-energy rays such as Gamma or X-rays to treat a tumor or a post-surgery tumor location. These rays are particularly effective at killing cancer cells that may remain after surgery or return where the tumor was removed. Treatments normally last five to seven weeks and are given five days a week. Each therapy is about 15 minutes long [38].

Chemotherapy: It is a form of drug therapy that is used to destroy cancerous cells. This therapy can be used alone in some cases, but it can be used in combination with other clinical treatments, for instance, surgery. The chemotherapeutic agents used in the management of breast cancer are shown in Table 2.2. Chemotherapy has a lot of unfavorable side effects, so talk to your doctor about them before you start [39].

TABLE 2.2: Chemotherapeutic drugs used in breast cancer management [39].

Sr. No.	Abbreviation	Components
1	AC	Day 1 Doxorubicin 60mg/m ² IV. Day1 Cyclophosphamide 400-600 mg/m ² IV (Repeat every 21 day). Day 1-14 Cyclophosphamide 100 mg /m ² PO. ”
2	CAF (FAC)	Day 1, 8 or 60 Doxorubicin25 mg/m ² day IV. Day 1, 8 Fluorouracil 500-600 mg/m ² IV (repeat every 28 days). Day 1 Cyclophosphamide 500-600 mg /m ² IV.
3	CMF (CNF, FNC)	Day 1 Fluorouracil 500-600 mg/m ² IV. Day 1 Mitoxantone 10-12 mg/ m ² IV (repeat every 21 days).

		Cyclophosphamide 100 mg /m ² PO day 1-14. Day 1-8 Methotrexate 40 mg / m ² IV.
4	CMF	Day 1 -8 Fluorouracil 600 mg/m ² IV (repeat every 28 days). Day 1 Mitoxantone 12 mg/ m ² IV. Day 1 -3 Fluorouracil 350 mg/m ² IV is given after leucovorin.
5	NFL	Days 1-3 Leucovorin 300 mg IV over 1 hr (repeat every 21 days).

Hormonal Therapy: The growth of breast tumors can be promoted with two hormones, estrogen, and progesterone, which are predominantly present in females. It works by inhibiting the synthesis of these hormones in your body, or by inhibiting receptors present on the surface of cancer cells. This mechanism can either slow down or stop the growth of cancer. Most breast cancers have a positive ER, three medications, tamoxifen, raloxifene, toremifene, are used to treat and/or prevent them. Tamoxifen use was linked to a lower risk of invasive breast cancer [40].

2.3 Medicinal Plant

Medicinal plants have been used for therapeutic purposes against several diseases since the dawn of human civilization. Natural-source drugs account for about 40% of newly approved drugs in the last two decades. They play a significant role in the discovery of drugs for cancer treatment and dealing with other infectious ailments [41].

The word "medicinal plant" refers to a variety of plants used in herbal medicine ("herbology" or "herbal medicine"). It is the practice of using plants for medicinal purposes as well as the study of such practices. Medicinal plants are thought

to be a rich source of ingredients that can be used to make pharmacopeia, non-pharmacopeia, or synthetic drugs. Plant parts that resembled parts of the human body were thought to be useful in treating ailments of certain body parts, according to the "Doctrine of Signature" theory of early herbalists [42].

Since ancient times, medicinal and aromatic plants have been used as therapeutic agents [43]. In ancient medical systems such as Ayurvedic, Unani, and Chinese traditional medicine, herbs have been used to cure diseases and restore and fortify body systems [44].

Various species of *Caralluma* are used in Arabic and IndoPak traditional medicine to treat diabetes, cancer, snake and scorpion bites, inflammation, and skin rashes. Drugs are made from various parts of medicinal plants, including the leaves, seeds, roots, flowers, and sometimes the whole plant [45] [46].

In the use of a few biochemicals, the plant kingdom provides a wide range of structural diversity. A variety of new pharmacophores have been discovered by phytochemical research on medicinal plants. In the development of drugs, pharmacophores have proven to be invaluable [47]. To meet demand, the number of plant-derived medicines and health foods has steadily increased. These medicinal plants are highly regarded and have few side effects, making them increasingly important around the world [48].

Most developing countries are promoting herbal medicines, which are also more cost-effective than prescription drugs [49]. According to one study, plant-based medicines are considered reliable in 70-80 percent of the developing world, considering the high cost of pharmaceuticals [50].

The United States, China, France, Japan, the United Kingdom, and Italy are currently the main global markets for medicinal plants. Medicinal plants have a promising future if they survive. In the world, there are approximately half a million plants, the bulk of which have yet to be examined in medical practice. As a result, current and future research on medicinal plants may be useful in the treatment of diseases [51].

2.4 Natural Compound in Treatment of Breast Cancer

Magnolol is a natural compound obtained from stem bark and root of plant *Magnolia officinalis* is known to prevent angiogenesis and inducing apoptosis [52]. 3,3'-Diindolylmethane (DIM) is known to inhibit COX -2 expression in breast cancer is a natural compound obtained from broccoli, cabbage, and cauliflower [53]. Grape stem extract is rich in quercetin and rutin thus is used in the treatment of breast cancer [54].

2.5 *Artemisia carvifolia*

With more than 300 species, *Artemisia* is a diverse and economically important genus in the Asteraceae family [55]. The name *Artemisia* is derived from the Greek Goddess Artemis, who was regarded as the Protector of the Wild. This genus produces secondary metabolites and essential oils that are used to treat various ailments. *Artemisias* are mostly biannual, perennial, annual herbaceous ornamental, aromatic plants or shrubs, and medicinal plants. Because of the presence of sesquiterpene and terpenoids lactones, their coloring is silver-green, dark green, or blue-green, and they have a sharp smell and bad taste [56]. *Artemisia carvifolia* is famous in the west as wormwood. It is a branched annual or biennial plant that grows 30 to 150cm tall. The plant is cultivated in the wild for use as a medicine and food in the region. Moist river channels, outer forest margins, canyons, waysides, and coastal beaches are among its ecosystem, which ranges in elevation from low to 4,600 meters. One of the significant uses of *Artemisia* species is it's used as a pain reliever. In the plants, the monoterpenes cooperate with the receptor channel to assuage pain and ache and sesquiterpenes help with the discomfort.

The plant has the same medicinal properties as *A. annua*, making it an essential anti-malarial. The plant is said to protect against malaria and repel mosquitoes.

It prevents the malaria parasite from maturing in the body. Low-grade fever, summer heatstroke, tidal fever, chronic diarrhea, phthisis, and purulent scabies are also treated with it [57].

This plant contains abrotanin which has antipyretic and antiphlogistic properties. It is commonly used in tropical areas as an effective antimalarial drug. The leaf of this plant is antiperiodic and antiseptic and often used to treat fever, cold, and diarrhea. The seed of *A. carvifolia* is used in the treatment of indigestion, flatulence, and night sweats. It produces allelopathic (secreting chemicals) that inhibit the growth of other plants in the region [58]. Plant basal stem leaves are withering, middle stem leaf is 5-10mm long, and elliptical and uppermost leaf is like pinnatisect and pectinasect as shown in Figure 2.2.



FIGURE 2.2: The figure represents the *Artemisia carvifolia* plant [59].

2.5.1 Taxonomic Hierarchy

Artemisia carvifolia is the binomial name of the plant belonging to the Asteraceae family. They are easily grown in an alkaline loamy soil. They are long-lived, harder, and more aromatic when grown in dry poor soil. It is widely distributed in different regions of the world. The taxonomic hierarchy is shown in Table 2.3.

TABLE 2.3: Taxonomic hierarchy of *Artemisia carvifolia*

Sr. No.	Domain	Eukarya
1	Kingdom	Plantae
2	Subkingdom	Tracheobionta (Vascular plant)
3	Division	Magnoliophyta (flowering plant)
4	Class	Magnoliophyta (Dicotyledons)
5	Subclass	Asteridae
6	Order	Asterales
7	Family	Asteraceae
8	Genus	Artemisia
9	Specie	A carvifolia

2.6 Anti-Cancer Mechanism of Action of Bioactive Constituent of Artemisia Species

Quercetin is known to induce apoptosis, prevent proliferation and metastasis and inhibit signal transduction in tumor cells. Quercetin also causes arrest in the cell cycle at the G2/M phase by causing downregulation of cyclin D1 [60]. Artesunate is also known to inhibit cell proliferation in breast cancer and is known to induce reactive oxygen species-dependent arrest at G1 and G2/M phase and apoptosis [61]. Artemisinin is also known to have anti-cancer properties and it causes cell cycle arrest and inhibits proliferation by decreasing the protein level of CDK2, transcriptional factor, and cyclin-dependent kinases [62].

2.7 Targeted Protein

3 different types of receptor proteins are used as targeted proteins for the molecular docking process such as estrogen receptor, HER2, and progesterone receptor.

2.7.1 Estrogen Receptor

Breast cancer development is linked to the estrogen receptor and estrogen signaling as the majority of breast cancer begins as estrogen-dependent. Estrogens are thought to play a key role in the proliferation of both normal and cancerous breast epithelial cells. Estrogen has been associated with enhanced breast cancer risk during postmenopausal years.

Research evidence has also shown a reduced risk of breast cancer with increase estrogen exposure during premenopausal years, childhood, by inducing the expression of DNA repair gene and by altering mammary gland development [63] [64]. Concerning increased risk, estrogen either act as a promoter by enhancing the growth of existing transformed cell or an initiator by inducing the genetic transformation. ER α is a major estrogen subtype that is involved in the progression of breast cancer [65].

The ER has an AF1 domain at the N-terminus, a DNA-binding domain at the C-terminus, and a ligand-binding region at the C-terminus with an AF2 domain [66]. The binding of estrogen to ER α , translocate the complex to the nucleus which in turn binds the responsive element of the promoter thus stimulate nuclear signaling [67]. ER signaling is considered complex as it involves many coregulatory proteins and extranuclear actions [68]. ER co-regulatory proteins have been shown to alter their functions in tumor cell lines leading to tumor progression [69]. Loss of breast cancer progression is associated with the loss of expression of E-cadherin which results from down-regulation of ER- coregulatory signaling [70]. Thus, ER α and ER coregulators modulate the expression of genes involved in metastasis.

ER α extranuclear signaling is associated with enhancing breast cancer cell motility and metastasis by stimulation of mitogen-activated protein kinase, protein kinase C, Src kinase, and phosphatidylinositol 3 kinase [71]. Since ER signaling pathways play a significant role in breast cancer metastasis, many therapies using non-endocrine and endocrine drugs are targeted against signaling pathways which may have a therapeutic effect and delay the metastasis process.

2.7.2 HER2

HER 2 belongs to the receptor family which is involved in signaling in the cancer cell. In normal cell activation of this family of tyrosine kinase receptors activates a complex pathway of signals that regulate differentiation of normal cell, its motility, growth, and adhesion [72]. The HER2 proto-oncogene produces p185HER2, a 185 kDa glycoprotein that is transmembranal with innate tyrosine kinase activity. Activation of HER1, HER2, and HER3 receptors by ligand results in heterodimerization and activation of HER 2. It acts as a heterodimerization partner with other receptors. HER 2 receptors are more expressed in carcinoma of the breast and its upregulation leads to tumor progression and metastasis. This receptor is overexpressed in up to 40% of cancer of the breast.

Overexpression of the HER2 gene, which is present in around 30% of ovarian and breast carcinomas, activates the survival pathway PI3K, which promotes the proliferation of cells by inhibiting the process of apoptosis [73]. HER2 family members secrete basement membrane degradative enzymes, which facilitate interaction between the tumor cell and its escape [74]. In addition, the interaction of HER2 with the integrin recruits the P13 pathway which causes the release of molecules that recruits multiprotein complexes which causes tumor cell migration [75]. Several therapies have been designed against HER2 which involve the use of (1) Growth inhibitory antibodies (2) Tyrosine Kinase inhibitors (3) Active immunotherapy [76]. Herceptin is a HER2-specific antibody whose antitumor effectivity is based on its ability to cause degradation of HER2 by undergoing Cbl depended on endocytosis.

2.7.3 Progesterone Receptor

Progesterone is a hormone that is steroidal and involves the normal development of the Breast. Progesterone plays its role in the differentiation and proliferation of breast cells. The critical role of the steroidal hormone in the progression of breast cancer was first observed by George Beatson. PR not only acts as a transcription

regulator but also activates many signal transduction pathways which cause proliferation in the breast. PR extranuclear action also activates many protein kinases such as MAPK and c-Src leading to increase cell growth. PR targeted gene WNT1 causes metalloprotease production and cleavage of heparin-binding EGF molecule. PR-dependent activation of EGFR causes sustained cyclin D1 expression, MAPK activation, and an increase in cell survival and proliferation [77].

2.8 Molecular Docking

Over the past three decades, molecular docking has been used to design drugs with the aid of computers and to find various structures in molecular biology. Docking is preferred when conducting virtual screening on compounds in databases or libraries for analysis of their functions; findings can be easily labeled, and one of the docking's key roles is to provide analysis of how the ligand interacted with the protein, locking it for optimizing lead compounds for drug production [78]. Protein and ligand docking are a crucial field of molecular docking that has gained a lot of attention and praise because of their role in structure-based drug design. The most widely used algorithms in molecular docking are molecular dynamics, distance geometry process, and genetics algorithm, among others, and the most used software for molecular docking is Auto Dock vina, Auto Dock, CB Dock, and ICM, among others [79].

The docking result provides an interaction score, and the precision of the scoring function makes docking more accurate for predicting ligand pose and, as a result, determining the ligand's binding site. It then predicts the binding affinity, which leads to the discovery of a new lead drug in combination with the target protein [80].

Chapter 3

Materials And Methods

3.1 Selection of Disease

Breast cancer is the most common cancer in women, accounting for one-fourth of all cancers in women. It poses a major threat to public health. Extremely precise targeted treatments have been developed due to rapid breakthroughs in molecular biology and immunotherapy. The estrogen, progesterone, and HER2 receptor, play an essential part in normal breast development and is present in most breast cancer subtypes. Thus, for this purpose, they provide potential target sites for drug treatment [81]. The greatest current challenge for breast cancer treatment is to create a winning strategy that is successful against various subtypes of breast cancer while still having limited side effects. Natural-derived compounds are gaining science and academic interest because they are believed to have less toxic side effects than conventional therapies like chemotherapy.

3.2 Selection of Proteins

The structure of estrogen, progesterone, and HER2 receptors was taken from Protein Data Bank (PDB). The PDB archive is the only site where you can learn

about the three-dimensional structure of large biological molecules like proteins and nucleic acids [82].

3.3 Primary Sequence Retrieval

The primary sequence of target proteins (Estrogen, Progesterone, and HER2 receptors) were obtained in FASTA format from UniProt Database with accession number P03372, P06401, P04626 respectively (<https://www.uniprot.org>) [83].

3.4 Analysis of Physiochemical Properties

The function of proteins is primarily determined by their physiochemical properties. These Properties were predicted using ProtParam. Mol. weight, number of amino acids, isoelectric point, instability index, grand average of hydropathicity (GRAVY), number of negatively charged residues (Asp + Glu), number of positively charged residues (Arg + Lys), Aliphatic index, and amino acid and atomic composition were all investigated using the ProtParam tool of ExPASy [84].

3.5 Cleaning of the Downloaded Proteins

The extra constituents attached to the proteins must be extracted after downloading the protein structures, which was achieved using the open-source system Pymol [85].

3.6 Functional Domains of Target Proteins

InterPro, a database that can analyze a protein and provide information about the families, functional sites, and domains of the protein, was used to determine the

domains of the target protein [86]. The polypeptide binding sites and homodimer interfaces were obtained by inserting the receptor protein FASTA sequence.

3.7 Selection of Active Metabolic Ligands

The ligands that have already shown antiviral, antioxidant, and antimalarial properties were chosen. Terpenes, sterols, monoterpenes, phenolic compounds, flavonoids, sesquiterpenes, coumarins, and monoterpenes are among them [87].

3.8 Ligands Preparation

The 3-dimensional structures of all of the above ligands were downloaded from the PubChem database. The National Center for Biotechnology Information manages PubChem, a database that contains information about chemical compounds (NCBI). The data is correlated with chemical names and molecular formulas, 3D or basic structures, their isomers, and canonic structures [88]. The structures of the ligands which were obtained from PubChem were downloaded and then the ligands MM2 energy was minimized by using Chem3D ultra. In the end, the SDF format was selected to save the energy minimized structures of the ligands.

3.9 Molecular Docking

To interpret docking effects, the interaction of the ligand's active pockets with the protein was measured. Ionic bonding, hydrogen bonding, and hydrophobic bonding are the three types of interactions investigated. CB-dock (Cavity detection directed blind docking) was used to perform molecular docking between the protein and the ligand. CB Dock automatically locates docking positions. CB-Dock is a docking method for proteins and ligands that measures the bonding sites, their duration, and their center [89].

3.10 Visualization of Docking Results via PyMol

Over the past few years, the PyMol has emerged as an efficient molecular tool of visualization. The graphics and its ability to view 3D structures have been extraordinary [90].

PyMol provides a plugin that can access the results and make their visualization clearer so that the docking results can be easily studied. The pictures of the docking result can be captured also. The docking results were saved in PDB formats throughout the process and were saved in PDB formats after visualization in PyMol.

3.11 Analysis of Docked Complexes via LigPlot

Once the docked complexes were obtained with the lowest vina score, the analysis of docking complexes was the next step. The complexes were stored as a PDB file. The program LigPlot was used to perform this research.

The schematic diagrams of the protein and ligand interactions were created automatically for the given PDB file format. The hydrophobic and hydrogen bonding interactions were studied using LigPlot. LigPlot provides a 2D representation of the protein-ligand complex using this tool [91].

3.12 Ligands ADMET Properties

In general, a more effective drug discovery needs a lead that is more like the drug. The compounds were then tested for drug score, drug similarity, and toxicity.

The ADMET, or Absorption, Distribution, Metabolism, Excretion, and toxicity, of the human body, can be optimized using the pkCSM [92].

3.13 Lead Compounds Analysis and Toxicity Measurement

The most active inhibitors were discovered after a careful study of proteins and ligands interactions, docking ratings, and toxicity studies. Our lead compounds are the ones we've chosen. After applying the rule of 5, the lead compound is defined.

1. The log value of the drug-like compound must be limited to 5.
2. The molecular weight of the compound should be less than 500.
3. The hydrogen bond acceptor's number should be ten.
4. Hydrogen bond donors' number should be five.

Once any compound fits these rules, it is selected as a lead compound [92].

3.14 Selection of Standard Drugs against Breast Cancer

Standard drugs against breast cancer were selected based on docking values, physicochemical properties and ADMET properties [93].

3.15 Comparison of Standard Drugs and Lead Compounds

The comparison between standard anti-cancer drugs and the proposed lead compounds was done by comparing docking values, physicochemical properties, and ADMET properties.

3.16 Context Diagram

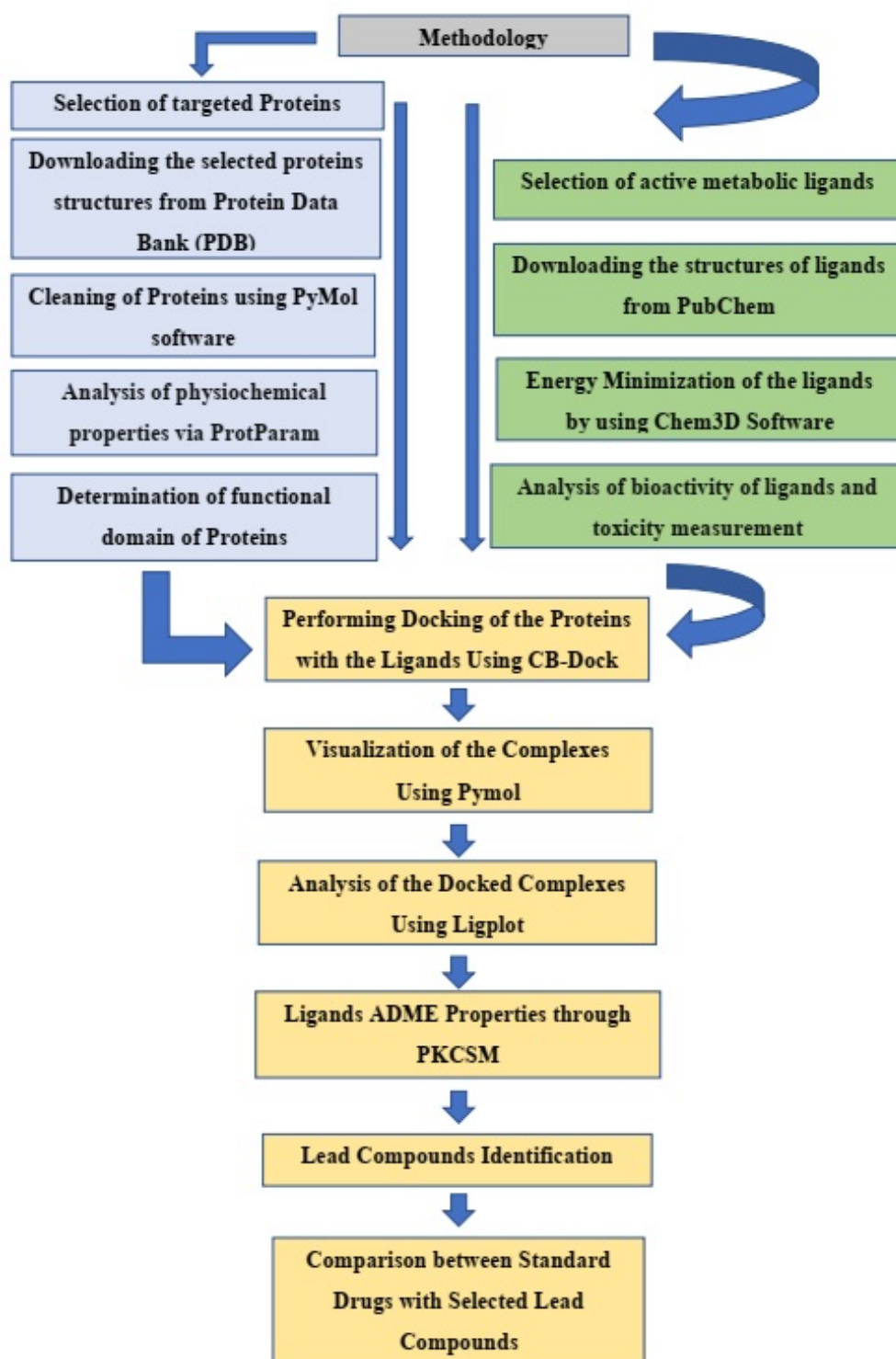


FIGURE 3.1: The methodology flow chart

Chapter 4

Results and Discussion

4.1 Structure Modeling

4.1.1 Primary Sequence Retrieval

The primary sequence of target proteins (ER, HER2, and PR) were taken in FASTA format from the Uniprot database (<http://www.uniprot.org>) under accession number P03372, P04626 and P06401 and residues length 595,1255, and 933 respectively.

```
>sp|P03372|ESR1_HUMAN Estrogen receptor OS=Homo sapiens OX=9606 GN=ESR1 PE=1 SV=2
MTMTLHTKASGMALLHQIQGNELEPLNRPQLKIPLERPLGEVYLDSSKPAVYNYPEGAAYEFNAAAAANA
QVYGQTGLPYGPGSEAAAFGSNGLGGFPPLNSVSPSPLMLLHPPPQLSPFLQPHGQVVPYYLENEPSGYTVR
EAGPPAFYRPNSDNRRQGGRERLASTNDKGSMAKESAKETRYCAVCNDYASGYHYGVWSCEGCKAFFK
RSIQGHNDYMCPATNQCTIDKNRRKSCQACRLRKCYEVGMMKGGIRKDRRGGRMLKHKRQRDDGEGRG
EVGSAGDMRAANLWPSPLMIKRSKKNLALSLTADQMVSALLDAEPPILYSEYDPTPFSEASMMGLLTNL
ADRELVHMINWAKRVPGFVDLTLHDQVHLLCAWLEILMIGLVWRSMEHPGKLLFAPNLLLDRNQGKCV
EGMVEIFDMLLATSSRFRMMNLQGEFVCLKSIILLNSGVYTFLSSTLKSLEEKDHIHRVLDKITDTLIHLMA
KAGLTLQQQHQLAQLLLILSHIRHMSNKGMEHLYSMKCKNVVPLYDILLEMLDAHRLHAPTSRGGASV
EETDQSHLATAGSTSSLSLQKYIITGEAEGFPATV
```

```
>sp|P04626|ERBB2_HUMAN Receptor tyrosine-protein kinase erbB-2 OS=Homo sapiens OX=9606GN=ERBB2
PE=1 SV=1
MELAALCRWGLLLALLPPGAASTQVCTGTDMLKRLPASPETHDMLRHL YQGCQVVQGNL
ELTYLPTNASLSFLQDIQEVQGYVLIHNVQRVPLQRLRIVRGTQLFEDNYALAVLDNGDPLNNTTPVTG
ASPGGLRELQLRSLTEILKGGVLIQRNPQLCYQDITLWKDIFHKNNQLALTLIDTNRSRACHPCSPMCKGSR
CWGESSEDCQSLTRTVCAAGGCARCKGPLPTDCHEQCAAGCTGPKHSDCLACLHFNHSGICELHCPALVT
YNTDTFESMPNPEGRYTFGASCVTACPYNYLSTDVGSCTLVCPHNLQEVTAEDGTQRCEKCSKPCARVCY
GLGMEHLREVRAVTSANIQEFAGCKKIFGSLAFLPESFDGDPASNTAPLQPEQLQVFETLEEITGYLYISAWP
```

DSLPLDSVFNQLQVIRGRILHNGAYSLLTQGLGISWGLRSLRELGSGLALIHHTLHCFVHTVPWDQLFRN
 PHQALLHTANRPEDECVEGLACHQLCARGHCWGPPTQCVCNCSQFLRGQECVEECRVLQGLPREYVNA
 RHCLPCHPECQPNQSVTCFGPEADQCVACAHYKDPFVCVARCPGSKVLPDL SYMPIWKFPDEEGACQPCPI
 NCTHSCVDLDDKGCPEQRASPLTSIISAVVVGILLVVVLGVVFGILIKRRQKIRKYTMRRLLQETELVEPLT
 PSGAMPNQAQMRILKETELRKVKVLGSGAFGTVYKGIWIPDGENVKIPVAIKVIRENTSPKANKEILDEAY
 VMAGVGSPPYVSRLLGICLTSTVQLVTQLMPYGCLLDHVRENRGRLGSQDLLNWCMIQAKGMSYLEDVRL
 VHRDLAARNVVKSPNHVKITDFGLARLLDIDE TEYHADGGKVPKWMALESILRRRFTHQSDVWSYGVV
 VWELMTFGAKPYDGPAREIPDLEKGERLPQPPICTIDVYMIMVKCWMIDSECRPRFREL VSEFSRMARDP
 QRFVVIQNE DLGPASPLDSTFYRSLLEDDDMGDLVDAEEYLVPQQGFFCPDPAPGAGGMVHHRHRSSTRS
 GGGDLTLGLEPSEEEAPRSPLAPSEGAGSDVFDGDLGMGAAGKGLQSLPHTDPSLQRYSEDPTVPLPSETDG
 YVAPLTCSPQPEYVNPDPVRQPPSPREGPLPAARPAGATLERPKTLSPGKNGVVKDVFAFGGAVENPEYL
 TPQGGAAPQPHPPAFSPAFDNLYYWDQDPPERGAPPSTFKGTPTAENPEYLGLDVPV

>sp|P06401|PRGR_HUMAN Progesterone receptor OS=Homo sapiens OX=9606 GN=PGR PE=1 SV=4
 MTELKAKGPRAPHVAGGPPSPEVGSPLLCPRAAGFPFGSQTSDTLPEVSAIPISLDGLLFFRPCQGGQDPSDEK
 TQDQQLSDVEGAYSRAEATRGAGGSSSSPPEKDSGLLDSVLDTLLAPSGPGQSQPSPPACEVTSSWCLFGP
 ELPEDPPAAPATQRVLSPLMSRSGCKVGDSSGTA AAHKVLPRLSPARQLLLPASESPHWSGAPVKPSPQA
 AAVEVEEEDGSESEESAGPLLK GKPRALGGAAGGAAAVPPGAAAGGVALVPKEDSRFSAPRVALVEQ
 DAPMAPGRSPLATTVMDFIHVPILPLNHALLAARTRQLLEDES YDGGAGAASAFAPPRSSPCASSTPVAVG
 DFPDCA YPPDAEPKDDAYPLYSDFPQPPALKIKEEEEGAEASARSPRSYL VAGANPAAFPDPFLGPPPLPPRA
 TPSRPGEA AVTAAPASASVSSASSSGSTLECILYKAEAGAPPQQGPFAPPCKAPGASGCLLPRDGLPSTSASA
 AAAGAAPALYPALGLNGLPQLGYQA AVLKEGLPQVYPPYLNLYLRPDSEASQSPQYSFESLPQKICLICGDE
 ASGCHYGVLTCGSCKVFFKRAMEGQHNYLCAGRND CIVDKIRRNKNCACRLRKCQAGMVLGGRKFKKF
 NKVRVVRALDAVALPQVGVPNESQALSQRF TSPGQDIQLIPPLINLLMSIEPDVYAGHDNTKPDTS SLL
 TSLNQLGERQLLSVVKWSKSLPGFRNLHIDDQITLIQYSWMSLMVFLGLGWRSYKHVSGQMLYFAPDLILNE
 QRMKESSFYSLCLTMWQIQEFVKLQVSQEEFLCMKVLLLNNTIPLEGLRSQTQFEEMRSSYIRELIKAIGLR
 QKGVVSSSRFYQLTKLLDNLHDLVKQLHL YCLNTFIQSRALSVEFPEMMSEVIAAQLPKILAGMVKPLLF
 HKK

Estrogen receptor, HER 2, and progesterone receptor were selected as the target proteins as they are considered breast cancer progression markers. Estrogen receptor has been associated with enhanced breast cancer risk by either acting as a promoter or an initiator by inducing genetic changes [65]. HER2 is more expressed in breast carcinoma and its upregulation results in tumor metastasis and progression [72]. Progesterone receptors play a role in the differentiation and proliferation of breast carcinoma [77].

4.1.2 Physiochemical Characterization of ER, HER2, PR

ProtParam is a tool of ExPasy which is used online for calculating various physical and chemical parameters for a protein recorded in Swiss-prot or TrEMBL, as well as a user-entered protein sequence. The molecular weight, amino acid composition, theoretical pI, atomic composition, extinction coefficient, estimated half-life, instability index, aliphatic index, and grand average of hydropathicity are among the calculated characteristics (GRAVY) [84].

The calculated pI greater than 7 represents the basic nature of the protein while less than 7 shows the acidic nature of the protein. The extinction coefficient represents light absorption. Instability index if less than 40 shows the stability of the protein while greater than 40 indicates the instability of protein [94]. The physicochemical properties of ER, HER2, and PR are shown in Tables 4.1, 4.2, and 4.3 respectively.

The aliphatic index represents the aliphatic content of a protein. The high value of the aliphatic index indicates the thermostability of the protein. Molecular weight includes both positive and negative charged residues of the protein. At 280nm the ranging extinction coefficient of 73980, 67965, 20105, and 112270 indicates Tyr and Trp high concentration [95]. Low GRAVY shows better interaction with water molecules. All these parameters which are selected for this research work are taken according to previous research work.

Results from Table 4.1, reveal that the protein estrogen receptor has a molecular weight of 66216.00 which is the collective weight of both negative and positive amino acid residues and pI is 8.30 which indicates that protein is basic. The values of light absorption in term of extinction coefficient is 62520 and 61770. The aliphatic index shows that protein is thermostable. Low GRAVY value showed that estrogen receptors show better interaction with water molecules.

TABLE 4.1: Physiochemical Properties of Human Estrogen receptor.

MW	PI	NR	PR	
66216.00	8.30	60	64	
Ext. Co1	Ext. Co2	Instability index	Aliphatic index	GRAVY
62520	61770	45.88	80.39	-0.354

Results from Table 4.2, reveal that the protein HER 2 has a molecular weight of 137910.50 which is the collective weight of both negative and positive amino acid

residues and pI is 5.58 which indicates that protein is acidic. The values of light absorption in term of extinction coefficient is 138275 and 134650. The aliphatic index shows that protein is thermostable. The low GRAVY value showed that HER 2 show better interaction with water molecules.

TABLE 4.2: Physiochemical Properties of HER 2.

MW	PI	NR	PR		
137910.50	5.58	142	110		
Ext. Co1	Ext. Co2	Instability index	Aliphatic index	GRAVY	
138275	134650	56.13	82.35	-0.247	

Results from Table 4.3 reveal that the progesterone receptor has a molecular weight of 98981.14 which is the collective weight of both negative and positive amino acid residues and pI is 6.09 which indicates that protein is acidic. The values of light absorption in term of extinction coefficient is 68770 and 67270. The aliphatic index shows that protein is thermostable. Low GRAVY value showed that progesterone receptor shows better interaction with water molecules.

TABLE 4.3: Physiochemical Properties of progesterone receptor.

MW	PI	NR	PR		
98981.14	6.09	90	83		
Ext. Co1	Ext. Co2	Instability index	Aliphatic index	GRAVY	
68770	67270	64.44	81.76	-0.177	

MW stands for molecular weight, pl for theoretical isoelectric point (pH at which protein is neutral, without any charge), NR for the total number of negatively charged residues (Asp + Glu), PR for the total number of positively charged residues (Arg + Lys), Ext.Co1 for extinction coefficients when assuming all pairs

of Cys residues form cystines, Ext.Co2 for extinction coefficients when assuming all Cys residues are reduced, and GRAVY for a grand average of hydrophobicity.

4.1.3 3D Structure Predictions of Proteins

3D Structures of targeted proteins were downloaded from RCSB PDB in PDB format. Protein Data Bank is a three-dimensional database of complex molecules of living organisms, such as proteins and nucleic acids. The 3D Structures of estrogen receptor, HER2, and progesterone receptor were obtained from PDB named as 3dt3,504g and 1e3k respectively and under accession number 10.2210/pdb3DT3/pdb, 10.2210/pdb5O4G/pdb and 10.2210/pdb1E3K/pdb respectively (Figure 4.1-4.3). The ER LBD structure obtained is already attached with ligand GW368 as shown in Figure 4.1 which needs to be removed for further processing. ER LBD is arranged in the antiparallel alpha-helical sandwich fold, having 11 helices namely H1-H12 arranged in a 3-layered sandwich structure. The helices H4, H5, H6, H8, H9 are flanked by H1, H3 on one side and by H7, H10, H11 on the other side [66].



FIGURE 4.1: Human estrogen receptor alpha LBD with GW368.

HER 2 structure obtained is already in complex with Herceptin Fab as shown in Figure 4.2. HER 2 ECD contains a small percentage of alpha-helical structure with a mixture of sheets and turns in protein structure [73].



FIGURE 4.2: HER2 in complex with Fab MF3958.

The structure of PR LBD is obtained in complex with ligand metribolone as shown in Figure 4.3. PR LBD has three layered globular structures consisting of 12 alpha helices and 1 beta-turn. Helix 12 is found in different orientations based on the nature of ligand-bound. If the bound ligand is agonist, helix 12 act as a lid and closes the LBD whereas when bound to antagonist helix 12 open the entrance of LBD [77].

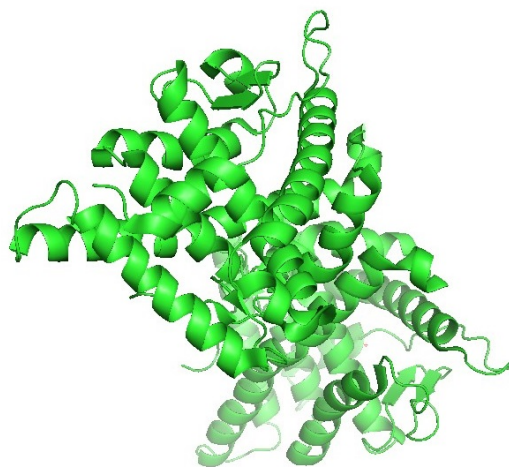


FIGURE 4.3: Human progesterone receptor LBD in complex with the ligand metribolone

4.1.4 Functional Domain Identification of Proteins

The functional domain of a protein is the region of the protein that interacts with other molecules. Proteins can have multiple functional domains, each of which performs a separate function. The N-terminal domain, DNA binding domain,

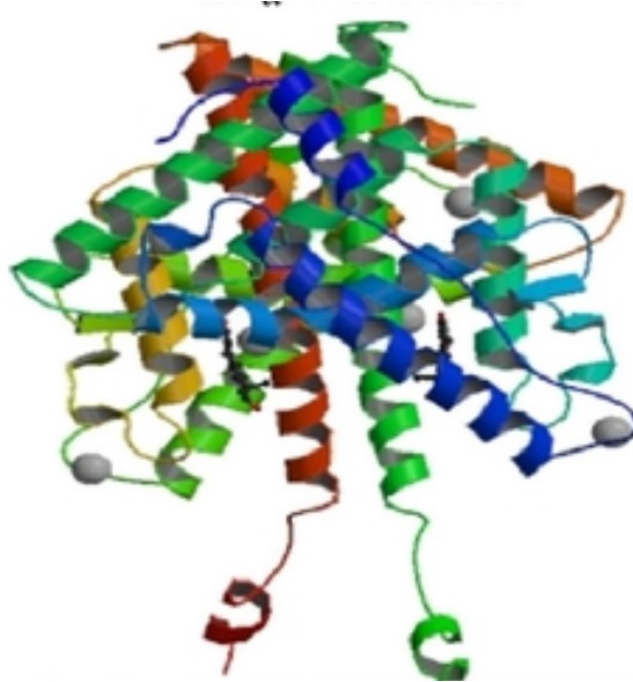


FIGURE 4.4A: Functional domain of ER [96].

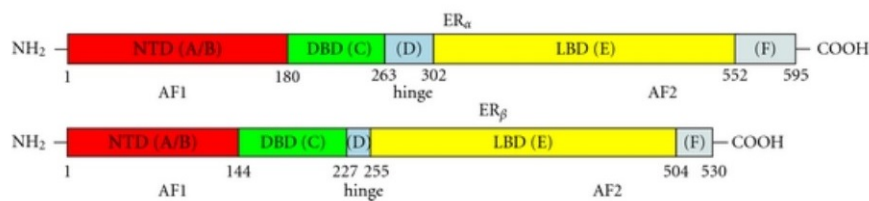


FIGURE 4.4B: Functional domains of ER with residue length [97].

and ligand-binding domain of the estrogen receptor have residue lengths of 1-180, 180-263, and 302-552, respectively.

NTD and LBD both have two activation domains (Figure 4.4). Different domains are indicated in different colors in the diagram: NTD stands for an amino-terminal domain is highlighted in red; DBD stands for DNA binding domain in green; LBD stands for a ligand-binding domain in yellow color [96].

HER 2 has an external ligand-binding domain, a transmembrane domain, a juxtamembrane domain, and an intracellular region that can interact with a variety of signaling molecules and can be ligand-dependent or ligand-independent (Figure 4.5). The ECD further consists of 4 subdomains, subdomain 1 on binding to ligand binds to subdomain 3 which causes conformational changes in subdomain

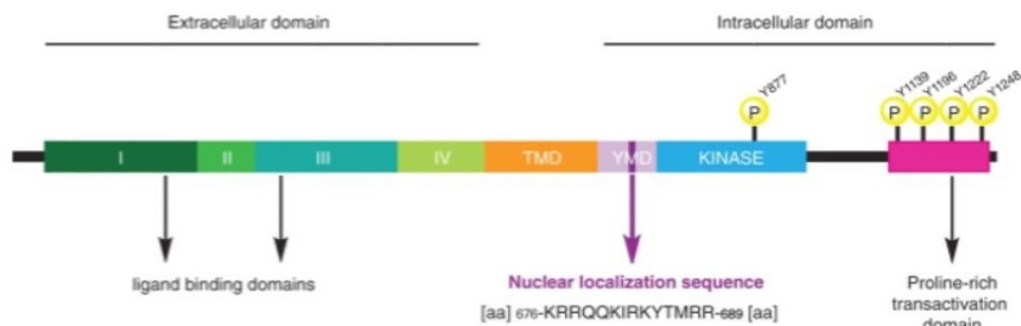


FIGURE 4.5A: Functional domains of HER2 [98].

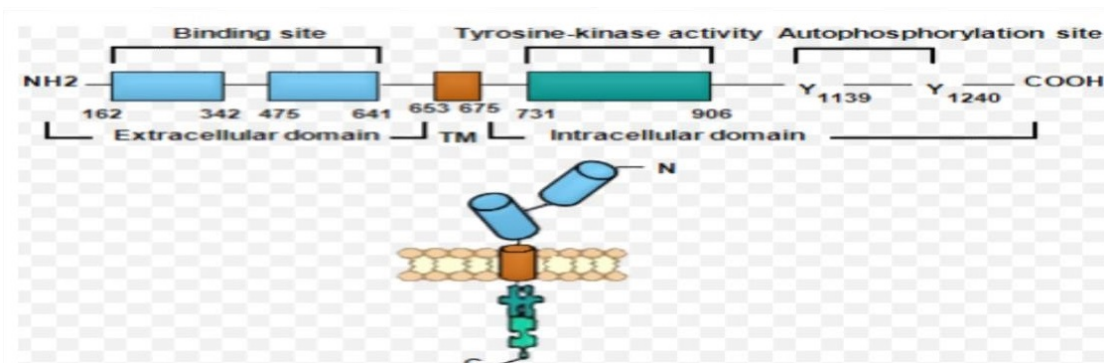


FIGURE 4.5B: Functional domains of HER2 with residue length [99].

2 leading to receptor kinase activation and dimerization. Domains 2 and 4 are further involved in disulfide bond formation [98].

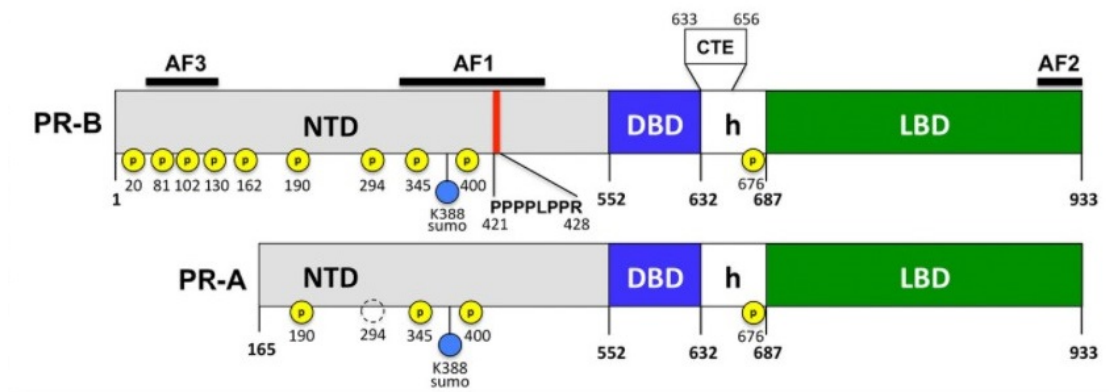


FIGURE 4.6: Functional domains of PR with residue length [99].

PR has a variable N-terminal domain, a highly conserved DNA binding domain, and a moderately conserved ligand-binding domain (LBD), each with residue lengths of 1-552, 552-632, and 687-933 respectively as shown in Figure 4.6 and Table 4.4 [99].

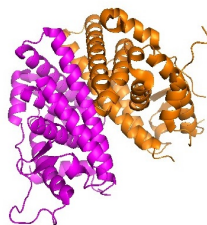

TABLE 4.4: Functional domain identification of ER, HER 2, and PR.

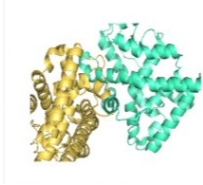
Sr. No.	Name	Domains	Start	End
1	ER	N -terminal, DNA binding domain, ligand-binding domain. Extracellular ligand- binding domain,	1,180,302	180,263,522
2	HER 2	Transmembrane domain, juxtamembrane domain, an intracellular domain N-terminal domain,	162,653,731	641,675,906
3	PR	DNA binding domain, ligand-binding domain	1,552,687	552,632,933

4.1.5 Templates Selection

Protein data bank contains a large amount of protein-ligand complex, especially for the protein target [82]. The 3 D structures of the selected templates were taken from the protein data bank (PDB) and listed in Table 4.5.

TABLE 4.5: Selected PDB Templates Structures

Sr. No.	Templates	Resolution	PDB ID	Structure
1	Human Estrogen receptor alpha LBD with GW368.	2.40	3DT3	
2	HER2 in complex with Fab MF3958.	3.00 Å	5O4G	

	Human progesterone receptor Ligand			
3	Binding Domain in complex with the ligand metribolone (R1881).	2.80 Å	1E3K	

4.1.6 Structure of Proteins Refined for Docking

The extra constituents attached to the proteins must be extracted after downloading the protein structures, which was achieved using Pymol [85]. The structures of proteins downloaded were already bound to some other ligands which need to be removed for further processing. The selected 3D structures were refined for docking and are shown in Figures 4.7, 4.8 & 4.9 respectively.

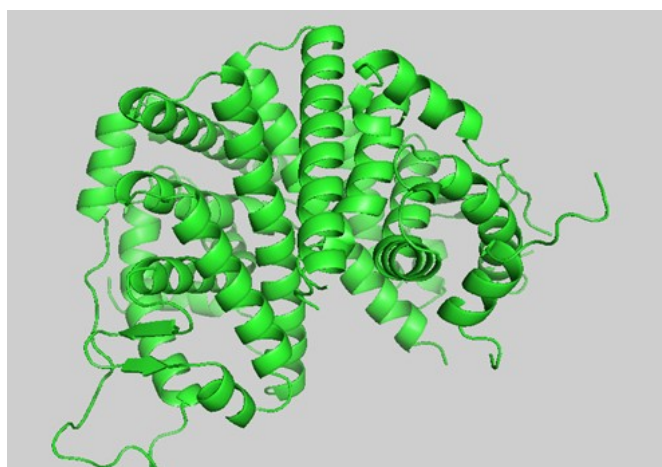


FIGURE 4.7: Refined 3D Structure of estrogen receptor.

4.2 Ligands Selection

The selection of ligands is based on the best resolution of the structure, the chemical class of the co-crystal ligand bound to the protein structure, and the best binding affinity. Conformational selection is a process in which ligand selectively

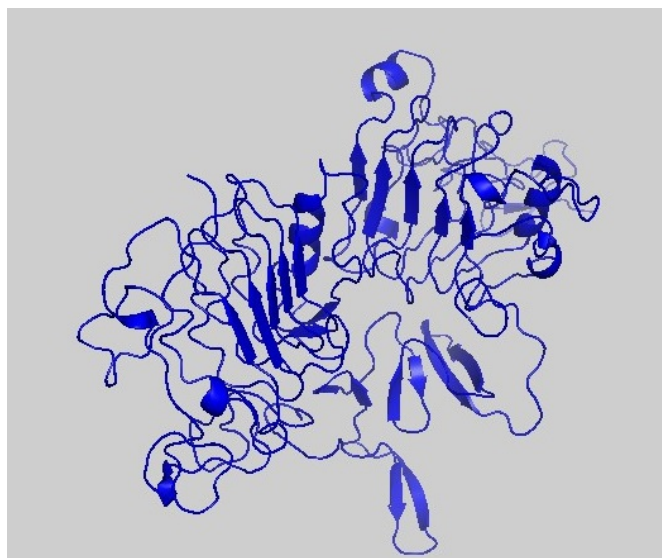


FIGURE 4.8: Refined 3D Structure of HER 2.

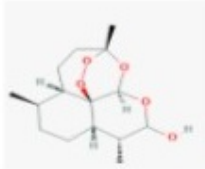
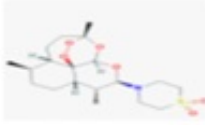
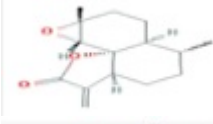

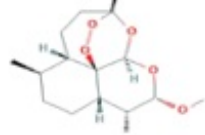

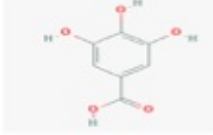
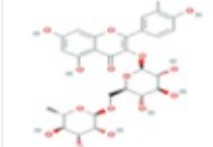


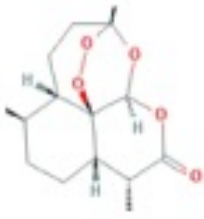
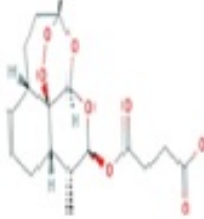
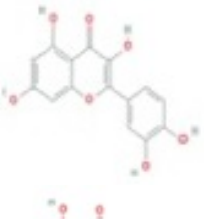

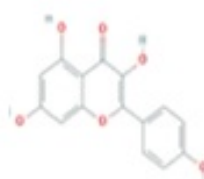
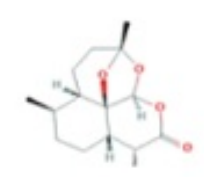
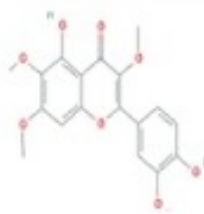
FIGURE 4.9: Refined 3D Structure of progesterone receptor.

binds to one of these conformers, strengthening it and increasing its population for the total population of the protein is ultimately resulting in the final observed complex. PubChem, the world's biggest freely accessible chemical information library, was used to find ligands (compounds of the chosen plant). Their 3-D structures were downloaded in SDF format from PubChem. Selected ligands were representing all the classes of compounds like phenols, terpenoids, essential oils, and steroids, etc. The 3 D structures and information of selected ligands that were Arteannuin B, Artemether, Artemisinin, Artesunate, Artenimol, Artemisone, Chrysosplenol D, Kaempferol, Luteolin, Isoquercetin, Quercetin, Rutin, Gallic acid, Dihydroartemisinin, and Caffeic acid were downloaded from PubChem [100].

After selection of ligands, energy minimization of ligands was done which was carried out by chem pro software (chem 3D v 12.0.2). This was a mandatory step in the preparation of ligands for docking because unstable ligands will show unreliable vina scores in docking results [101]. Bioactive antioxidant compounds of *Artemisia carvifolia* were selected as ligands for the present study and are listed in Table 4.6.

TABLE 4.6: Selected Ligands with Structural Information.

Sr. No.	Name	Molecular Formula	Molecular Weight g/mol	Structure
1	Artemimol	$C_{15}H_{24}O_5$	284.35	
2	Artemisone	$C_{19}H_{31}NO_6S$	401.5	
3	Arteannuin B	$C_{15}H_{20}O_3$	248.32	
4	Caffeic acid	$C_9H_8O_4$	180.16	
5	Artemether	$C_{16}H_{26}O_5$	298.3	
6	Isoquercetin	$C_{21}H_{20}O_{12}$	464.4	
7	Gallic acid	$C_7H_6O_5$	170.12	
8	Rutin	$C_{27}H_{30}O_{16}$	610.5	

9	Artemisinin	$C_{15}H_{22}O_5$	282.33	
10	Artesunate	$C_{19}H_{28}O_8$	384.4	
11	Quercetin	$C_{15}H_{10}O_7$	302.23	
12	Luteolin	$C_{15}H_{10}O_6$	286.24	
13	Kaempferol	$C_{15}H_{10}O_6$	286.24	
14	Dihydroartemisinin	$C_{15}H_{22}O_4$	266.33	
15	Chrysoptanol D	$C_{18}H_{16}O_8$	360.3	

4.3 Applicability of Lipinski's Rule

Drug-like and non-drug-like substances are distinguished by using Lipinski's rule of five and the ADMET characteristics test [92]. The original rules of five deal with four physicochemical factors connected with orally active chemicals (MWT 500, log

P 5, H-bond donors 5, H-bond acceptors 10) [102]. A compound is considered to have drug-likeness if it is complying with three or more of the RO5. If a compound violates more than two of these rules, it is assumed to be poorly absorbed [103]. Table 4.7 showed the applicability of Lipinski's rule of five on selected ligands. All ligands follow these rules. There is one ligand that complying with only 1 rule that is Rutin. Rutin has M.W 610 Dalton, 16 H-bond acceptors, and 10 H-bond donors. Rutin is not considered to have a drug-likeness.

TABLE 4.7: Applicability of Lipinski Rule on Ligands.

Sr. No.	Ligand	logP Value	Molecular Weight	H-Bond Acceptor	H-Bond Donor
1	Artemisinin	2.3949	282.336 g/-mol	5	0
2	Artemether	2.8408	298.379 g/-mol	5	0
3	Artesunate	2.6024	384.425 g/-mol	7	1
4	Dihydroartemisinin	2.4633	266.337 g/-mol	4	0
5	Arteannuin B	2.4518	248.322 g/-mol	3	0
6	Artenimol	2.1867	284.352 g/-mol	5	1
7	Artemisone	1.9248	401.5 g/-mol	7	0
8	Quercetin	1.988	302.238 g/-mol	7	5
9	Isoquercetin	-0.5389	464.379 g/-mol	12	8
10	Rutin	-1.6871	610.521 g/-mol	16	10
11	Gallic acid	0.5016	170.12 g/-mol	4	4
12	Kaempferol	2.2824	152.237 g/-mol	6	4
13	Chrysofenol D	2.6026	360.318 g/-mol	8	3
14	Luteolin	2.2824	286.239 g/-mol	6	4
15	Caffeic acid	1.1956	180.159 g/-mol	3	3

4.3.1 Toxicity Prediction

PkCSM is an online tool used to discover the ADMET properties of bioactive compounds and drugs. By using this tool, we will determine the toxicity of selected

ligands [92].

AMES toxicity test is used to test the mutagenic potential of the compound by using bacteria. If it shows a positive response, then the ligand is mutagenic which can also act as a carcinogen.

The maximum tolerated dose (MRTD) provides a measure of toxic chemical limits on individuals. This will help in directing the first recommended dose of the treatment regimen in phase 1 clinical trials. MRTD is expressed in the form of logarithms ($\log \text{ mg/kg/day}$). In a given compound MRTD less than or equal to $0.477 \log (\text{mg} / \text{kg} / \text{day})$ is considered lower, whereas MRTD greater than $0.477 \log (\text{mg} / \text{kg} / \text{day})$ is considered higher [104].

The hERG I & II inhibitors model determines the potential of any compound to cause the inhibition of potassium channels induced by the h ERG (human ether-a-go-go gene). An inhibitor of these channels could probably lead to chronic QT syndrome and on a long-term basis the person could develop fatal ventricular arrhythmia. Many pharmaceuticals have been withdrawn from the market due to the blockage of hERG channels.

The LD₅₀ value of a chemical is the amount that kills 50% of experimental animals (mice). It predicts the toxicity of a probable compound whereas LOAEL aims to identify the lowest dosage of a compound with a significant adverse effect. Exposure to low to moderate chemical doses for a long time is very important in medicine and is expressed in a $\log (\text{mg} / \text{kg-bw} / \text{day})$ [104].

Hepatotoxicity reveals a drug that can cause liver damage and is a major drug development safety concern. Skin sensitivity is a potential adverse effect of skincare & applied products. *T. pyriformis* is a protozoan bacteria, whose toxin is often used as a toxic endpoint (IGC₅₀) and inhibits 50% growth. In $\log \text{ ug} / \text{L}$, pIGC₅₀ (negative concentration logarithm required to halt 50% growth) anticipated value $> -0.5 \log \text{ ug} / \text{L}$ is hazardous.

The lethal concentrations (LC₅₀) show the number of molecules required to kill 50 percent of Flathead Minnows (small bait fishes). LC₅₀ values below 0.5 m M

(log LC₅₀ below 0.3) are considered significant acute toxicity in Minnow poisoning [104]. Toxicity predicted values of selected ligands are listed in Tables 4.8 to 4.22.

4.3.1.1 Arteannuin-B

Arteannuin B is non-carcinogenic, and it shows low Max. tolerated dose. It is a supporter of potassium channels and is non-hepatotoxic. The compound is considered toxic against *T. pyriformis* (might not be harmful to human cells) but nontoxic to Minnow. Toxicity predicted values of arteannuin B are shown in Table 4.8. The toxicity properties of arteannuin B were previously reported by Zarina Khurshid in 2021 [105].

TABLE 4.8: The Toxicity Values of Arteannuin B.

Sr. No	Model Name	Predicted Values
1	AMES toxicity	No
2	Max.tolerated dose (human)	0.195 mg/Kg
3	hERG I inhibitor	No
4	hERG II inhibitor	No
5	Oral rat acute toxicity	2.052 mol/Kg
6	Oral rat chronic toxicity	1.589 mg/Kg
7	Hepatotoxicity	No
8	Skin sensitization	No
9	<i>T. pyriformis</i> toxicity	0.45 log ug/L
10	Minnow toxicity	1.53 log mM

4.3.1.2 Artemether

Artemether is non-carcinogenic and it shows low Max. tolerated dose. It is a supporter of potassium channels and is non-hepatotoxic. The compound is considered toxic against *T. pyriformis* (might not be harmful to human cells) but nontoxic to Minnow. Toxicity predicted values of artemether are shown in Table 4.9. Some

models of toxicity of artemether were previously reported by Tabish Qidwai in 2017 [106].

TABLE 4.9: The Toxicity Values of Artemether.

Sr. No	Model Name	Predicted Values
1	AMES toxicity	No
2	Max.tolerated dose (human)	0.074 mg/Kg
3	hERG I inhibitor	No
4	hERG II inhibitor	No
5	Oral rat acute toxicity	2.429 mol/Kg
6	Oral rat chronic toxicity	1.043 mg/Kg
7	Hepatotoxicity	No
8	Skin sensitization	No
9	<i>T. pyriformis</i> toxicity	0.304 log ug/L
10	Minnow toxicity	0.587 log mM

4.3.1.3 Artemisinin

Artemisinin is carcinogenic and it shows low Max. tolerated dose. It is a supporter of potassium channels and is non-hepatotoxic. The compound is considered toxic against *T. pyriformis* (might not be harmful to human cells) but nontoxic to Minnow. Toxicity predicted values of artemisinin are shown in Table 4.10. Some models of toxicity of artemisinin were previously reported by Tabish Qidwai in 2017 [106].

TABLE 4.10: Toxicity prediction of Artemisinin.

Sr. No	Model Name	Predicted Values
1	AMES toxicity	Yes
2	Max.tolerated dose(human)	0.065 mg/Kg
3	hERG I inhibitor	No
4	hERG II inhibitor	No

5	Oral rat acute toxicity	2.459 mol/Kg
6	Oral rat chronic toxicity	1 mg/Kg
7	Hepatotoxicity	No
8	Skin sensitization	No
9	<i>T. pyriformis</i> toxicity	0.322 log ug/L
10	Minnow toxicity	1.406 log mM

4.3.1.4 Artesunate

Artesunate is non-carcinogenic and it shows low Max. tolerated dose. It is a supporter of potassium channels and is non-hepatotoxic. The compound is considered toxic against *T. pyriformis* (might not be harmful to human cells) but nontoxic to Minnow. Toxicity predicted values of artesunate are shown in Table 4.11. The toxicity properties of artesunate were previously reported by Zarina Khurshid in 2021 [105].

TABLE 4.11: The Toxicity Values of Artesunate.

Sr. No	Model Name	Predicted Values
1	AMES toxicity	No
2	Max.tolerated dose (human)	0.256 mg/Kg
3	hERG I inhibitor	No
4	hERG II inhibitor	No
5	Oral rat acute toxicity	3.112 mol/Kg
6	Oral rat chronic toxicity	1.549 mg/Kg
7	Hepatotoxicity	No
8	Skin sensitization	No
9	<i>T. pyriformis</i> toxicity	0.285 log ug/L
10	Minnow toxicity	1.499 log mM

4.3.1.5 Chrysosplenol D

Chrysosplenol D is non-carcinogenic, and it shows low Max. tolerated dose. It is a supporter of potassium channels and is non-hepatotoxic. The compound is considered toxic against *T. pyriformis* (might not be harmful to human cells) but nontoxic to Minnow. Toxicity predicted values of chrysosplenol D are shown below in Table 4.12. The toxicity properties of chrysosplenol D were previously reported by Zarina Khurshid in 2021 [105].

TABLE 4.12: The Toxicity Values of Chrysosplenol D.

Sr. No	Model Name	Predicted Values
1	AMES toxicity	No
2	Max.tolerated dose (human)	0.284 mg/Kg
3	hERG I inhibitor	No
4	hERG II inhibitor	No
5	Oral rat acute toxicity	2.345 mol/Kg
6	Oral rat chronic toxicity	2.658 mg/Kg
7	Hepatotoxicity	No
8	Skin sensitization	No
9	<i>T. pyriformis</i> toxicity	0.323 log ug/L
10	Minnow toxicity	2.254 log mM

4.3.1.6 Dihydroartemisinin

Dihydroartemisinin is non-carcinogenic, and it shows low Max. tolerated dose. It is a supporter of potassium channels and is non-hepatotoxic. The compound is considered toxic against *T. pyriformis* (might not be harmful to human cells) but nontoxic to Minnow. Toxicity predicted values of dihydroartemisinin are shown in Table 4.13. Some models of toxicity of dihydroartemisinin were previously reported by Tabish Qidwai in (2017) [106].

TABLE 4.13: The Toxicity Values of Dihydroartemisinin

Sr. No	Model Name	Predicted Values
1	AMES toxicity	No
2	Max.tolerated dose (human)	0.174 mg/Kg
3	hERG I inhibitor	No
4	hERG II inhibitor	No
5	Oral rat acute toxicity	2.161 mol/Kg
6	Oral rat chronic toxicity	1.506 mg/Kg
7	Hepatotoxicity	No
8	Skin sensitization	No
9	<i>T. pyriformis</i> toxicity	0.363 log ug/L
10	Minnow toxicity	1.538 log mM

4.3.1.7 Kaempferol

Kaempferol is non-carcinogenic and has a high maximum tolerated dose. It is a supporter of potassium channels and is non-hepatotoxic. The compound is considered toxic against *T. pyriformis* (might not be harmful to human cells) but nontoxic to Minnow. Toxicity predicted values of kaempferol are shown in Table 4.14. The toxicity properties of kaempferol were previously reported by Al-Nor in 2019 [107].

TABLE 4.14: The Toxicity Values of Kaempferol.

Sr. No	Model Name	Predicted Values
1	AMES toxicity	No
2	Max.tolerated dose (human)	0.531 mg/Kg
3	hERG I inhibitor	No
4	hERG II inhibitor	No
5	Oral rat acute toxicity	2.449 mol/Kg
6	Oral rat chronic toxicity	2.505 mg/Kg

7	Hepatotoxicity	No
8	Skin sensitization	No
9	<i>T. pyriformis</i> toxicity	0.312 log ug/L
10	Minnow toxicity	2.885 log mM

4.3.1.8 Luteolin

Luteolin is non-carcinogenic and shows a high maximum tolerated dose. It is a supporter of potassium channels and is non-hepatotoxic. The compound is considered toxic against *T. pyriformis* (might not be harmful to human cells) but nontoxic to Minnow. Toxicity predicted values of luteolin are shown in Table 4.15. The toxicity properties of luteolin were previously reported by Gangarapur Kiran and his colleagues in 2020.

Luteolin is non-carcinogenic and shows a high maximum tolerated dose. The compound is considered toxic against *T. pyriformis* (might not be harmful to human cells) but nontoxic to Minnow. The toxicity properties of luteolin were previously reported by Gangarapur Kiran and his colleagues in 2020 [108].

TABLE 4.15: The Toxicity Values of Luteolin

Sr. No	Model Name	Predicted values
1	AMES toxicity	No
2	Max.tolerated dose (human)	0.499 mg/Kg
3	hERG I inhibitor	No
4	hERG II inhibitor	No
5	Oral rat acute toxicity	2.455 mol/Kg
6	Oral rat chronic toxicity	2.409 mg/Kg
7	Hepatotoxicity	No
8	Skin sensitization	No
9	<i>T. pyriformis</i> toxicity	0.326 log ug/L
10	Minnow toxicity	3.169 log mM

4.3.1.9 Quercetin

This compound is non-carcinogenic and shows a high maximum tolerated dose. Maximum recommended tolerated dose helps in deciding the maximum recommended starting dose in phase I clinical trials. It is a supporter of potassium channels and is non-hepatotoxic.

The compound is considered toxic against *T. pyriformis* (might not be harmful to human cells) but nontoxic to Minnow. Toxicity predicted values of quercetin are shown in Table 4.16. The toxicity properties of quercetin were previously reported by Al-Nor in 2019 [107].

TABLE 4.16: The Toxicity Values of Quercetin.

Sr. No	Model Name	Predicted values
1	AMES toxicity	No
2	Max.tolerated dose (human)	0.499 mg/Kg
3	hERG I inhibitor	No
4	hERG II inhibitor	No
5	Oral rat acute toxicity	2.471 mol/Kg
6	Oral rat chronic toxicity	2.612 mg/Kg
7	Hepatotoxicity	No
8	Skin sensitization	No
9	<i>T. pyriformis</i> toxicity	0.288 log ug/L
10	Minnow toxicity	3.721 log mM

4.3.1.10 Rutin

Rutin is non-carcinogenic and shows a high maximum tolerated dose. It is non-hepatotoxic. Rutin predicted value shows it as an h ERG II inhibitor which predicts its possible withdrawal from to be an effective drug. The compound is considered toxic against *T. pyriformis* (might not be harmful to human cells) but nontoxic to Minnow. Toxicity predicted values of rutin are shown in Table 4.17.

The toxicity properties of rutin were previously reported by Zarina Khurshid in 2021 [105].

TABLE 4.17: The Toxicity Values of Rutin

Sr. No	Model Name	Predicted values
1	AMES toxicity	No
2	Max.tolerated dose (human)	0.452 mg/Kg
3	hERG I inhibitor	No
4	hERG II inhibitor	Yes
5	Oral rat acute toxicity	2.491 mol/Kg
6	Oral rat chronic toxicity	3.673 mg/Kg
7	Hepatotoxicity	No
8	Skin sensitization	No
9	<i>T. pyriformis</i> toxicity	0.285 log ug/L
10	Minnow toxicity	7.677 log mM

4.3.1.11 Isoquercetin

Isoquercetin is non-carcinogenic and shows a high maximum tolerated dose. It is non-hepatotoxic. Isoquercetin predicted value shows it as an h ERG II inhibitor which predicts its possible withdrawal from to be an effective drug. The compound is considered toxic against *T. pyriformis* (might not be harmful to human cells) but nontoxic to Minnow. Toxicity predicted values of isoquercetin are shown in Table 4.18. The toxicity properties of isoquercetin were previously reported by Maghfiroh Gesty Maharani and his colleagues in 2020 [109].

TABLE 4.18: The Toxicity Values of Isoquercetin.

Sr. No	Model Name	Predicted values
1	AMES toxicity	No
2	Max.tolerated dose (human)	0.569 mg/Kg
3	hERG I inhibitor	No

4	hERG II inhibitor	Yes
5	Oral rat acute toxicity	2.541 mol/Kg
6	Oral rat chronic toxicity	4.417 mg/Kg
7	Hepatotoxicity	No
8	Skin sensitization	No
9	<i>T. pyriformis</i> toxicity	0.285 log ug/L
10	Minnow toxicity	8.061 log mM

4.3.1.12 Artemimol

Artemimol is non-carcinogenic and shows a low maximum tolerated dose. It is a supporter of potassium channels and is non-hepatotoxic.

The compound is considered toxic against *T. pyriformis* (might not be harmful to human cells) but nontoxic to Minnow.

Toxicity predicted values of artemimol are shown in Table 4.19.

TABLE 4.19: The Toxicity Values of Artemimol.

Sr. No	Model Name	Predicted values
1	AMES toxicity	No
2	Max.tolerated dose (human)	0.014 mg/Kg
3	hERG I inhibitor	No
4	hERG II inhibitor	No
5	Oral rat acute toxicity	2.227 mol/Kg
6	Oral rat chronic toxicity	0.995 mg/Kg
7	Hepatotoxicity	No
8	Skin sensitization	No
9	<i>T. pyriformis</i> toxicity	0.298 log ug/L
10	Minnow toxicity	1.067 log mM

4.3.1.13 Artemisone

Artemisone is non-carcinogenic and shows a low maximum tolerated dose. It is a supporter of potassium channels and is non-hepatotoxic. The compound is considered toxic against *T. pyriformis* (might not be harmful to human cells) but nontoxic to Minnow. Toxicity predicted values of artemisone are shown in Table.

TABLE 4.20: The Toxicity Values of Artemisone.

Sr. No	Model Name	Predicted values
1	AMES toxicity	No
2	Max.tolerated dose (human)	-0.475 mg/Kg
3	hERG I inhibitor	No
4	hERG II inhibitor	No
5	Oral rat acute toxicity	2.98 mol/Kg
6	Oral rat chronic toxicity	1.066 mg/Kg
7	Hepatotoxicity	Yes
8	Skin sensitization	No
9	<i>T. pyriformis</i> toxicity	0.285 log ug/L
10	Minnow toxicity	2.089 log mM

4.3.1.14 Caffeic acid

Caffeic acid is non-carcinogenic and shows a high maximum tolerated dose. It is a supporter of potassium channels and is non-hepatotoxic. The compound is considered toxic against *T. pyriformis* (might not be harmful to human cells) but nontoxic to Minnow. Toxicity predicted values of caffeic acid are shown in Table.

TABLE 4.21: The Toxicity Values of Caffeic acid.

Sr. No	Model Name	Predicted values
1	AMES toxicity	No
2	Max.tolerated dose (human)	1.145 mg/Kg

3	hERG I inhibitor	No
4	hERG II inhibitor	No
5	Oral rat acute toxicity	2.383 mol/Kg
6	Oral rat chronic toxicity	2.092 mg/Kg
7	Hepatotoxicity	No
8	Skin sensitization	No
9	<i>T. pyriformis</i> toxicity	0.293 log ug/L
10	Minnow toxicity	2.246 log mM

4.3.1.15 Gallic acid

Gallic acid is non-carcinogenic and shows high maximum tolerated doses. It is a supporter of potassium channels and is non-hepatotoxic.

The compound is considered toxic against *T. pyriformis* (might not be harmful to human cells) but non-toxic to Minnow. Toxicity predicted values of gallic acid are shown in Table 4.22. The toxicity properties of Gallic acid were previously reported by Gangarapur Kiran and his colleagues in 2020 [108].

TABLE 4.22: The Toxicity Values of Gallic acid.

Sr. No	Model Name	Predicted values
1	AMES toxicity	No
2	Max.tolerated dose (human)	0.7 mg/Kg
3	hERG I inhibitor	No
4	hERG II inhibitor	No
5	Oral rat acute toxicity	2.218 mol/Kg
6	Oral rat chronic toxicity	3.06 mg/Kg
7	Hepatotoxicity	No
8	Skin sensitization	No
9	<i>T. pyriformis</i> toxicity	0.285 log ug/L
10	Minnow toxicity	3.188 log mM

4.4 Molecular Docking

Molecular Docking is a technique used to estimate the strength of a bond between a ligand and a target protein through a special scoring function and to determine the correct structure of the ligand within the target binding site. The 3D structure of the target proteins and the ligands are taken as the input for docking.

After preparing proteins and ligands ready for docking, docking is performed by CB dock which is a well-trusted online blind auto docking tool. The results and time required for docking depend upon structures of receptors, ligands, refinements, and net speed. It may take several hours for a single result, so patience was shown while doing docking. CB dock gave us five possible possess and receptor models and among these possess best one was selected by observing certain properties like vena score and size of cavity etc. Molecular docking without knowledge of binding sites is accomplished using CB Dock, a user-friendly blind docking web server that predicts and estimates a binding site for a given protein calculates centers and sizes using a novel rotation cavity detection method, and docks with the popular docking program Auto dock Vina [110]. Molecular dockings are performed by using estrogen, HER 2, and progesterone as receptors and 15 selected compounds as ligands [111]. After submitting input files (receptor file in PDB format & ligand file in SDF format), CB-Dock examines the input files and converts them using OpenBabel and MGLTools to pdb formatted files.

After that, the docking program determines the cavities of the receptor and calculates the size and centers of the top N cavities (n=5 by default). Each center, size, and pdb file are given in to Auto Dock Vina for docking. Among the 5 best confirmations, the best one is selected based on the highest affinity score of receptor-ligand interaction. Ligands with the best binding score values with estrogen receptor, HER 2, and progesterone receptor are shown in Tables 4.23 to 4.25. Docking results of selected ligands with estrogen receptors are shown in Table 4.23. Among the selected ligands, the binding scores of Quercetin and Isoquercetin (-9.2 kcal/mol) are the highest followed by Luteolin by having the second-highest binding score of -9.0 kcal/mol. The binding scores of Kaempferol, Artemisinin,

Artenimol, and Dihydroartemisinin are -8.9 kcal/mol, -8.9 kcal/mol, -8.8 kcal/mol, and -8.8 kcal/mol respectively. The rest of the ligands have a binding score of less than -8.5 kcal/mol.

The ligand Gallic acid showed the lowest binding score of -6.2 kcal/mol. The ligands Quercetin, Luteolin, and Kaempferol had been reported earlier to be docked against ER using a molecular modelling approach.

The binding energies reported by Ninad V.Puranik and his colleagues in 2019 were quite similar to the binding values listed in the table [112].

TABLE 4.23A: Ligands with Best Binding Score Values with estrogen receptor.

Sr. No.	Compound	Artem- isinin	Artem- ether	Artes- unate	Dihydroar- temisinin	Artean- nuin B
1	Binding scores	-8.9	-8.3	-8.3	-8.8	-8.4
2	Cavity size	1905	1905	1905	1905	1905
3	HBD	0	0	1	0	0
4	HBA	5	5	7	4	3
5	Log P	2.3949	2.8408	2.6024	2.4633	2.4518
6	Molecular weight g/mol	282.336	298.379	384.425	266.337	248.322
7	Rotatable bond	0	1	4	0	0
8	Grid map	42	42	42	42	42
9	Min energy kcal/mol	0	0	0	0	0
10	Max eenergy kcal/mol	1.60E+00	1.60E+00	1.60E+00	1.60E+00	1.60E+00

TABLE 4.23B: Ligands with Best Binding Score Values with estrogen receptor.

Sr. No.	Compound	Artenimol	Artem- isone	Querc- etin	Isoquer- cetin	Rutin
1	Binding scores	-8.8	-7.3	-9.2	-9.2	-7.2
2	Cavity size	1905	1905	1905	1905	1905
3	HBD	1	0	5	8	10
4	HBA	5	7	7	12	16
5	Log P	2.1867	1.9248	1.988	-0.5389	-1.6871
6	Molecular weight g/mol	284.352	401.5	302.238	464.379	610.521
7	Rotatable bond	0	1	1	4	6
8	Grid map	42	42	42	42	42
9	Min energy kcal/mol	0	0	0	0	0
10	Max energy kcal/mol	1.60E +00	1.60E +00	1.60E +00	1.60E +00	1.60E +00

TABLE 4.23C: Ligands with Best Binding Score Values with estrogen receptor.

Sr. No	Compound	Gallic acid	Kaempferol	Chryso- plenol D	luteolin	Caffeic acid
1	Binding scores	-6.2	-8.9	-7.4	-9.0	-6.4
2	Cavity size	1905	1905	1905	1905	1905
3	HBD	4	4	3	4	3
4	HBA	4	6	8	6	3
5	Log P	0.5016	2.2824	2.6026	2.2824	1.1956

6	Molecular weight g/mol	170.12	152.237	360.318	286.239	180.159
7	Rotatable bond	1	1	4	1	2
8	Grid map	42	42	42	42	42
9	Min energy kcal/mol	0	0	0	0	0
10	Max energy kcal/mol	1.60E+00	1.60E+00	1.60E+00	1.60E+00	1.60E+00

Docking results of selected ligands with HER 2 are shown in Table 4.24. Among the selected ligands, the binding score of Artesunate (-9.1 kcal/mol) is the highest followed by Artemisone and Rutin having the second-highest binding score of -8.9 kcal/mol. The binding scores of Arteannuin B and Quercetin are -8.7 kcal/mol and -8.5 kcal/mol respectively. The rest of the ligands have shown a binding score of less than -8.5 kcal/mol.

The ligand Gallic acid showed the lowest binding score of -5.8 kcal/mol. The ligands Artesunate, Artemisinin, Artemisone, Artemether, and Dihydroartemisinin had been reported earlier to be docked against HER2 using Autodock 4.2.3 by Muhammad Rizki Fadhil Pratama in 2015 [113].

The ligands artemisinin, artemether, dihydroartemisinin, artemisone showed better binding energy of -8.0 kcal/mol, -8.2 kcal/mol, -8.4 kcal/mol, -8.8 kcal/mol respectively when docked against HER2 using CB dock as compared to binding energies of -7.28 kcal/mol, -8.1 kcal/mol, -7.86 kcal/mol, -7.85 kcal/mol when docked using Autodock 4.2.3.

However, Artesunate showed better binding energy of -10.59 kcal/mol when docked using Autodock 4.2.3 as compared to binding energies of -9.1 kcal/mol when docked using CB dock.

TABLE 4.24A: Ligands with Best Binding Score Values with HER2.

Sr. No	Compound	Artem- isinin	Artem- ether	Artes- unate	Dihydroar- temisinin	Artean- nuin B
1	Binding scores	-8.0	-8.2	-9.1	-8.4	-8.7
2	Cavity size	665	665	665	665	665
3	HBD	0	0	1	0	0
4	HBA	5	5	7	4	3
5	Log P	2.3949	2.8408	2.6024	2.4633	2.4518
6	Molecular weight g/smol	282.336	298.379	384.425	266.337	248.322
7	Rotatable bond	0	1	4	0	0
8	Grid map	88	88	88	88	88
9	Min energy kcal/mol	0	0	0	0	0
10	Max eenergy kcal/mol	1.60E +00	1.60E +00	1.60E +00	1.60E +00	1.60E +00

TABLE 4.24B: Ligands with Best Binding Score Values with HER2.

Sr. No	Compound	Arten- imol	Artem- isone	Quercetin	Isoque- rcetin	Rutin
1	Binding scores	-8.4	-8.8	-8.5	-8.0	-8.8
2	Cavity size	665	665	665	1288	387
3	HBD	1	0	5	8	10
4	HBA	5	7	7	12	16
5	Log P	2.1867	1.9248	1.988	-0.5389	-1.6871

6	Molecular weight	284.352	401.5	302.238	464.379	610.521
7	Rotatable bond	0	1	1	4	6
8	Grid map	88	88	88	75	84
9	Min energy kcal/mol	0	0	0	0	0
10	Max energy kcal/mol	1.60	1.60	1.60	1.60	1.60
		E+00	E+00	E+00	E+00	E+00

TABLE 4.24C: Ligands with Best Binding Score Values with HER2.

Sr. No.	Compound	Gallic acid	Kaempferol	Chryso-phenol- D	luteolin	Caffeic acid
1	Binding scores	-5.8	-8.3	-7.4	-8.1	-6.4
2	Cavity size	1288	665	665	665	599
3	HBD	4	4	3	4	3
4	HBA	4	6	8	6	3
5	Log P	0.5016	2.2824	2.6026	2.2824	1.1956
6	Molecular weight	170.12	152.237	360.318	286.239	180.159
7	Rotatable bond	1	1	4	1	2
8	Grid map	75	88	88	88	94
9	Min energy kcal/mol	0	0	0	0	0
10	Max energy kcal/mol	1.60	1.60	1.60	1.60	1.60
		E+00	E+00	E+00	E+00	E+00

Docking results of selected ligands with progesterone receptors are shown in Table 4.25. Among the selected ligands, the binding score of Kaempferol (-9.2 kcal/mol) is highest followed by Luteolin having the second-highest binding score of -9.0 kcal/mol. The binding scores of Artemisinin, Arteannuin B, and Quercetin are -8.5 kcal/mol, -8.0 kcal/mol, and -8.5 kcal/mol respectively. The rest of the ligands have a binding score of less than -8.0 kcal/mol. The ligand Gallic acid showed the lowest binding score of -6.2 kcal/mol. The ligands Quercetin, Luteolin, and Kaempferol had been reported previously to be docked against PR using the Autodock tool by Vahid Zarezade and his colleagues in 2018 [114]. The ligands Luteolin, and Kaempferol showed better binding energy of -9.0 kcal/mol, -9.2 kcal/mol, -8.4 kcal/mol respectively when docked using CB dock as compared to binding energies of -8.2 kcal/mol, -9.0 kcal/mol using Autodock tool. However, Quercetin showed better binding energy of -9.6 kcal/mol when docked using Autodock 4.2.3 as compared to binding energies of -8.5 kcal/mol when docked using CB dock.

TABLE 4.25A: Ligands with Best Binding Score Values with progesterone receptor.

Sr. No	Compound	Artem- isinin	Artem- ether	Artes- unate	Dihydroar- temisinin	Artean- nuin B
1	Binding scores	-8.5	-7.3	-7.8	-7.8	8.1
2	Cavity size	1178	1178	1178	1178	1178
3	HBD	0	0	1	0	0
4	HBA	5	5	7	4	3
5	Log P	2.3949	2.8408	2.6024	2.4633	2.4518
6	Molecular weight g/mol	282.336	298.379	384.425	266.337	248.322
7	Rotatable bond	0	1	4	0	0
8	Grid map	30	30	30	30	30

9	Min energy kcal/mol	0	0	0	0	0
10	Max energy kcal/mol	1.60 E+00	1.60 E+00	1.60 E+00	1.60 E+00	1.60 E+00

TABLE 4.25B: Ligands with Best Binding Score Values with progesterone receptor.

Sr. No	Compound	Artenimol	Artem- isone	Querc- etin	Isoque- rcetin	Rutin
1	Binding scores	-7.8	-7.6	-8.5	-7.4	-7.9
2	Cavity size	1178	1178	1178	1178	285
3	HBD	1	0	5	8	10
4	HBA	5	7	7	12	16
5	Log P	2.1867	1.9248	1.988	-0.5389	-1.6871
6	Molecular weight g/mol	284.352	401.5	302.238	464.379	610.521
7	Rotatable bond	0	1	1	4	6
8	Grid map	30	30	30	30	14
9	Min energy kcal/mol	0	0	0	0	0
10	Max energy kcal/mol	1.60E +00	1.60E +00	1.60E +00	1.60E +00	1.60E +00

TABLE 4.25C: Ligands with Best Binding Score Values with progesterone receptor.

Sr. No	Compound	Gallic- acid	Kaem- pferol	Chryso- plenol D	luteolin	Caffeic acid
1	Binding scores	-6.2	-9.2	-8.0	-9.0	-6.6
2	Cavity size	1178	1178	1178	1178	1178
3	HBD	4	4	3	4	3
4	HBA	4	6	8	6	3
5	Log P	0.5016	2.2824	2.6026	2.2824	1.1956
6-	Molecular weight g/mol	170.12	152.237	360.318	286.239	180.159
7	Rotatable bond	1	1	4	1	2
8	Grid map	30	30	30	30	30
9	Min energy kcal/mol	0	0	0	0	0
10	Max energy kcal/mol	1.60	1.60	1.60	1.60	1.60

4.5 Interaction of Ligands and Target Protein

The docking analysis is performed by using LigPlot+ (version v.1.4.5) and PyMol Edu (v1.7.4.5). Interactions of ligands and target proteins are predicted by using Ligplot plus (version v.1.4.5). LigPlot +'s graphical system generates several 2D diagrams of interactions from 3D coordinates automatically. The hydrogen-bond interaction pattern and hydrophobic interactions between the ligand and the protein's main-chain or side-chain components are depicted in these 2D representations [115]. The 2D diagrams of the best binding score ligands with respective

proteins are shown in Figures 4.10 to 4.54 while their hydrogen bonds and hydrophobic interactions are listed in Tables 5.1 to 5.3.

4.5.1 Interaction of Ligands with Estrogen Receptor

Figure 4.10 shows the interaction of Artemisinin with the estrogen receptor. As evident from the 2D diagram ligand show only hydrophobic interactions with the protein. Ligand consists of 15 carbons and shows hydrophobic interactions with residues Met 343, Leu 525, Leu 346, Thr 347, Ala 350, Leu 349, Leu 387, Glu 353, Phe 404, Leu 391, Met 388, and Leu 384 as evident also from Table 5.1.

Artemether, Dihydroartemisinin, Arteannuin B, Artenimol, Artemisone ligands are without hydrogen bonds as it is evident from the 2D structures they are mostly without active oxygen atoms. The ligands Artemether and Dihydroartemisinin made hydrophobic interactions with 12 residues as shown in Figure 4.11 and Figure 4.12 respectively. Artesunate made 1 hydrogen bond and maximum hydrophobic interactions with 14 residues as shown in Figure 4.13. The ligands Arteannuin B, Artenimol, and Artemisone made hydrophobic interactions with 9, 12, and 7 residues respectively as shown in Figure 4.14, Figure 4.15, and Figure 4.16. Maximum hydrogen bonds are shown by Gallic acid, Kaempferol, Luteolin, Quercetin, Rutin, and Isoquercetin as 4, 4, 5, 4, 5, and 7 respectively. The ligand Quercetin made 4 hydrogen bonds and hydrophobic interactions with 9 residues. The residues involved in hydrogen bonding are His, Met, Glu, and Arg as shown in Figure 4.17. The ligand Isoquercetin made 7 hydrogen bonds and hydrophobic interactions with 13 residues. The residues involved in hydrogen bonding are His, Met, Glu, Thr, and Arg as shown in Figure 4.18. The ligand Rutin made 5 hydrogen bonds and hydrophobic interactions with 10 residues. The residues involved in hydrogen bonding are Met Thr and Asp as shown in Figure 4.19. The ligand Gallic acid made 4 hydrogen bonds and hydrophobic interactions with 6 residues. The residues involved in hydrogen bonding are Leu and Arg as shown in Figure 4.20. The ligand Kaempferol made 4 hydrogen bonds and hydrophobic interactions with 8 residues. The residues involved in hydrogen bonding are Met,

His, Glu, and Arg as shown in Figure 4.21. The ligand Chryso splenol D made 3 hydrogen bonds and hydrophobic interactions with 10 residues.

The residues involved in hydrogen bonding are Thr, Leu, and Arg as shown in Figure 4.22. The ligand Luteolin made 5 hydrogen bonds and hydrophobic interactions with 8 residues. The residues involved in hydrogen bonding are Glu, Met, His, and Arg as shown in Figure 4.23. The ligand Caffeic acid made 3 hydrogen bonds and hydrophobic interactions with 5 residues. The residues involved in hydrogen bonding are Thr, Leu, and Arg as shown in Figure 4.24.

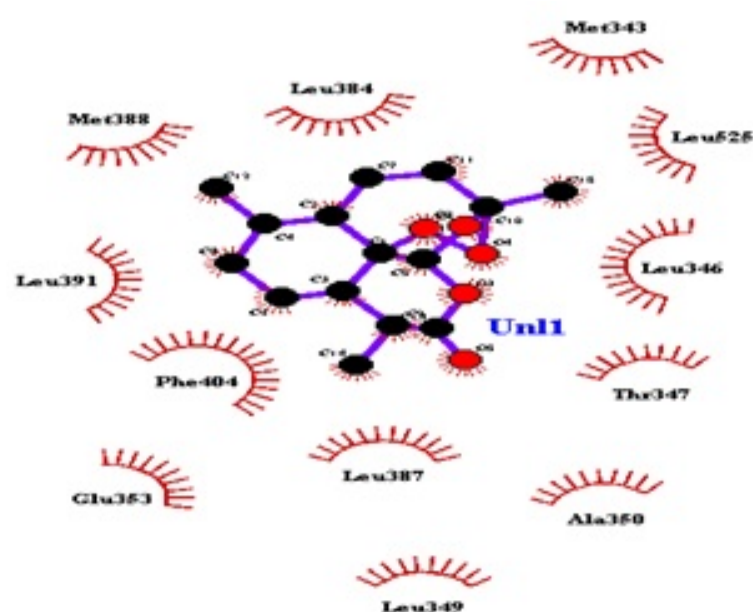


FIGURE 4.10: Interactions of Artemisinin with ER by Ligplot.

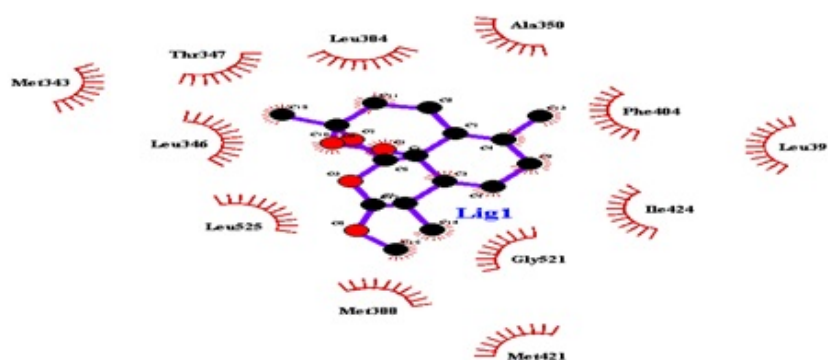


FIGURE 4.11: Interactions of Artemether with ER by Ligplot.

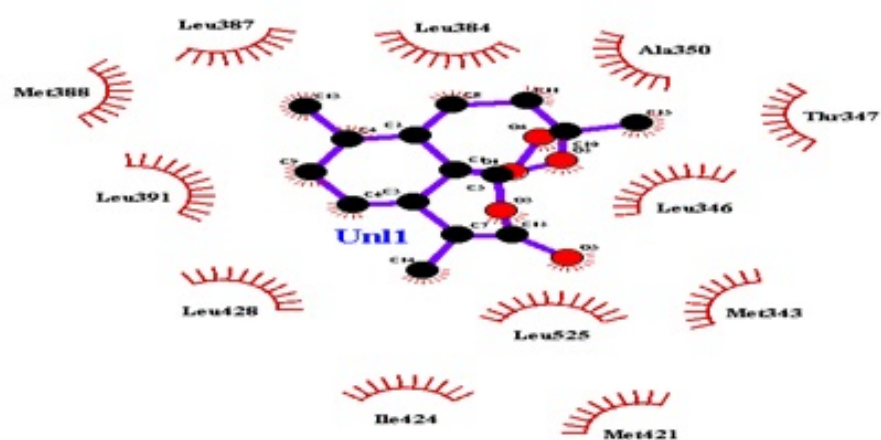


FIGURE 4.12: Interactions of Dihydroartemisinin with ER by Ligplot.

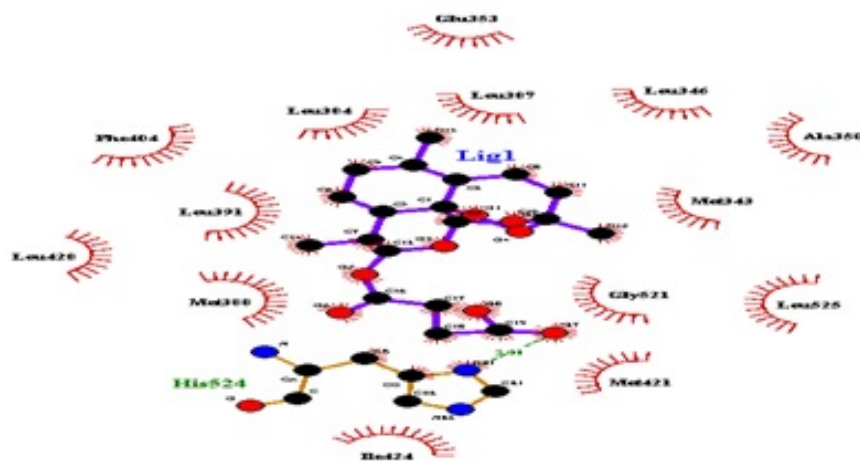


FIGURE 4.13: Interactions of Artesunate with ER by Ligplot.

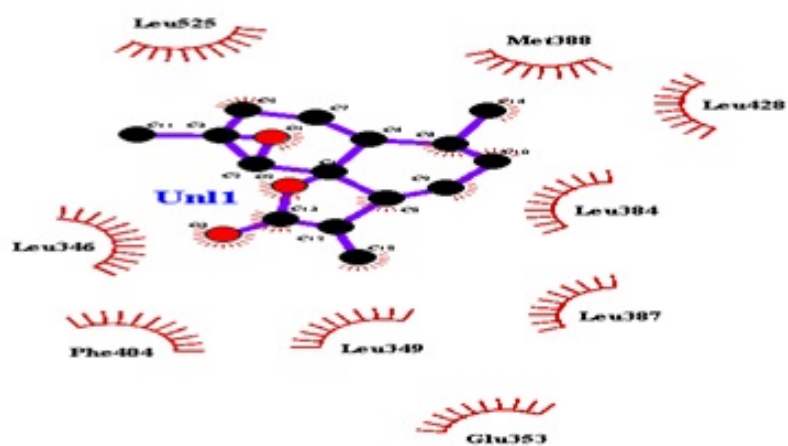


FIGURE 4.14: Interactions of Arteannuin B with ER by Ligplot.

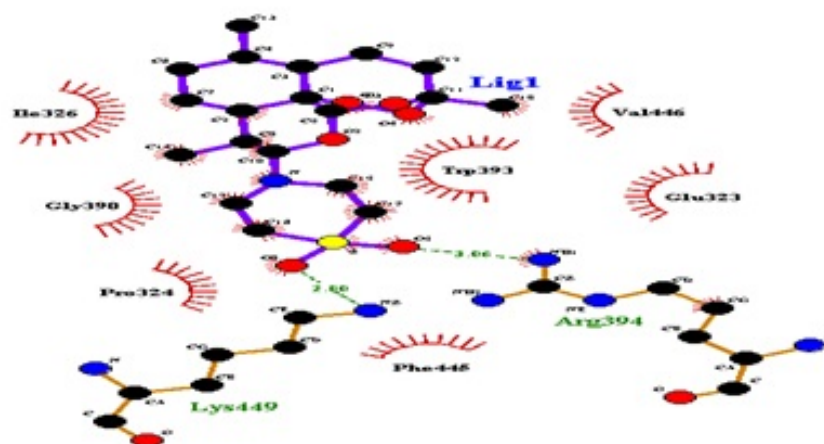


FIGURE 4.15: Interactions of Artemisone with ER by Ligplot.

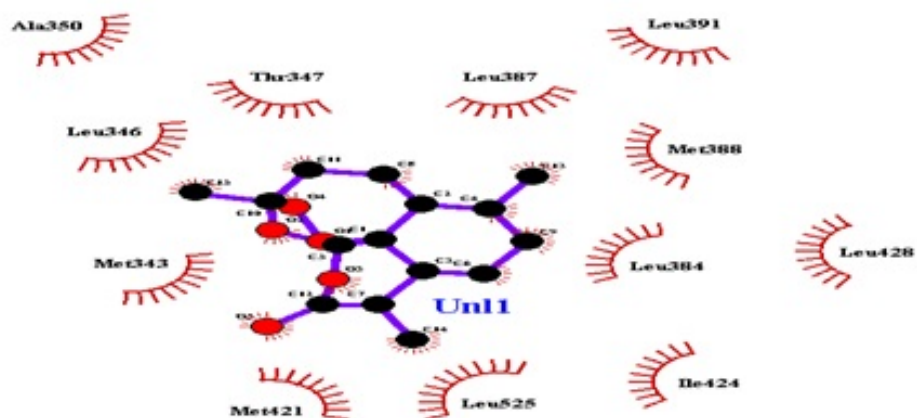


FIGURE 4.16: Interactions of Artemimol with ER by Ligplot.

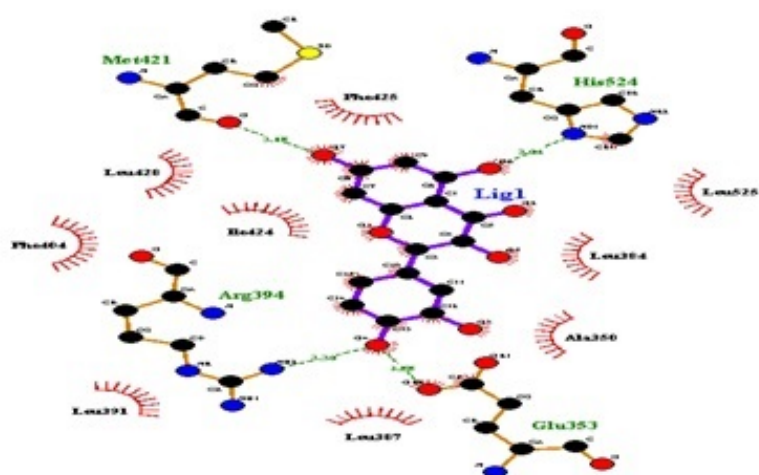


FIGURE 4.17: Interactions of Quercetin with ER by Ligplot.

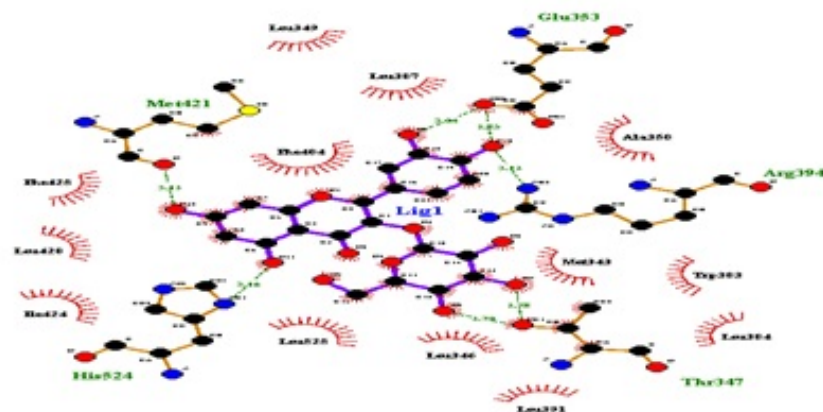


FIGURE 4.18: Interactions of Isoquercetin with ER by Ligplot.

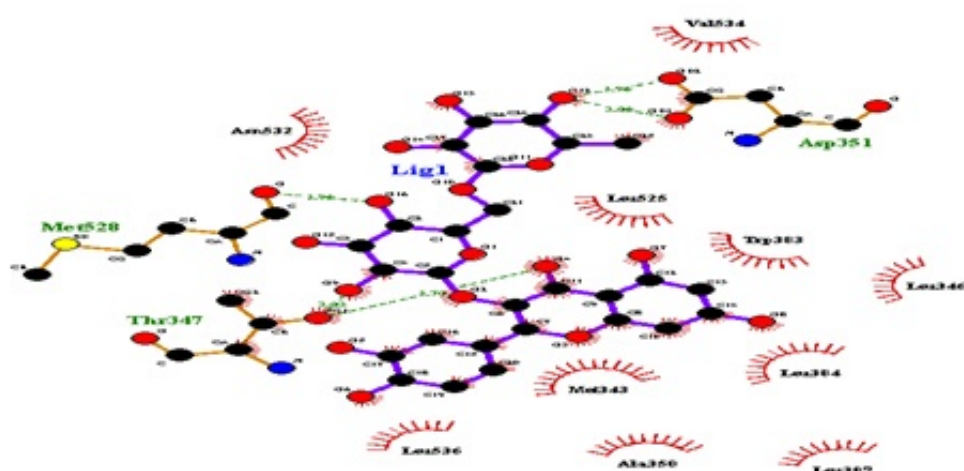


FIGURE 4.19: Interactions of Rutin with ER by Ligplot.

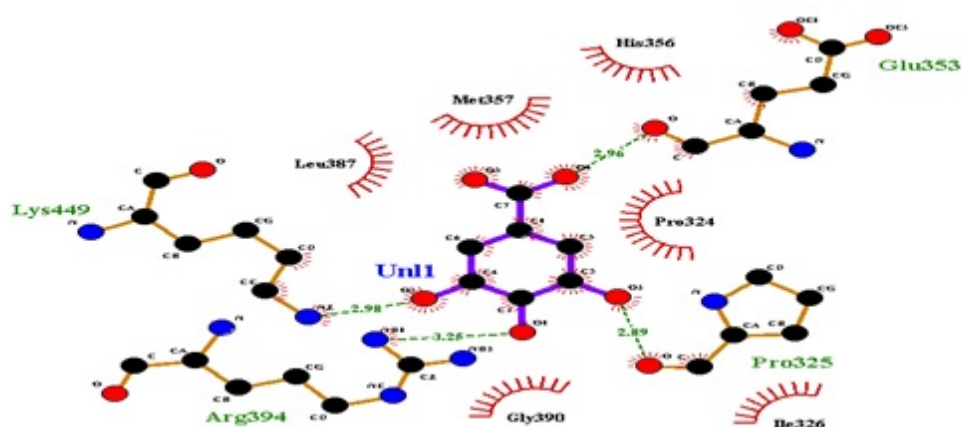


FIGURE 4.20: Interactions of Gallic acid with ER by Ligplot.

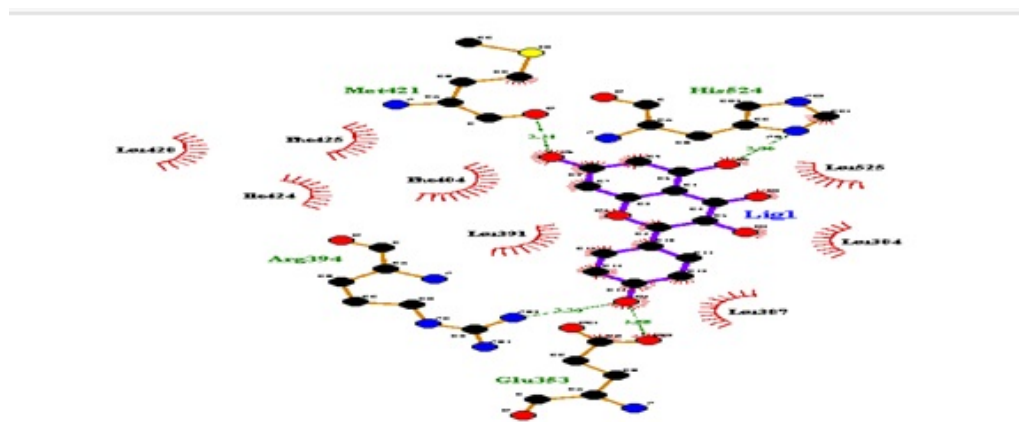


FIGURE 4.21: Interactions of kaempferol with ER by Ligplot

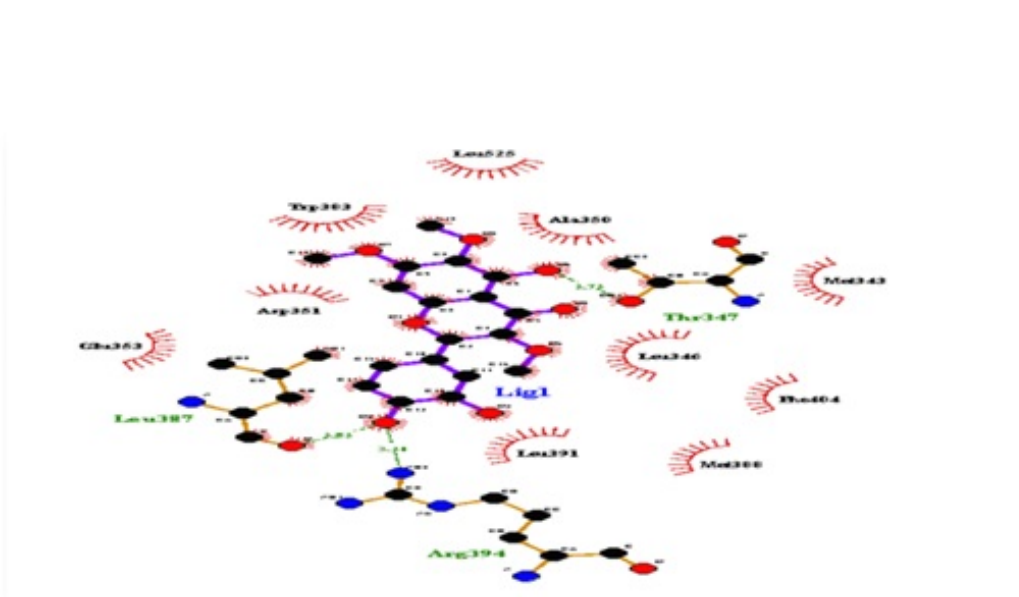


FIGURE 4.22: Interactions of Chrysoptanol D with ER by Ligplot.

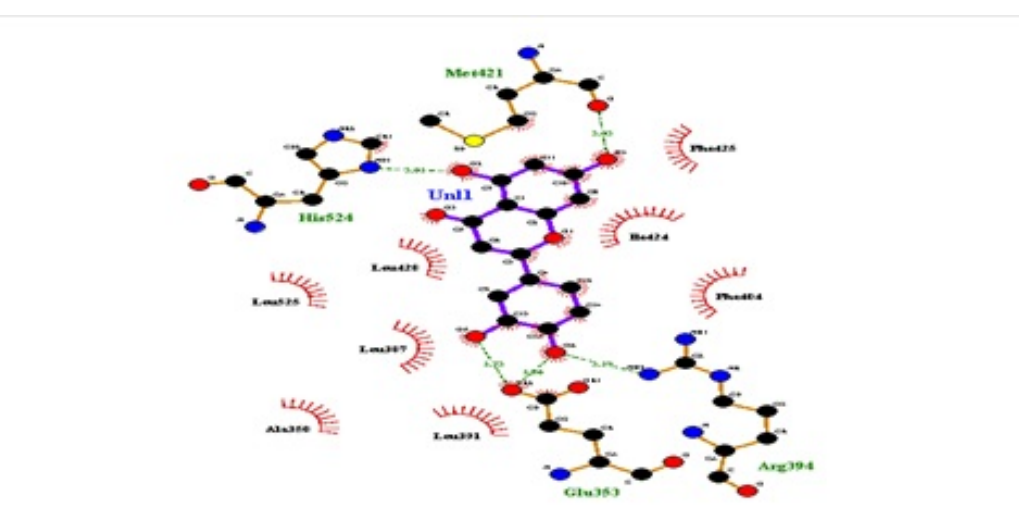


FIGURE 4.23: Interactions of Luteolin with ER by Ligplot.

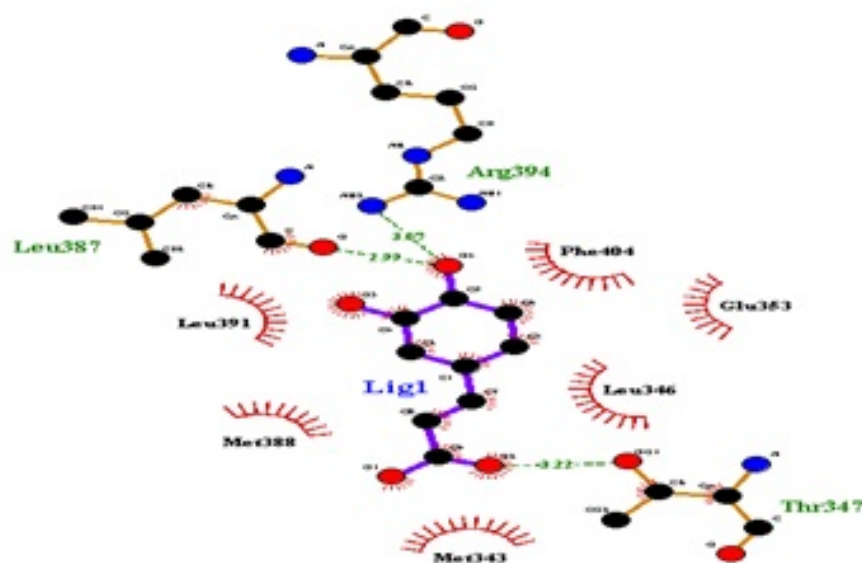


FIGURE 4.24: Interactions of Caffeic acid with ER by Ligplot.

4.5.2 Interaction of Ligands with HER 2

Figure 4.25 shows the interaction of Artemisinin with HER 2. As evident from the 2D diagram ligand show only hydrophobic interactions with the protein. Ligand consists of 15 carbons and shows hydrophobic interactions with residues Pro278, Arg 465, Asn 466, Set 441, Thr 5, Tyr 281, Phe 269, Val 3, Thr 1, and Tyr 279 as evident also from Table 5.2. Only Artemisinin and Chrysosplenol D ligands are without hydrogen bonds as it is evident from the 2D structures they are mostly without active oxygen atoms. Maximum hydrogen bonds are shown by Quercetin, Isoquercetin, Rutin, and Gallic acid, Kaempferol as 5, 7, 10, 7, and 4 respectively. Artemether and Artemisone show maximum hydrophobic interactions with 11 protein residues. Artemether made only 1 hydrogen bond with residue Thr as shown in Figure 4.26. Artesunate made 3 hydrogen bonds and hydrophobic interactions with 10 residues as shown in Figure 4.27.

The residues involved in hydrogen bonding are Thr and Ser. Dihydroartemisinin made 2 hydrogen bonds and hydrophobic interactions with 7 residues as shown in

Figure 4.28. The residues involved in hydrogen bonding are Thr and Asn. Arteannuin B made 3 hydrogen bonds and hydrophobic interactions with 5 residues as shown in

Figure 4.29. The residues involved in hydrogen bonding are Thr, Gly, and Asn. Artemimol made 2 hydrogen bonds and hydrophobic interactions with 7 residues as shown in Figure 4.30.

The residues involved in hydrogen bonding are Thr and Asn. Artemisone made 1 hydrogen bond and hydrophobic interactions with 11 residues as shown in Figure 4.31.

The residue involved in hydrogen bonding is Gln. Quercetin made 5 hydrogen bonds and hydrophobic interactions with 5 residues as shown in Figure 4.32.

The residues involved in hydrogen bonding are Gly, Val, Leu, Ser, and Asn. Isoquercetin made 7 hydrogen bonds and hydrophobic interactions with 8 residues as shown in Figure 4.33.

The residues involved in hydrogen bonding are Gln, Cys, Arg, and Glu. Rutin made 10 hydrogen bonds and hydrophobic interactions with 7 residues as shown in Figure 4.34.

The residue involved in hydrogen bonding are Gln, Thr, Ser, Arg, and Glu. Gallic acid made 7 hydrogen bonds and hydrophobic interactions with 3 residues as shown in Figure 4.35.

The residues involved in hydrogen bonding are Gln, Asn, Ala, Ser, Arg, and Glu. Kaempferol made 4 hydrogen bonds and hydrophobic interactions with 8 residues as shown in Figure 4.36.

The residues involved in hydrogen bonding are Val, Thr, and Gly. Chrysopterin D has eight oxygen atoms, but no one is involved in hydrogen bonding and has hydrophobic interactions with 11 residues as shown in Figure 4.37.

Luteolin made 3 hydrogen bonds and hydrophobic interactions with 8 residues as shown in Figure 4.38.

The residues involved in hydrogen bonding are Val, Asn, and Leu. Caffeic acid made 5 hydrogen bonds and hydrophobic interactions with 5 residues as shown in Figure 4.39. The residue involved in hydrogen bonding are Pro, Asn, and Thr.

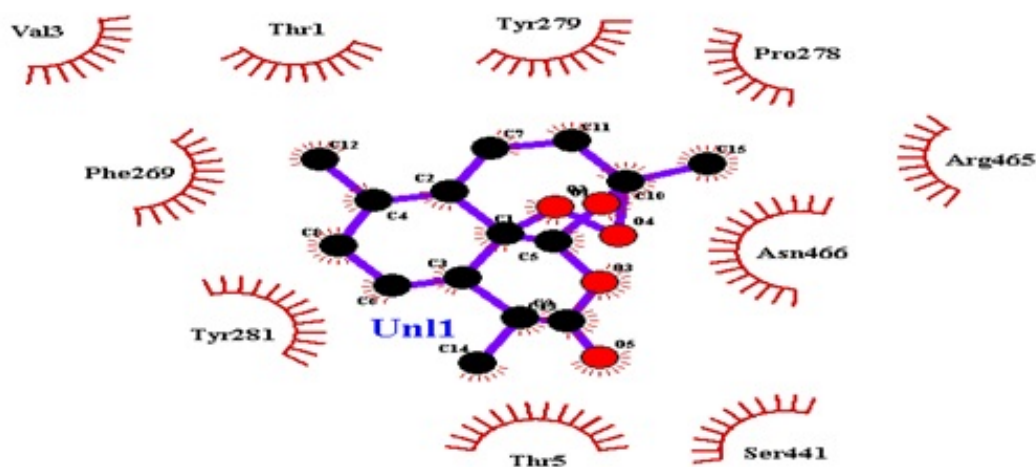


FIGURE 4.25: Interactions of Artemisinin with HER 2 by Ligplot.

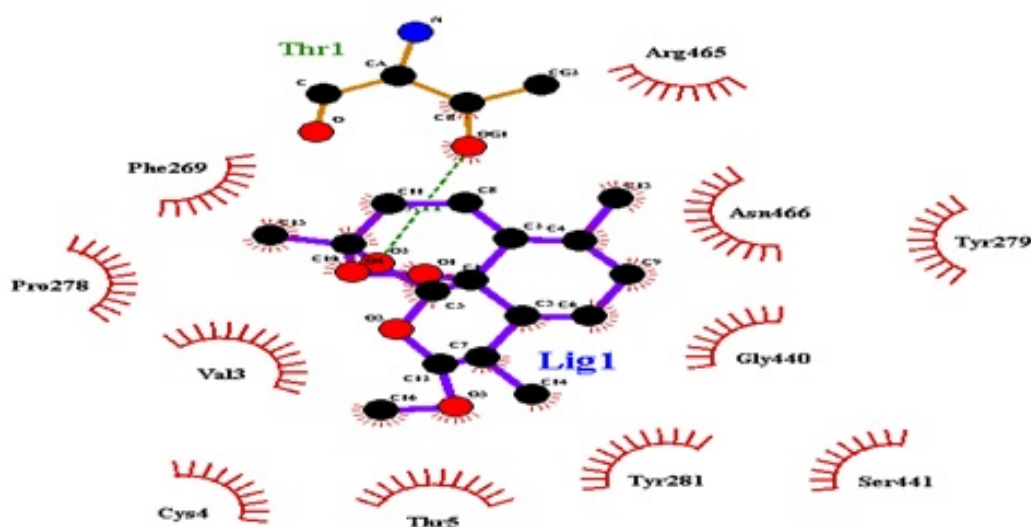


FIGURE 4.26: Interactions of Artemether with HER 2 by Ligplot.

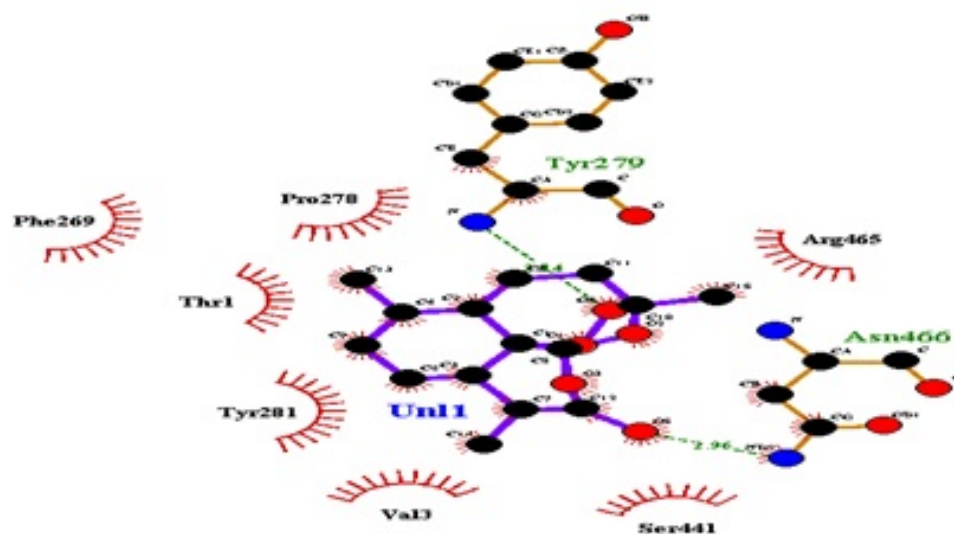


FIGURE 4.30: Interactions of Artemimol with HER 2 by Ligplot.

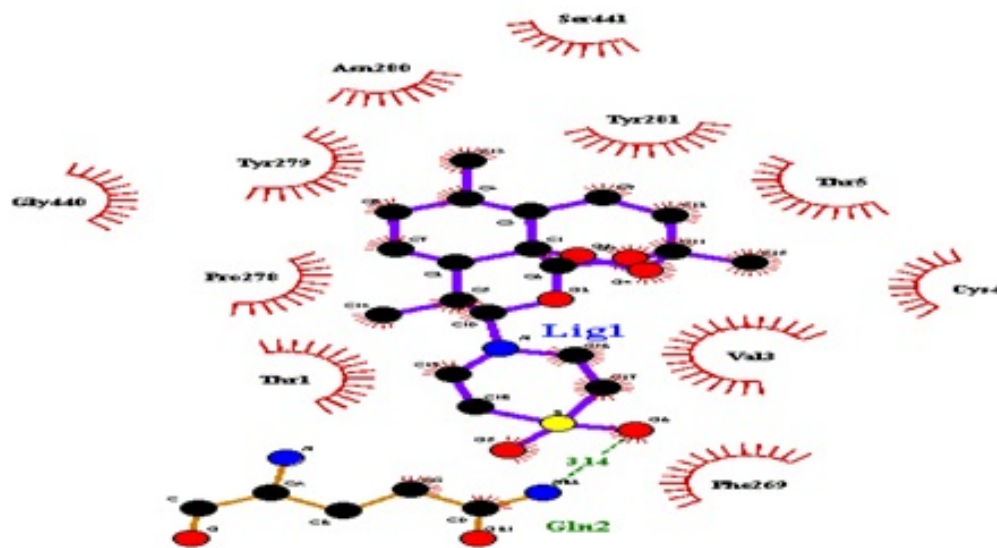


FIGURE 4.31: Interactions of Artemisone with HER 2 by Ligplot.

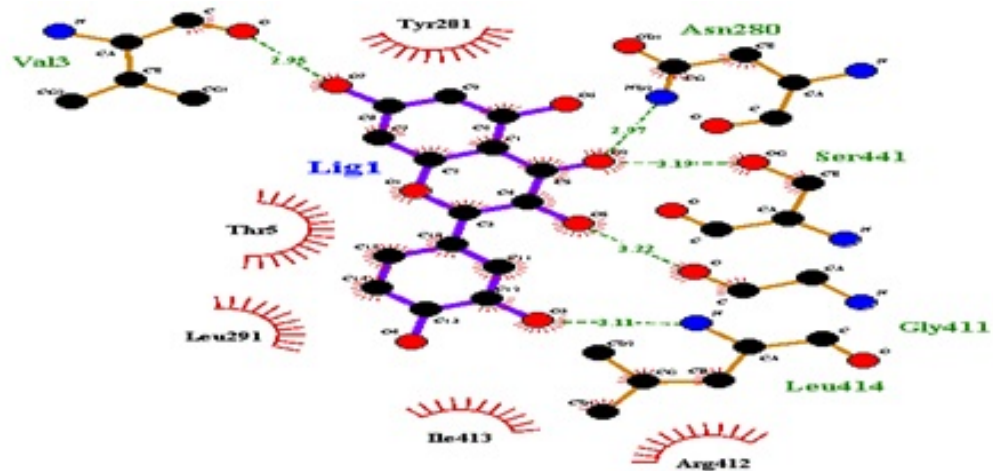


FIGURE 4.32: Interactions of Quercetin with HER 2 by Ligplot.

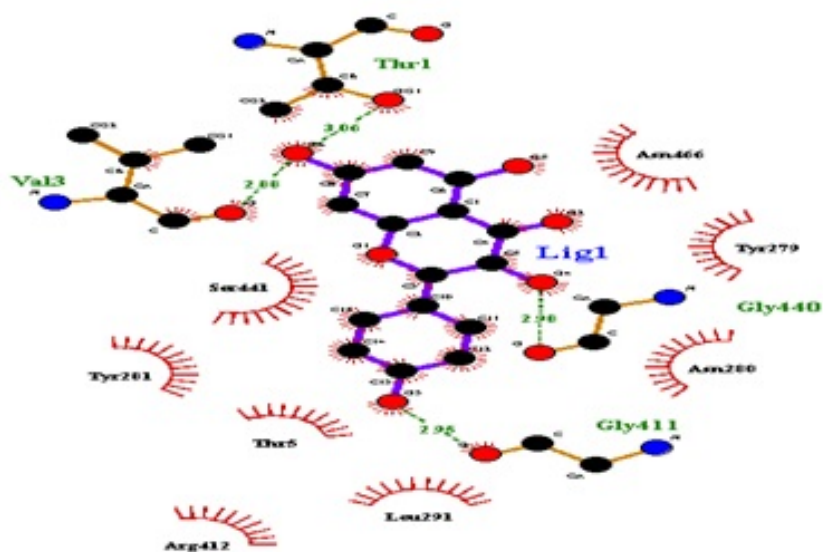


FIGURE 4.36: Interactions of kaempferol with HER 2 by Ligplot.

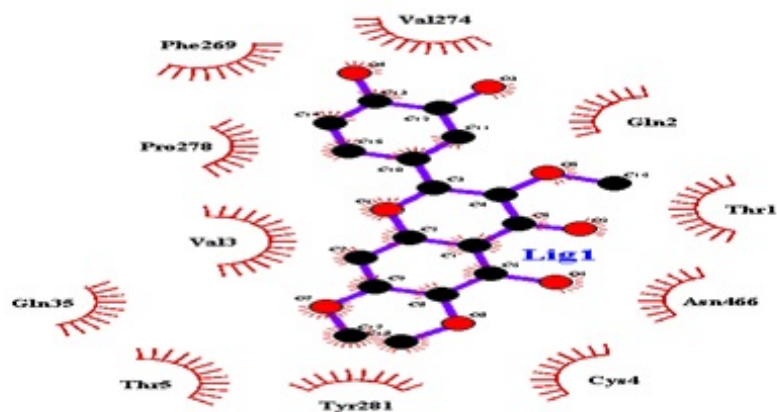


FIGURE 4.37: Interactions of Chrysoptanol D with HER 2 by Ligplot.

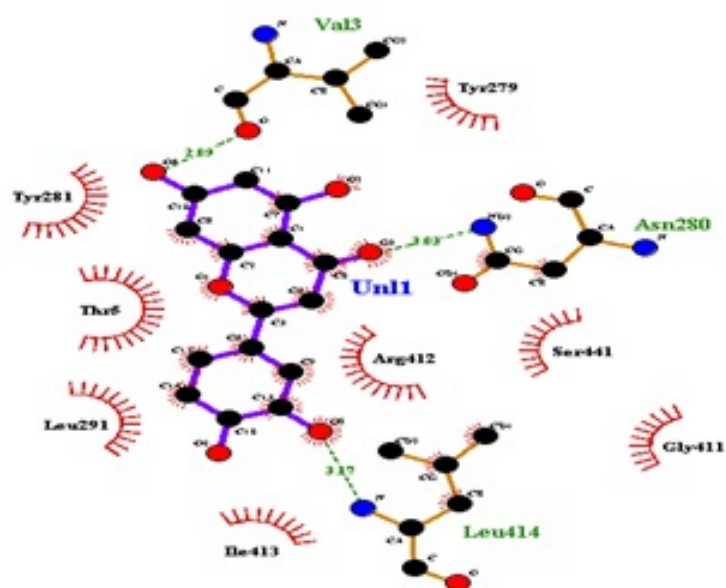


FIGURE 4.38: Interactions of Luteolin with HER 2 by Ligplot.

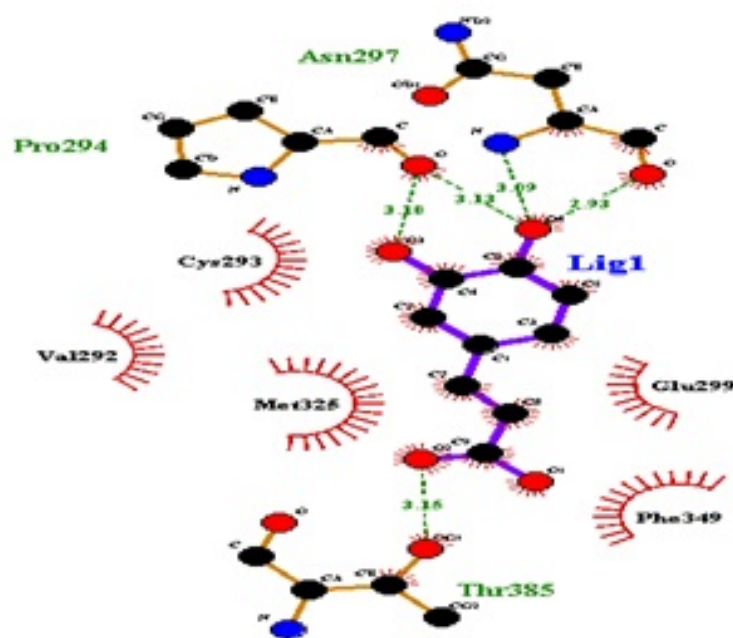


FIGURE 4.39: Interactions of Caffeic acid with HER 2 by Ligplot.

4.5.3 Interaction of Ligands with Progesterone Receptor

Figure 4.40 shows the interaction of Artemisinin with the progesterone receptor.

As evident from the 2D diagram ligand show only hydrophobic interactions with the protein. Ligand consists of 15 carbons and shows hydrophobic interactions with residues Asn 719, Met 909, Phe 778, Met 759, Val 760, Met 756, Met 801, Leu 887, Tyr 890, Leu 797, and Leu 718 as evident also from Table 4.28.

Artemether and Quercetin ligands are without hydrogen bonds as it is evident from the 2D structures they are mostly without active oxygen atoms.

Maximum hydrogen bonds are shown by Isoquercetin, Rutin, Kaempferol, and Luteolin as 4, 6, 4, and 4 respectively. Quercetin and Arteannuin B show maximum hydrophobic interactions with 12 protein residues. Artemether made hydrophobic interactions with 11 residues as shown in Figure 4.41.

Artesunate made 2 hydrogen bonds with residues Gln and Ile and hydrophobic interactions with 8 residues as shown in Figure 4.42.

Dihydroartemisinin made 2 hydrogen bonds with residues Lys and Arg and hydrophobic interactions with 11 residues as shown in Figure 4.43.

Arteannuin B made 1 hydrogen bond with residue Cys and hydrophobic interactions with 12 residues as shown in Figure 4.44.

Artemimol made 2 hydrogen bonds with residues Lys and Arg and hydrophobic interactions with 11 residues as shown in Figure 4.45.

Artemisone made 1 hydrogen bond with residue Pro and hydrophobic interactions with 9 residues as shown in Figure 4.46.

Quercetin has seven oxygen atoms, but no one involves in hydrogen bonding as shown in Figure 4.47.

Isoquercetin made 4 hydrogen bonds with residues Ile and Gln and hydrophobic interactions with 8 residues as shown in Figure 4.48.

Rutin made 6 hydrogen bonds with residues His, Lys, and Asp and hydrophobic interactions with 9 residues as shown in Figure 4.49.

Gallic acid made 1 hydrogen bond with residues Gln and hydrophobic interactions with 9 residues as shown in Figure 4.50.

Kaempferol made 4 hydrogen bonds with residues Gln, Leu, and Arg and hydrophobic interactions with 11 residues as shown in Figure 4.51.

Chrysosplenol D made 2 hydrogen bonds with residues Leu and Trp and hydrophobic interactions with 8 residues as shown in Figure 4.52.

Luteolin made 4 hydrogen bonds with residues Gln, Leu, Met, and Arg and hydrophobic interactions with 9 residues as shown in Figure 4.53.

Caffeic acid made 2 hydrogen bonds with residues Gln and Met and hydrophobic interactions with 6 residues as shown in Figure 4.54.

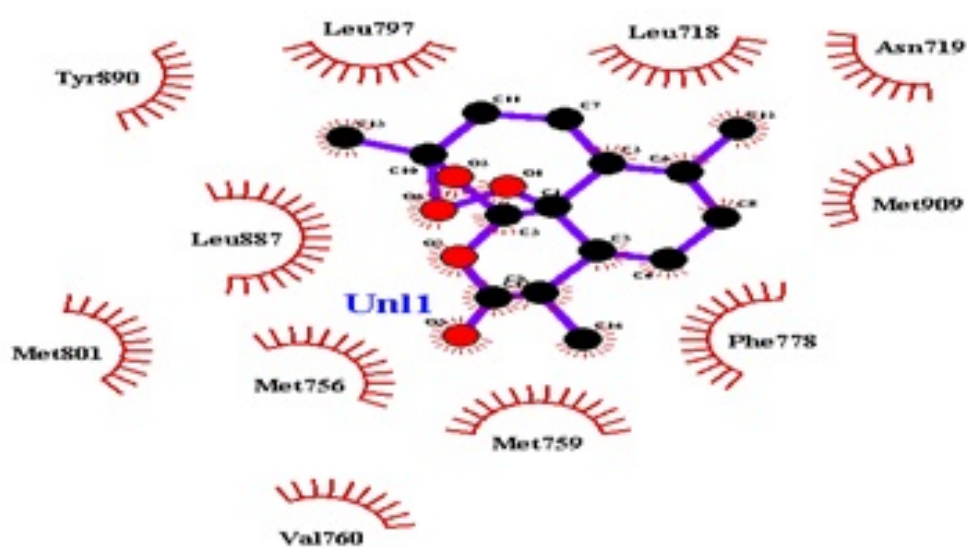


FIGURE 4.40: Interactions of Artemisinin with PR by Ligplot.

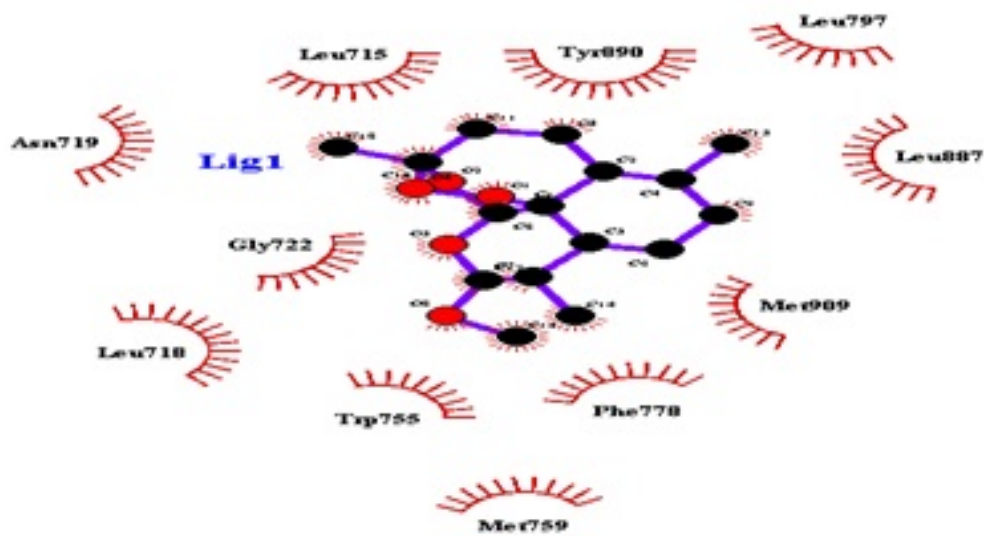


FIGURE 4.41: Interactions of Artemether with PR by Ligplot.

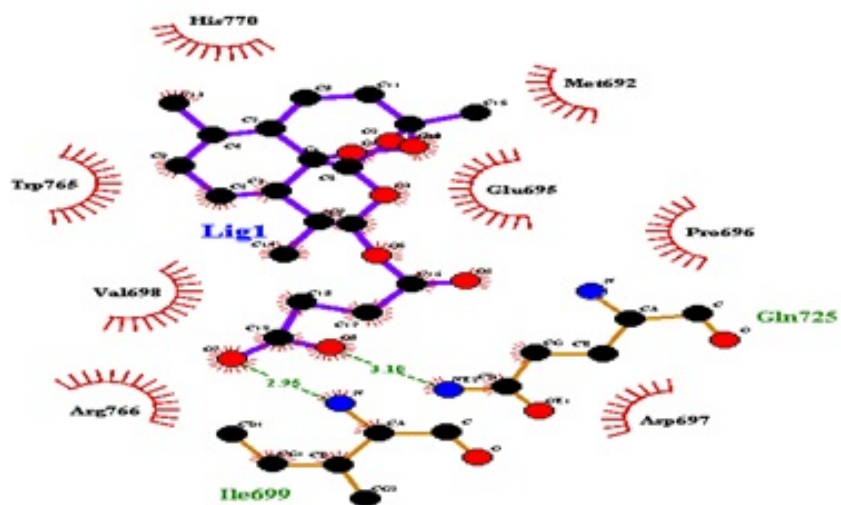


FIGURE 4.42: Interactions of Artesunate with PR by Ligplot.

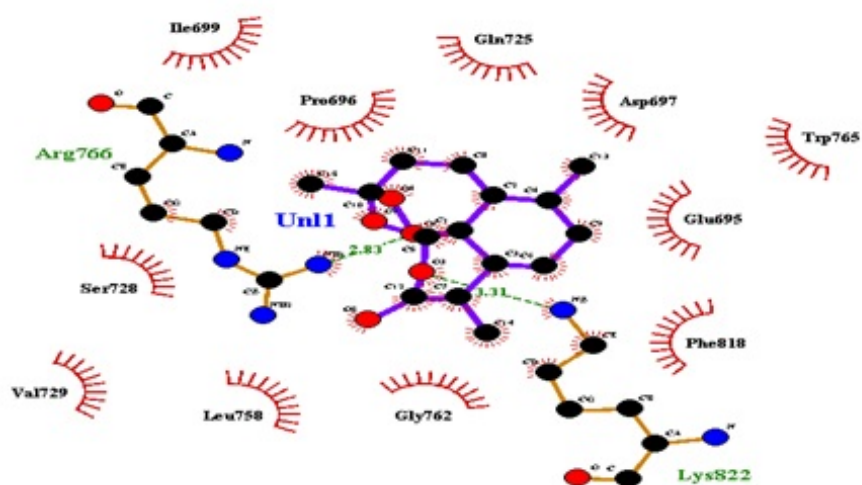


FIGURE 4.43: Interactions of Dihydroartemisinin with PR by Ligplot.

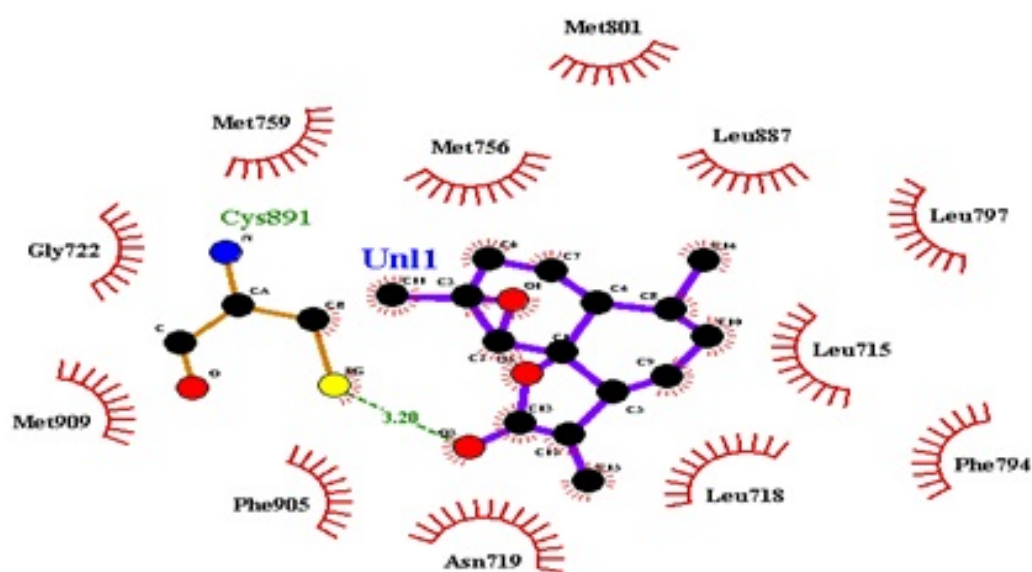


FIGURE 4.44: Interactions of Arteannuin B with PR by Ligplot.

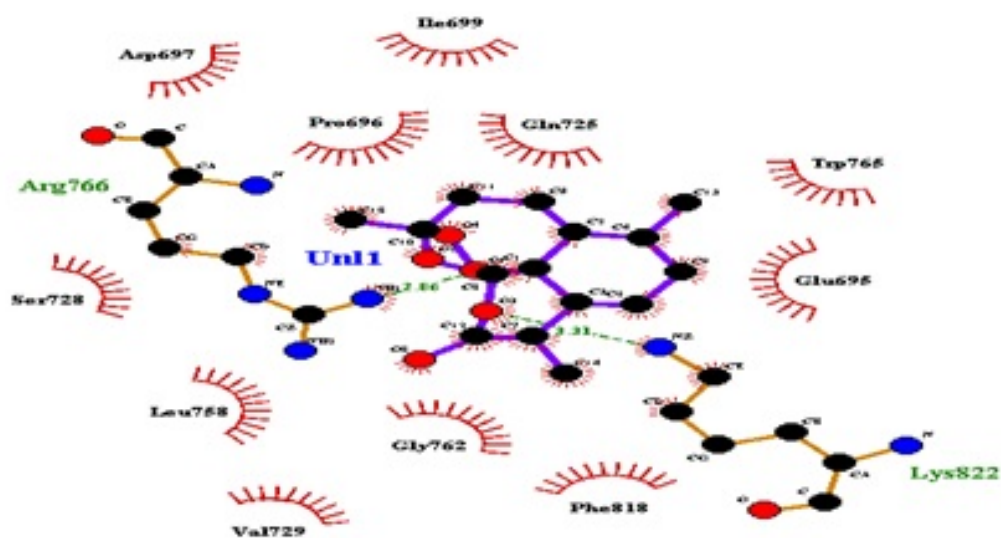


FIGURE 4.45: Interactions of Arteminol with PR by Ligplot.

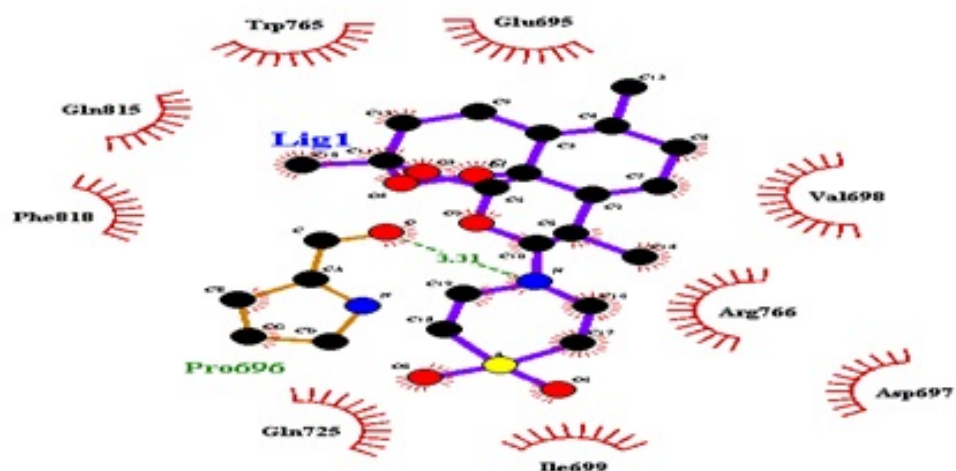


FIGURE 4.46: Interactions of Artemisone with PR by Ligplot.

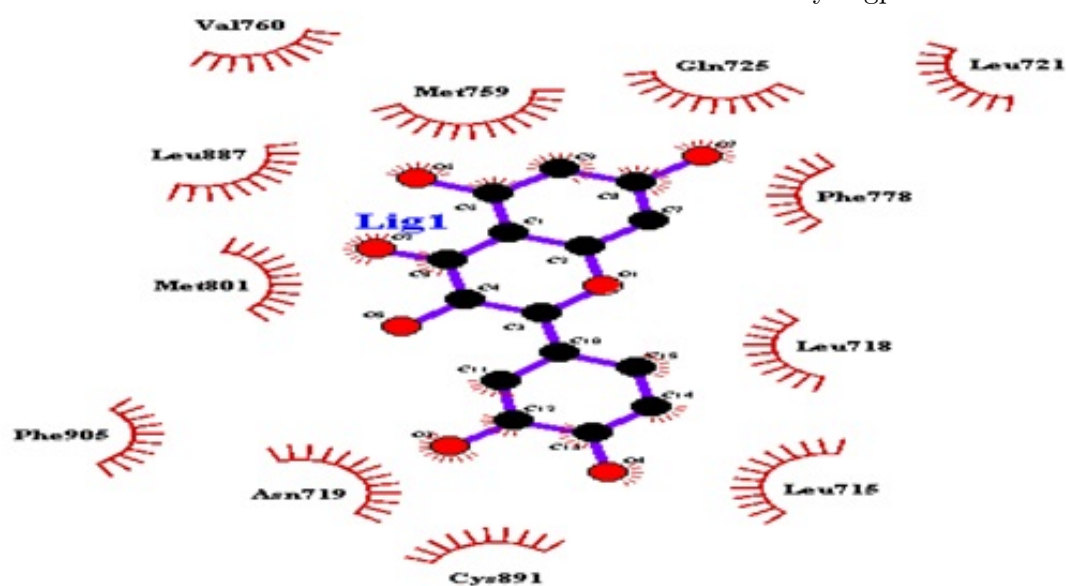


FIGURE 4.47: Interactions of Quercetin with PR by Ligplot.

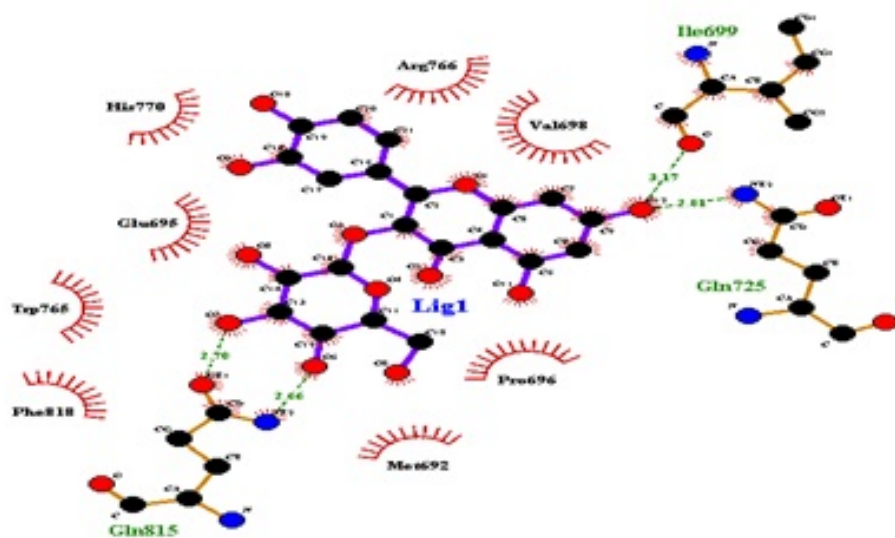


FIGURE 4.48: Interactions of Isoquercetin with PR by Ligplot.

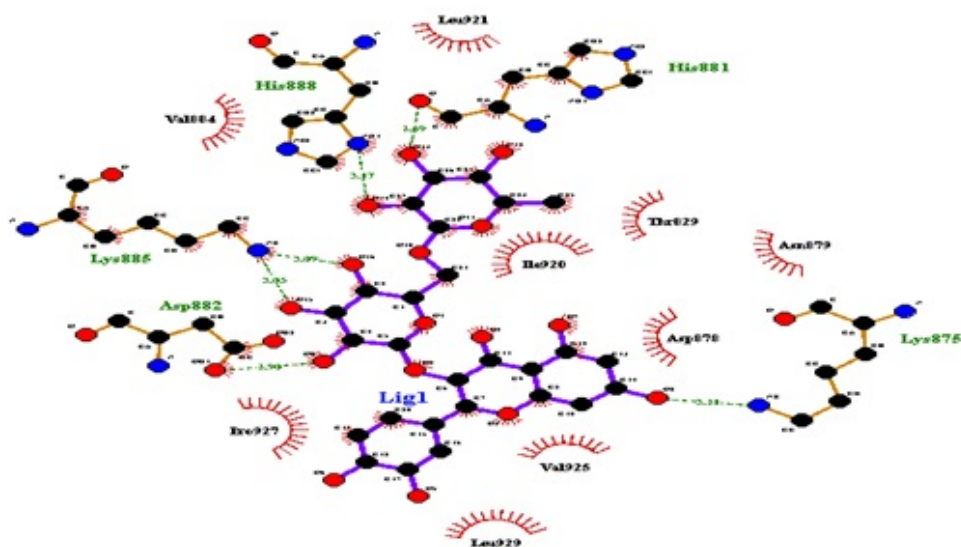


FIGURE 4.49: Interactions of Rutin with PR by Ligplot.

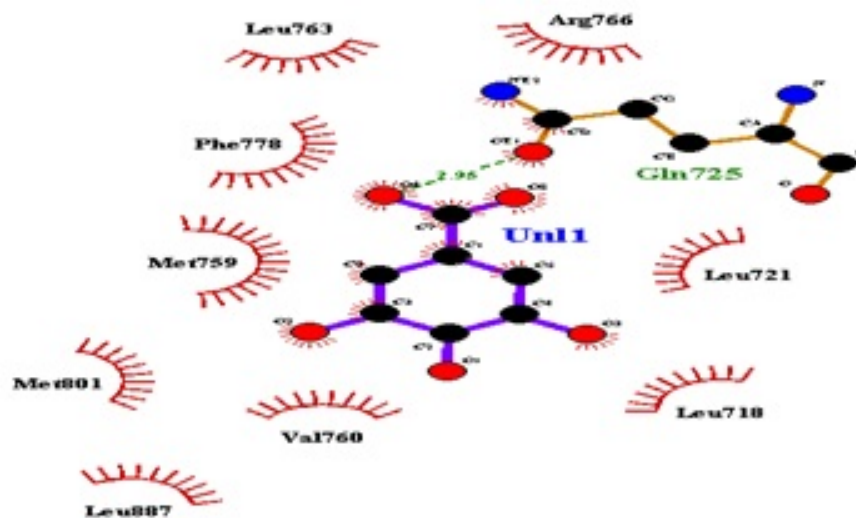


FIGURE 4.50: Interactions of Gallic acid with PR by Ligplot.

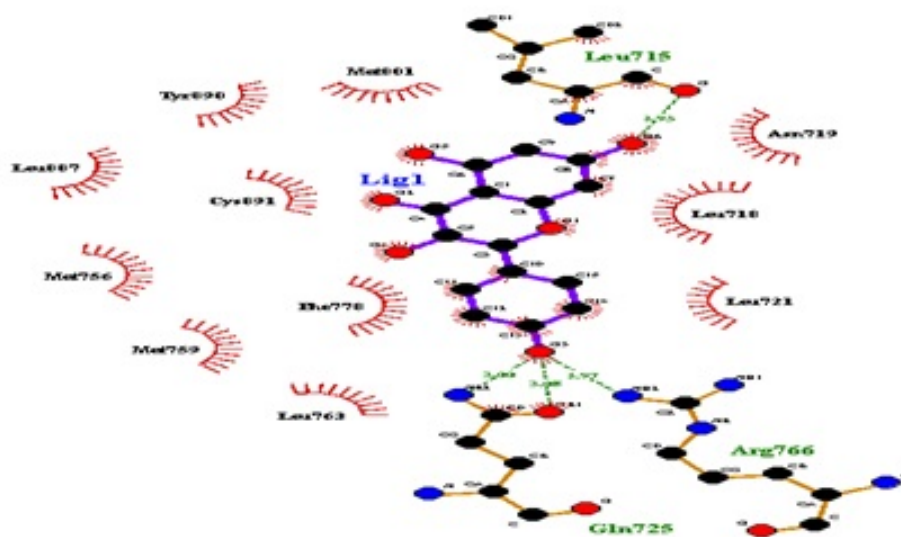


FIGURE 4.51: Interactions of kaempferol with PR by Ligplot.

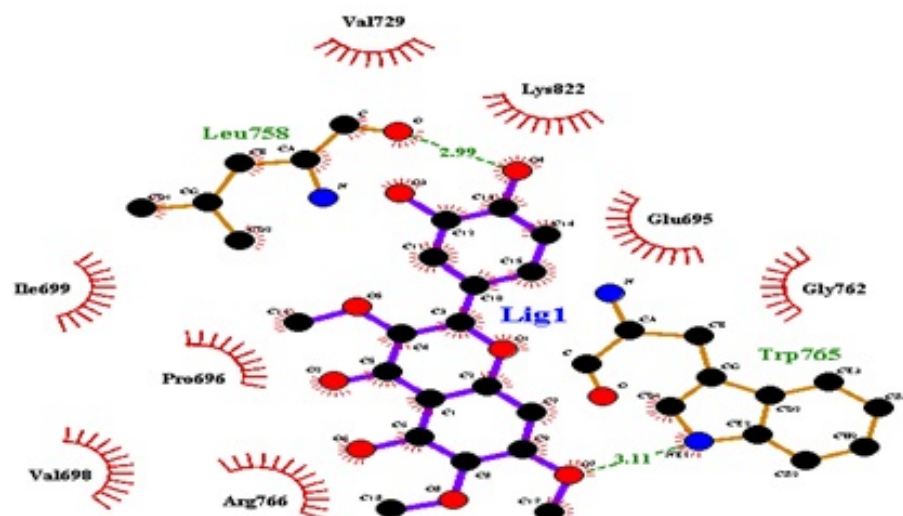


FIGURE 4.52: Interactions of Chrysoptanol D with PR by Ligplot.

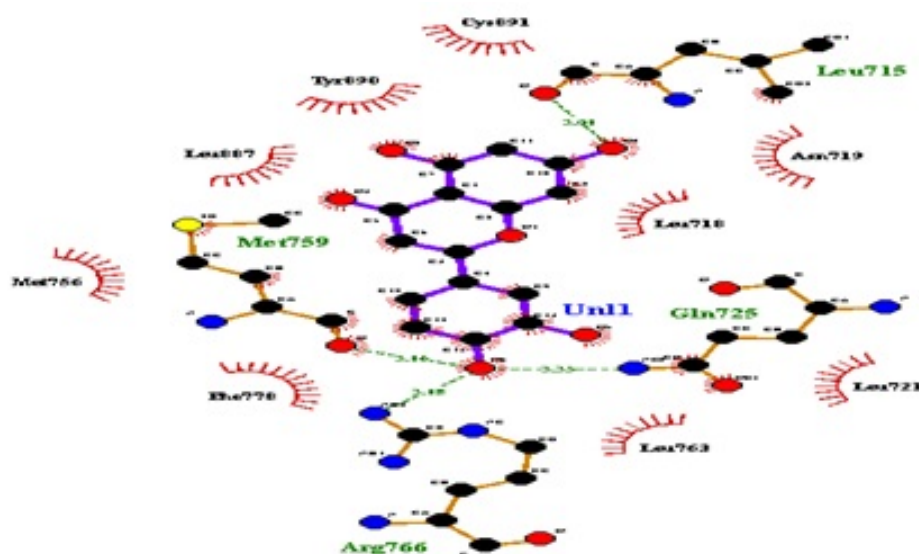


FIGURE 4.53: Interactions of Luteolin with PR by Ligplot.

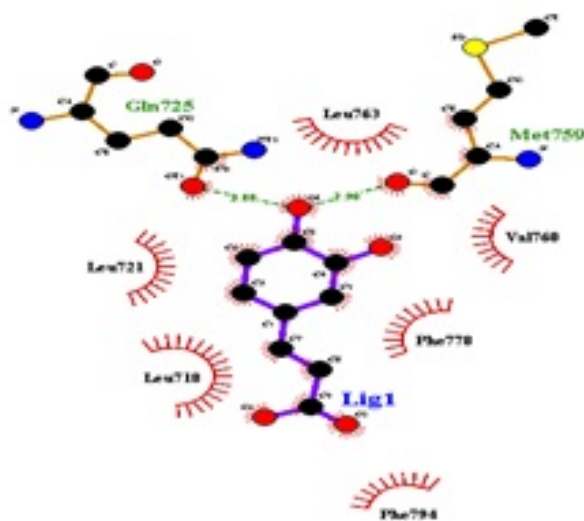


FIGURE 4.54: Interactions of Caffeic acid with PR by Ligplot.

4.6 ADME Properties of Ligands

Lipinski's five-drug law is used as a first step in assessing verbal bioavailability and artificial availability. Toxicity provides insights into the nature of ligands, which must be considered before designing a drug. A second study was performed as a measure of pharmacokinetics. PkCSM is used to find the toxicity and ADME properties of ligands [116]. In pharmacology, there are two broad terms the one is pharmacodynamics and the other is pharmacokinetics.

4.6.1 Pharmacodynamics

It is one of the broad terms used in pharmacology in which we study the drug effects on the body [92].

4.6.2 Pharmacokinetics

The other term used in pharmacology in which we study of the effect of the body on the drugs. In pharmacokinetics, we study the absorption of drugs, distribution of drugs, and metabolism of the drug, and excretion of the drugs [116].

4.6.3 Absorption

Absorption is the process of a drug passing from the bloodstream to the tissues in pharmacology (particularly pharmacokinetics). As a result, both the chemical composition of a drug and the environment in which it is administered play a role in determining the rate and degree of drug absorption [104]. Water solubility, CaCo₂ permeability, Intestinal absorption, Skin permeability, P-glycoprotein substrate, and P-glycoprotein I & II inhibitors are some of the ADME features that predict drug absorption when given orally. A compound's water solubility (log S) forecasts its solubility in water at 25 °C. It's calculated as a logarithm of molar concentration (log mol / L). Lipid-soluble medications are less water-soluble than water-soluble

drugs. The logarithm of the apparent permeability coefficient ($\log P_{app}$; $\log \text{cm/s}$) is predicted by the CaCO_2 permeability model. If a compound's P_{app} is greater than $8 \times 10^{-6} \text{ cm/s}$ (0.9 in terms of the pkCSM prediction model), it has high CaCO_2 absorbency [104].

Intestinal absorption predicts the percentage that will enter a person's small intestine. A compound with less than 30% absorption is less absorbent. The skin permeability model predicts the absorbency in $\log K_p$, and this model has a special interest in the formation of transdermal drugs. The element with the $\log K_p > -2.5$ means it has low skin penetration [104].

Toxins and xenobiotics are removed from the cells by the P-glycoprotein substrate, which acts as a natural barrier. This model determines whether a given substance is a potential P-glycoprotein (P-gp) substrate. If a substance is a P-glycoprotein substrate (which is categorically true), it may have minimal oral absorption. To limit the absorption of P-glycoprotein substrates, they can be quickly pushed out of the cells. The P-glycoprotein I/II inhibitor model predicts that the compound is likely to be a P-gp I/II inhibitor or not. P-gp inhibitors reduce the pumping activity of P-gp and may have high absorption [117].

4.6.3.1 Absorption Properties of Artemisinin, Artemether, Artesunate, Dihydroartemisinin, and Arteannuin B

All these ligands showed less water solubility. CaCO_2 permeability in the form of $\log P_{app}$ in 10^{-6} cm/s is within normal range except for Artesunate. Their intestinal absorption values are good in the line of 90%, highest among them is 98.347% of Arteannuin B. Artemisinin, Artesunate, Dihydroartemisinin, Arteannuin B and Artemether showed low skin permeability values in the form of $\log K_p$. Artesunate is predicted as a P-glycoprotein substrate while Artemether is a P-glycoprotein I inhibitor as shown in Table 4.26. The absorption properties of artemether, artemisinin, and dihydroartemisinin were previously reported by Tabish Qidwai in 2017 [106] and that of artesunate and Arteannuin B by Zarina Khurshid in 2021 [105].

TABLE 4.26: Absorption Properties of Ligands.

Sr. No.	Ligands	Artem- isinin	Artem- ether	Artes- unate	Dihydro- artemisinin	Artean- nuin B
1	Water solubility	-3.678 mol/L	-3.927 mol/L	-3.097 mol/L	-3.396 mol/L	-3.221 mol/L
2	CaCo ₂ permeability	1.295 cm/S	1.311 cm/S	0.863 cm/S	1.318 cm/S	1.537 cm/S
3	Intestinal absorption (human)	97.543 %	96.855 %	72.19 %	97.828 %	98.347 %
4	Skin Permeability	-3.158 log Kp	-2.929 log Kp	-2.735 log Kp	-3.279 log Kp	-3.322 log Kp
5	P-glyco- protein substrate	No	No	Yes	No	No
6	P-glyco- protein I inhibitor	No	Yes	No	No	No
7	P-glyco- protein II inhibitor	No	No	No	No	No

4.6.3.2 Absorption Properties of Artenimol, Artemisone, Quercetin, Isoquercetin, and Rutin

All these ligands showed less water solubility. CaCo₂ permeability in the form of log P_{app} in 10⁻⁶ cm/s is within normal range except for Rutin, Quercetin, and Isoquercetin.

Their intestinal absorption values are good except for Rutin which has 23.446% and the highest among them is 95.812% of Artemisone. Artenimol, Artemisone,

Quercetin, Isoquercetin, and Rutin showed low skin permeability values in the form of log Kp. The absorption properties of quercetin were previously reported by Al-Nor in 2019 [107] and that of isoquercetin by Maghfiroh Gesty Maharani and his colleagues in 2020 [109]. Quercetin, Isoquercetin, and Rutin are predicted as P-glycoprotein substrates as shown in Table 4.27.

The absorption properties of quercetin were previously reported by Al-Nor in 2019 [107] and that of isoquercetin by Maghfiroh Gesty Maharani and his colleagues in 2020 [109] and rutin by Zarina Khurshid in 2021 [105].

TABLE 4.27: Absorption Properties of Ligands

Sr. No.	Ligands	Artem- imol	Artem- isone	Quer- cetin	Isoque- rcetin	Rutin
1	Water solubility	-3.699 mol/L	-3.788 mol/L	-2.925 mol/L	-2.925 mol/L	-2.892 mol/L
2	CaCO ₂ permeability	1.249 cm/S	1.124 cm/S	-0.229 cm/S	0.242 cm/S	-0.949 cm/S
3	Intestinal absorption (human)	94.965 %	95.812 %	77.207 %	47.999 %	23.446 %
4	Skin Permeability	-3.354 log Kp	-2.74 log Kp	-2.735 log Kp	-2.735 log Kp	-2.735 log Kp
5	P-glyco- protein substrate	No	No	Yes	Yes	Yes
6	P-glyco- protein I inhibitor	No	No	No	No	No
7	P-glyco- protein II inhibitor	No	No	No	No	No

4.6.3.3 Absorption Properties of Gallic acid, Kaempferol, Chryso-splenol D, Luteolin and Caffeic acid

All these ligands showed less water solubility. CaCO_2 permeability in the form of $\log P_{app}$ in 10^{-6} cm/s is not within the normal range. Their intestinal absorption values are good, the highest among them is 81.386% of Chryso-splenol D. Gallic acid, Kaempferol, Chryso-splenol D, Luteolin, and Caffeic acid showed low skin permeability values in the form of $\log K_p$. Kaempferol, Chryso-splenol D, Luteolin are predicted as P-glycoprotein substrates while Chryso-splenol D is a P-glycoprotein II inhibitor as shown in Table 4.28. The absorption properties of Kaempferol were previously reported [107] and that of Luteolin and Gallic acid [108] and of chryso-splenol D Zarina Khurshid in 2021 [105].

TABLE 4.28: Absorption Properties of Ligands

Sr. No	Ligands	Gallic acid	Kaem- pferol	Chryso-s- plenol D	Luteolin	Caffeic - acid
1	Water solubility	-2.56 mol/L	-3.04 mol/L	-3.328 mol/L	-3.094 mol/L	-2.33 mol/L
2	CaCO_2 permeability	-0.081 cm/S	0.032 cm/S	0.402 cm/S	0.096 cm/S	0.634 cm/S
3	Intestinal absorption (human)	43.354 %	74.29 %	81.386 %	81.13 %	69.407 %
4	Skin Permeability	-2.735 log K_p	-2.735 log K_p	-2.735 log K_p	-2.735 log K_p	-2.722 log K_p
5	P-glycoprotein substrate	No	Yes	Yes	Yes	No
6	P-glycoprotein I inhibitor	No	No	No	No	No
7	P-glycoprotein II inhibitor	No	No	Yes	No	No

4.6.4 Distribution

In pharmacology, distribution is a branch of pharmacokinetics that deals with the transport of drugs from one area to another inside the body. The volume of distribution in humans (VD_{ss} expressed as $\log L/kg$), Fraction unbound in humans (F_u), Blood-brain barrier (BBB) permeability expressed as $\log BBB$, and Central nervous system permeability (CNS permeability) expressed as $\log PS$ are four ADME properties [118].

Model-1 describes the notional volume in which the complete amount of medicine must be equally distributed to achieve the same concentration as blood plasma. VD_{ss} is low if it is less than 0.71 L / kg ($\log VD_{ss} 0.15$) and high if it is more than 2.81 L / kg ($\log VD_{ss} > 0.45$). When VD_{ss} is high, it suggests that the medication is still being delivered to the tissues rather than the plasma. If a compound shows more F_u value, it means it is more effective [118]. BBB protects the brain from exogenous compounds, so BBB permeability is an important parameter. If the predicted value of $\log BBB > 0.3$ then it means the given substance can cross BBB and if value < -1 then not permeable to the brain. $\log PS$ is the product of blood-brain permeability and surface area, with a value of > -2 indicate penetration of the CNS and a value < -3 indicate poor permeability [118].

Distribution Properties Artemisinin, Artemether, Artesunate, Dihydroartemisinin, and Arteannuin B are listed in Table 4.29. From Table 4.29, Artemisinin and Artemether have high VD_{ss} values, while values of Artesunate, Dihydroartemisinin, and Arteannuin B are below 0.45. The fraction unbound values are within the acceptable range. The ligands Artemether and Arteannuin B can penetrate brain tissue while Artemisinin, Artesunate, and Dihydroartemisinin have poor permeability. The ligands artemisinin, Dihydroartemisinin, and Arteannuin B have values > -3 but less than -2 while the ligands Artemether and Artesunate have poor CNS permeability. The distribution properties of artemether, artemisinin, and dihydroartemisinin were previously reported by Tabish Qidwai in 2017 [106] and that of artesunate and Arteannuin B by Zarina Khurshid in 2021 [105].

TABLE 4.29: The Distribution Properties of Ligands.

Sr. No	Ligands	Artem- isinin	Arte- methers	Arte- sunate	Dihydro- artemisinin	Artean- nuin B
1	VDss	0.457	0.611	0.172	0.356	0.401
	(human)	L/Kg	L/Kg	L/Kg	L/Kg	L/Kg
2	Fraction unbound	0.4	0.384	0.36	0.411	0.426
	(human)	Fu	Fu	Fu	Fu	Fu
3	BBB permeability	0.235	0.861	-0.954	0.28	0.434
		log BB	log BB	log BB	log BB	log BB
4	CNS permeability	-2.909	-3.239	-3.039	-2.999	-2.951
		log PS	log PS	log PS	log PS	log PS

From Table 4.30, Artemimol, Quercetin, Isoquercetin, and Rutin have high VDss value, except for Artemisone, that has a value below 0.45. The fraction unbound values are within the acceptable range. The ligand Artemimol can penetrate brain tissue while the rest have poor permeability. The ligand Artemimol has a value >-3 but less than -2 is permeable to CNS while the rest of the ligands have poor CNS permeability. The distribution properties of quercetin were previously reported by Al-Nor in 2019 [107] and that of isoquercetin by Maghfiroh Gesty Maharani and his colleagues in 2020 [109] and rutin by Zarina Khurshid in 2021 [105].

TABLE 4.30: The Distribution Properties of Ligands.

Sr. No.	Ligands	Artem- imol	Artem- isone	Querc- etin	Isoque- rcetin	Rutin
1	VDss	0.613	0.075	1.559	1.846	1.663
	(human)	L/Kg	L/Kg	L/Kg	L/Kg	
2	Fraction unbound	0.452	0.493	0.206	0.228	0.187
	(human)	Fu	Fu	Fu	Fu	Fu

3	BBB	0.783	-0.331	-1.098	-1.688	-1.899
	permeability	log BB	log BB	log BB	log BB	log BB
4	CNS	-2.952	-3.081	-3.065	-4.093	-5.178
	permeability	log PS	log PS	log PS	log PS	log PS

From Table 4.31, Kaempferol and Luteolin have high VDss values while values of Gallic acid, Caffeic acid, and Chrysofenol D are below range. The fraction unbound values are within the acceptable range.

All the ligands have poor BBB permeability. The ligand Gallic acid has poor CNS permeability while the rest of the ligands have values >-3 but less than -2 .

The distribution properties of Kaempferol were previously reported by Al-Nor in 2019 [107] and that of luteolin and Gallic acid by Gangarapur Kiran and his colleagues in 2020 [108] and of chrysofenol D Zarina Khurshid in 2021 [105].

TABLE 4.31: The Distribution Properties of Ligands.

Sr. No	Ligands	Gallic acid	Kaempferol	Chrysofenol D	Luteolin	Caffeic acid
1	VDss	-1.855	1.274	0.287	1.153	-1.098
	(human)	L/Kg	L/Kg	L/Kg	L/Kg	L/Kg
2	Fraction unbound	0.617 Fu	0.178 Fu	0.093 Fu	0.168 Fu	0.529 Fu
	(human)					
3	BBB permeability	-1.102	-0.939	-1.607	-0.907	-0.647
		log BB	log BB	log BB	log BB	log BB
4	CNS permeability	-3.74	-2.228	-3.298	-2.251	-2.608
		log PS	log PS	log PS	log PS	log PS

4.6.5 Metabolism

Cytochrome P450 is an enzyme held responsible for the detoxification of toxins in the liver. This enzyme facilitates the release of xenobiotics by reacting with them. Some drugs are triggered by this enzyme while most drugs are neutralized by it [92]. The ligands listed in Table 4.32 act as a substrate of only one isoform CYP 3A4 and inhibitor of only one isoform CYP1A2 except for artesunate which does not act as an inhibitor of any isoform. The metabolic properties of artemether, artemisinin, and dihydroartemisinin were previously reported by Tabish Qidwai in 2017 [106] and that of artesunate and Arteannuin B by Zarina Khurshid in 2021 [105].

TABLE 4.32: Metabolic Properties of Ligands.

Sr. No	Ligands	Artem- isinin	Artem- ether	Artes- unate	Dihydro- artemisinin	Artean- nuin B
1	CYP2D6 substrate	No	No	No	No	No
2	CYP3A4 substrate	Yes	Yes	Yes	Yes	Yes
3	CYP1A2 inhibitor	Yes	Yes	No	Yes	Yes
4	CYP2C19 inhibitor	No	No	No	No	No
5	CYP2C9 inhibitor	No	No	No	No	No
6	CYP2D6 inhibitor	No	No	No	No	No
7	CYP3A4 inhibitor	No	No	No	No	No

The ligands listed in Table 4.32 do not act as a substrate of any isoform and

inhibitor of any isoform except for quercetin which acts as an inhibitor of CYP1A2 isoform. The metabolic properties of quercetin were previously reported by Al-Nor in 2019 [107] and that of isoquercetin by Maghfiroh Gesty Maharani and his colleagues in 2020 [109] and rutin by Zarina Khurshid in 2021 [105].

TABLE 4.33: Metabolic Properties of Ligands.

Sr. No	Ligands	Arten- imol	Artem- isone	Quer- cetin	Isoque- rcetin	Rutin
1	CYP2D6 substrate	No	No	No	No	No
2	CYP3A4 substrate	No	No	No	No	No
3	CYP1A2 inhibitor	No	No	Yes	No	No
4	CYP2C19 inhibitor	No	No	No	No	No
5	CYP2C9 inhibitor	No	No	No	No	No
6	CYP2D6 inhibitor	No	No	No	No	No
7	CYP3A4 inhibitor	No	No	No	No	No

The ligands listed in Table 4.33 do not act as a substrate of any isoform except for chryso splenol D which acts as a substrate of CYP3A4, Gallic acid, and Caffeic acid does not act as an inhibitor of any isoform. Kaempferol and chryso splenol D act as an inhibitor of CYP1A2 and Luteolin as an inhibitor of CYP1A2 and CYP2C9 isoform.

The metabolic properties of Kaempferol were previously reported by Al-Nor in 2019 [107] and that of Luteolin and Gallic acid by Gangarapur Kiran and his colleagues in 2020 [108] and of chryso splenol D Zarina Khurshid in 2021 [105].

TABLE 4.34: Metabolic Properties of Ligands

Sr. No	Ligands	Gallic acid	Kaempferol	Chryso-plenol D	Luteolin	Caffeic acid
1	CYP2D6 substrate	No	No	No	No	No
2	CYP3A4 substrate	No	No	Yes	No	No
3	CYP1A2 inhibitor	No	Yes	Yes	Yes	No
4	CYP2C19 inhibitor	No	No	No	No	No
5	CYP2C9 inhibitor	No	No	No	Yes	No
6	CYP2D6 inhibitor	No	No	No	No	No
7	CYP3A4 inhibitor	No	No	No	No	No

4.6.6 Excretion

The kidneys, which play a key part in drug excretion (renal excretion), and the liver are two organs implicated in drug excretion (biliary excretion). Other organs, such as the lungs for volatile or gaseous substances, may also be involved in excretion. Sweat, saliva, and tears can all be used to eliminate drugs. Total Clearance (CL_{tot}) represented as log (CL_{tot}) in ml/min/kg is one model of excretion property, while Renal OCT2 substrate predicts findings as Yes/No. The renal uptake transporter OCT2 (organic cation transporter 2) is involved in drug disposition and renal clearance [119]. Excretory properties of ligands are listed in Tables 4.35 to 4.38. From Table 4.35, the predicted value of Total clearance of Artemisinin, Artemether, Artesunate, Dihydroartemisinin, and Arteannuin B

is within the recommended range. All ligands showed a negative result for model Renal OCT2 substrate.

The excretion properties of artemether, artemisinin, and dihydroartemisinin were previously reported by Tabish Qidwai in 2017 [106] and that of artesunate and arteannuin B by Zarina Khurshid in 2021 [105].

TABLE 4.35: Excretory Properties of Ligands.

Sr. No	Ligands	Artem- isinin	Artem- ether	Artes- unate	Dihydro- artemisinin	Artean- nuin B
1	Total	0.98	1.031	0.969	0.803	0.965
	Clearance Renal	ml/Kg	ml/Kg	ml/Kg	ml/Kg	ml/Kg
2	OCT2 substrate	No	No	No	No	No

From Table 4.36, the predicted value of Total clearance of Artenimol, Artemisone, Quercetin, and Isoquercetin are within recommended range while Rutin exhibits poor total clearance. All ligands showed a negative result for model Renal OCT2 substrate. The excretion properties of quercetin were previously reported by Al-Nor in 2019 [107] and that of isoquercetin by Maghfiroh Gesty Maharani and his colleagues in 2020 [109] and rutin by Zarina Khurshid in 2021 [105].

TABLE 4.36: Excretory Properties of Ligands.

Sr. No	Ligands	Arten- imol	Artem- isone	Quer- cetin	Isoque- rcetin	Rutin
1	Total	1.002	0.377	0.407	0.394	-0.369
	Clearance Renal	ml/Kg	ml/Kg	ml/Kg	ml/Kg	ml/Kg
2	OCT2 substrate	No	No	No	No	No

From Table 4.37, the predicted value of Total clearance of Gallic acid, Kaempferol, Chrysofenol D, Luteolin, and Caffeic acid are within the recommended range. All ligands showed a negative result for model Renal OCT2 substrate. The excretion properties of Kaempferol were previously reported by Al-Nor in 2019 [107] and that of Luteolin and Gallic acid by Gangarapur Kiran and his colleagues in 2020 [108] and of chrysofenol D Zarina Khurshid in 2021 [105].

TABLE 4.37: Excretory Properties of Ligands

Sr. No	Ligands	Gallic acid	Kaempferol	Chrysofenol D	Luteolin	Caffeic acid
1	Total	0.518	0.477	0.502	0.495	0.508
	Clearance	ml/Kg	ml/Kg	ml/Kg	ml/Kg	ml/Kg
2	Renal					
	OCT2 substrate	No	No	No	No	No

4.7 Lead Compound Identification

Physicochemical and Pharmacokinetics properties determine the final destiny of compounds as drug or non-drug compounds. Physicochemical properties or Lipinski's rule of five works as primary filter and Pharmacokinetics studies as a secondary filter in the screening of potential compounds. Rutin does not obey Lipinski's rule of five, so it is knocked out in primary screening. Pharmacokinetic studies of these compounds screen out Artemisinin as it is considered carcinogenic. Isoquercetin and Rutin act as h ERG II inhibitors are thus knock out in secondary screening. The best five compounds based on primary and secondary filters, toxicity predicted values, and binding scores are Quercetin, Isoquercetin Luteolin, Artemisinin, Kaempferol against estrogen receptor, Artesunate, Artemisone, Arteannuin B, Quercetin and Dihydroartemisinin, against HER 2 receptor, Kaempferol, Luteolin, Artemisinin, Quercetin, Chrysofenol D

against progesterone receptor. As quercetin is already known for its use in the treatment of breast cancer [54]. So, the less common compound Luteolin is selected as the lead compound. Similarly, artesunate has been already used as Her 2 inhibitor and used in breast cancer treatment so instead of artesunate, artemisone is selected as the lead compound against Her 2 [61]. Kaempferol is selected as the lead compound against the progesterone receptor. Luteolin has been previously reported to act as an inhibitor of Epidermal Growth Factor Receptor [120]. Similarly, kaempferol has been reported as an inhibitor of mTORC1 against Hepatocellular carcinoma by exhibiting better affinity to receptor FKPB12 and AKT serine/threonine-protein kinase [121]. Binding scores with all three receptors are shown in Tables 4.38-4.40. Lead Compounds of this research work are Luteolin for estrogen receptor, Artemisone for HER 2, and Kaempferol for progesterone.

TABLE 4.38: Hit Compounds with Binding Scores with ER.

Sr. No	Name of Potential Compound	Binding Score with estrogen receptor
1	Quercetin	-9.2
2	Luteolin	-9
3	Kaempferol	-8.9
4	Dihydroartemisinin	-8.8
5	Artesunate	-8.3

TABLE 4.39: Hit Compounds with Binding Scores with HER2.

Sr. No	Name of Potential-Compound	Binding Score with HER2
1	Artesunate	-9.1
2	Artemisone	-8.8
3	Arteannuin B	-8.7
4	Quercetin	-8.5
5	Dihydroartemisinin	-8.4

TABLE 4.40: Hit Compounds with Binding Scores with PR.

Sr. No	Name of Potential-Compound	Binding Score with progesterone receptor
1	Kaempferol	-9.2
2	Luteolin	-9.0
3	Quercetin	-8.5
4	Artemisone	-8.5
5	Chrysofenol D	-8.0

4.8 Selection of Standard Drugs

For the selection of the most efficient drug, physicochemical parameters including molecular formula, molecular weight, absorption, water solubility, log P, H-bond donors and acceptors, bioavailability, polarizability, ADMET probability (must be less than 1), and side effects of these drugs were studied by using PubChem, and Drug bank databases and pkCSM online tool.

Mechanism of these selected drugs with references are shown in Table 4.41. The physicochemical properties of selected drugs are listed in Table 4.41. Tamoxifen has been selected as a standard drug against the estrogen receptor.

Tamoxifen is the oldest estrogen receptor modulator known which is used to treat hormone-positive breast cancer [122]. Capecitabine has been selected as a standard drug against HER 2. It is a chemotherapeutic drug used in the treatment of colon, breast, and rectal cancer [123]. Mifepristone has been selected as a standard drug against the progesterone receptor.

It is a synthetic steroid that blocks the progesterone hormone thus help fight breast cancer [124]. The 2-D structures of the selected drugs downloaded from PubChem are shown in Figure 4.55-4.57.

TABLE 4.41: Drugs and Their Mechanism of Action.

Sr. No	Drugs	Mechanism of Action	Ref.
1	Tamoxifen	Tamoxifen (TAM) has a dual mode of action: (1) it competes with 17-estradiol (E2) at the receptor site, blocking E2's development of breast cancer; and (2) it binds DNA following metabolic activation, and prevent carcinogenesis.	[122]
2	Capecitabine	Capecitabine is a prodrug that thymidine phosphorylase converts to its cytotoxic component, fluorouracil, in a tumor-specific manner. Fluorouracil is further converted in normal and malignant cells to two active metabolites, 5-fluoro-2-deoxyuridine monophosphate (FdUMP) and 5-fluorouridine triphosphate (FUTP). FUTP competes with uridine triphosphate to decrease RNA and protein synthesis, while FdUMP inhibits DNA synthesis by lowering normal thymidine biosynthesis.	[123]
3	Mifepristone	Mifepristone's anti-pregnant activity is due to a competitive interaction with progesterone at progesterone-receptor sites. At lower concentrations, MF suppresses the proliferation of many cancer cell lines with a cytostatic impact, which is associated with a decrease in	

the activity of the cell cycle regulatory
protein Cdk2.

[124]

TABLE 4.42: Physiochemical Properties of Drugs.

Sr. No	Properties	Tamoxifen	Capecitabine	Mifepristone
1	Chemical formula	$C_{26}H_{29}NO$	$C_{15}H_{22}FN_3O_6$	$C_{29}H_{35}NO_2$
2	Absorption	5 hours	Readily absorbed through the GI tract (~70%)	The absolute bioavailability of a 20mg oral dose is 69%
3	Water solubility mg/ml	0.00102	0.248 mg/mL	0.00336 mg/mL
4	LogP	5.9961	0.7602	5.4065
5	H-bond donor	0	3	1
6	H-bond Acceptor	2	8	3
7	Mol. weight	371.524 g/mol	359.3501 g/mol	429.5937
8	Rotatable bonds	8	6	2
9	Bio-availability	1	1	1
10	Polarizability	44.19 Å ³	35.81 Å ³	50.69 Å ³
11	ADMET probability	0.997	0.9513	1.0
12	Side Effects	Respiratory difficulty	Diarrhea, nausea, stomatitis, vomiting,	Lethargy, nausea,

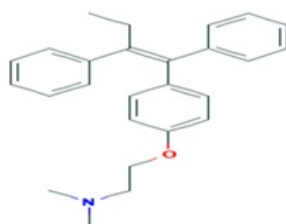


FIGURE 4.55: 2D Structure of Tamoxifen Drug- PubChem.

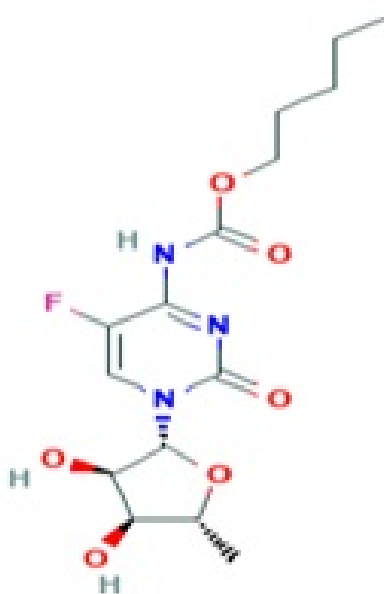


FIGURE 4.56: 2D Structure of Capecitabine Drug- PubChem.

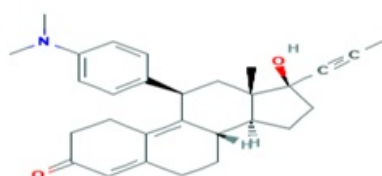


FIGURE 4.57: 2D Structure of Mifepristone Drug- PubChem.

4.9 Drug ADMET Properties

ADMET properties of reference drugs were explored by the pkCSM online prediction tool.

4.9.1 Toxicity Prediction of Reference Drugs

The predicted toxicity values of reference drug tamoxifen are listed in Table 4.43. The maximum tolerated dose value is as shown as 0.313 whereas this drug predicts itself as an hERG II inhibitor that means it inhibits potassium channels. LD₅₀ predicts toxic potency of drug and LOAEL tells about the lowest dose that causes adverse effects. Tamoxifen does not show itself as hepatotoxic that means it does not induce liver injury. *T. pyriformis* toxicity is used as a toxic endpoint. Tamoxifen is considered toxic against *T. pyriformis* (might not be harmful to human cells). Tamoxifen predicts minnow toxicity value as 0.6 log mM.

TABLE 4.43: Toxicity Values of Tamoxifen

Sr. No	Model Name	Predicted value
1	AMES toxicity	No
2	Max.tolerated dose(human)	0.313 mg/Kg
3	hERG I inhibitor	Yes
4	hERG II inhibitor	Yes
5	Oral rat acute toxicity	2.285 mg/Kg
6	Oral rat chronic toxicity	0.41 mg/Kg
7	Hepatotoxicity	No
8	Skin sensitization	No
9	<i>T. pyriformis</i> toxicity	0.316 log ug/L
10	Minnow toxicity	0.6 log mM

The predicted toxicity values of reference drug capecitabine are listed in Table 4.44. The maximum tolerated dose value is as shown as 1.051 whereas this drug does not predict itself as an hERG II inhibitor that means it does not inhibit potassium channels.

LD₅₀ predicts toxic potency of drug and LOAEL tells about the lowest dose that causes adverse effects. Capecitabine does show itself as hepatotoxic that means it does induce liver injury. Capecitabine is considered toxic against *T. pyriformis*

(might not be harmful to human cells). Capecitabine predicts minnow toxicity value as 2.893 mM.

TABLE 4.44: Toxicity Values of Capecitabine

Sr. No	Model Name	Predicted value
1	AMES toxicity	No
2	Max.tolerated dose(human)	1.051 mg/Kg
3	hERG I inhibitor	No
4	hERG II inhibitor	No
5	Oral rat acute toxicity	2.459 mg/Kg
6	Oral rat chronic toxicity	2.401 mg/Kg
7	Hepatotoxicity	Yes
8	Skin sensitization	No
9	<i>T. pyriformis</i> toxicity	0.288 log ug/L
10	Minnow toxicity	2.893 log Mm

The predicted toxicity values of the reference drug mifepristone are listed in Table 4.45. The maximum tolerated dose value is low as shown as -0.342 whereas this drug predicts itself as an hERG II inhibitor that means it inhibits potassium channels.

LD₅₀ predicts toxic potency of drug and LOAEL tells about the lowest dose that causes adverse effects. Mifepristone does not show itself as hepatotoxic that means it does not induce liver injury. Mifepristone is considered toxic against *T. pyriformis* (might not be harmful to human cells). Mifepristone predicts minnow toxicity value as -0.659 mM.

TABLE 4.45: Toxicity Values of Mifepristone.

Sr. No	Model Name	Predicted value
1	AMES toxicity	No
2	Max.tolerated dose(human)	-0.342 mg/Kg
3	hERG I inhibitor	No

4	hERG II inhibitor	Yes
5	Oral rat acute toxicity	2.61mg/Kg
6	Oral rat chronic toxicity	1.212mg/Kg
7	Hepatotoxicity	No
8	Skin sensitization	No
9	<i>T. pyriformis</i> toxicity	0.62 log ug/L
10	Minnow toxicity	-0.659 log mM

4.9.2 Absorption Properties

Tamoxifen shows absorption properties as shown in Table 4.46. As clear from the table, Tamoxifen is less soluble in water and has 96.85 % absorption in the small intestine of humans.

Skin permeability is low and shows a positive result as Pgp-substrate and Pgp I/II inhibitor. It means the standard drug has low oral absorption. Pgp I/II inhibitor 'YES' means tamoxifen has reduced pumping activity to pump out xenobiotics from cells and have high absorption.

TABLE 4.46: Absorption Properties of Tamoxifen.

Sr. No	Model Name	Value
1	Water solubility	-5.929 mol/L
2	CaCo ₂ permeability	1.065 cm/S
3	Intestinal absorption (human)	96.885%
4	Skin Permeability	-2.737 log Kp
5	P-glycoprotein substrate	Yes
6	P-glycoprotein I inhibitor	Yes
7	P-glycoprotein II inhibitor	Yes

Capecitabine shows absorption properties as shown in Table 4.47. As clear from the table, Capecitabine is less soluble in water and has 68.027 % absorption in the

small intestine of humans. Skin permeability is low and shows the negative result as Pgp-substrate and Pgp I/II inhibitor. It means the standard drug has high oral absorption. Pgp I/II inhibitor 'No' means capecitabine does not have reduced pumping activity to pump out xenobiotics from cells and have high absorption.

TABLE 4.47: Absorption Properties of Capecitabine.

Sr. No	Model Name	Value
1	Water solubility	-3.135 mol/L
2	CaCO ₂ permeability	0.255 cm/S
3	Intestinal absorption (human)	68.027 %
4	Skin Permeability	-2.755 log Kp
5	P-glycoprotein substrate	No
6	P-glycoprotein I inhibitor	No
7	P-glycoprotein II inhibitor	No

Mifepristone shows absorption properties as shown in Table 4.48. As clear from the table, Mifepristone is less soluble in water and mifepristone has 98.03 % absorption in the small intestine of humans. Skin permeability is low and shows the negative result as Pgp-substrate, but a Positive result as Pgp I/II inhibitor. It means the standard drug has high oral absorption. Pgp I/II inhibitor 'YES' means mifepristone has reduced pumping activity to pump out xenobiotics from cells and have high absorption.

TABLE 4.48: Absorption Properties of Mifepristone.

Sr. No	Model Name	Value
1	Water solubility	-5.97 mol/L
2	CaCO ₂ permeability	1.297 cm/S
3	Intestinal absorption (human)	98.023%
4	Skin Permeability	-2.9 log Kp
5	P-glycoprotein substrate	No

TABLE 4.48: Absorption Properties of Mifepristone.

Sr. No	Model Name	Value
6	P-glycoprotein I inhibitor	Yes
7	P-glycoprotein II inhibitor	Yes

4.9.3 Distribution Properties

Distribution properties consist of four models, among the first one is a volume of distribution in humans (VDss) expressed as log L/kg. Tamoxifen shows high VDss which means more of the drug is distributed in tissue rather than plasma. Fu (fraction unbound) predicts the unbounded friction in plasma, if it is more then the drug may be more effective. Our standard drug has a 0.093 Fu predicted value. The third model BBB permeability shows a value of 1.329 which is more than 0.3 thus it can penetrate the brain. The last model named CNS permeability expressed as log PS $>$ -3 is considered as poorly permeable while tamoxifen shows log PS = -1.473. The distribution properties of the standard drug are listed in Table 4.48.

TABLE 4.49: Distribution Properties of Tamoxifen.

Sr. No	Model Name	Value
1	VDss (human)	0.83 L/Kg
2	Fraction unbound (human)	0.093 Fu
3	BBB permeability	1.329 log BB
4	CNS permeability	-1.473 log PS

Capecitabine shows low VDss which means less of the drug is distributed in tissue rather than plasma. Our standard drug has a 0.394 Fu predicted value. The third model BBB permeability shows a value of -1.448 which is less than -1 thus poorly permeable to the brain. The last model named CNS permeability expressed as log

PS capecitabine shows $\log PS = -3.315$ thus considered poorly permeable to CNS. The distribution properties of the standard drug are listed in Table 4.50.

TABLE 4.50: Distribution Properties of Capecitabine.

Sr. No	Model Name	Value
1	VD _{ss} (human)	-0.396 L/Kg
2	Fraction unbound (human)	0.394 Fu
3	BBB permeability	-1.448 log BB
4	CNS permeability	-3.315 log PS

Distribution properties consist of four models, among the first one is a volume of distribution in humans (VD_{ss}) expressed as log L/kg. Mifepristone shows high VD_{ss} which means more of the drug is distributed in tissue rather than plasma.

Fu (fraction unbound) predicts the unbounded friction in plasma, if it is more than the drug may be more effective. Our standard drug has a 0.0Fu predicted value. The third model BBB permeability shows a value of -0.042 which is less than -1 thus considered poorly permeable to the brain.

The last model named CNS permeability expressed as log PS, mifepristone shows $\log PS = -2.266$ which is greater than -3 but less than -2. The distribution properties of the standard drug are listed in Table 4.54.

TABLE 4.51: Distribution Properties of Mifepristone.

Sr. No	Model Name	Value
1	VD _{ss} (human)	0.585 L/Kg
2	Fraction unbound (human)	0 Fu
3	BBB permeability	-0.042 log BB
4	CNS permeability	-2.266 log PS

4.9.4 Metabolic Properties

Reference drug's metabolic properties are given below in Table 4.52. Cytochrome P450 is a detoxification enzyme present in the liver and plays role in the excretion of exogenous compounds by oxidizing them. CYP2D6 & CYP3A4 are the two main isoforms of cytochrome P450. First & second model result shows that tamoxifen is metabolized by one isoform of cytochrome P450 (CYP3A4). Model no 4-5, 7 shows that drug is not an inhibitor for these isoforms of cytochrome P450 whereas model 3 and 6 named as CYP2D6 and CYP1A2 shows tamoxifen as an inhibitor for this isoform which changes the pharmacokinetics of tamoxifen.

TABLE 4.52: Metabolic Properties of Tamoxifen.

Sr. No	Model Name	Predicted Value
1	CYP2D6 substrate	No
2	CYP3A4 substrate	Yes
3	CYP1A2 inhibitor	Yes
4	CYP2C19 inhibitor	No
5	CYP2C9 inhibitor	No
6	CYP2D6 inhibitor	Yes
7	CYP3A4 inhibitor	No

Reference drug metabolic properties are given below in Table 4.53. Cytochrome P450 is a detoxification enzyme present in the liver and plays role in the excretion of exogenous compounds by oxidizing them. CYP2D6 & CYP3A4 are the two main isoforms of cytochrome P450. First & second model result shows that capecitabine is not metabolized by both isoforms of cytochrome P450. Model, no 3-7 shows that the drug is not an inhibitor for these isoforms of cytochrome P450.

TABLE 4.53: Metabolic Properties of Capecitabine.

Sr. No	Model Name	Predicted Value
1	CYP2D6 substrate	No

2	CYP3A4 substrate	No
3	CYP1A2 inhibitor	No
4	CYP2C19 inhibitor	No
5	CYP2C9 inhibitor	No
6	CYP2D6 inhibitor	No
7	CYP3A4 inhibitor	No

Reference drug's metabolic properties are given below in Table 4.54. Cytochrome P450 is a detoxification enzyme present in the liver and plays role in the excretion of exogenous compounds by oxidizing them. CYP2D6 & CYP3A4 are the two main isoforms of cytochrome P450. First & second model result shows that mifepristone is metabolized by one isoform of cytochrome P450 (CYP3A4). Model no 5-6, 7 shows that drug is not an inhibitor for these isoforms of cytochrome P450 whereas model 3 and 4 named as CYP2C19 and CYP1A2 shows mifepristone as an inhibitor for this isoform which changes the pharmacokinetics of mifepristone.

TABLE 4.54: Metabolic Properties of Mifepristone

Sr. No	Model Name	Predicted Value
1	CYP2D6 substrate	No
2	CYP3A4 substrate	Yes
3	CYP1A2 inhibitor	Yes
4	CYP2C19 inhibitor	Yes
5	CYP2C9 inhibitor	No
6	CYP2D6 inhibitor	No
7	CYP3A4 inhibitor	No

4.9.5 Excretion Properties

The predicted values of excretion of the reference drug are given in Table 4.55. Total clearance expressed as log (CL tot) value is 0.556 ml/min/kg which indicates

the hepatic and renal clearance of tamoxifen. Tamoxifen predicts Renal OCT2 substrate 'No' which means it is not interfering in the functioning of OCT2 in the cell,

TABLE 4.55: The Excretion Properties of Tamoxifen.

Sr. No	Model Name	Predicted Value
1	Total Clearance	0.556 ml/Kg
2	Renal OCT2 substrate	No

The predicted values of excretion of Capecitabine drug are given in Table 4.56. Total clearance expressed as log (CL tot) value is 1.054 ml/min/kg which indicates the hepatic and renal clearance of capecitabine. Capecitabine predicts Renal OCT2 substrate 'No' which means it is not interfering in the functioning of OCT2 in the cell.

TABLE 4.56: The Excretion Properties of Capecitabine.

Sr. No	Model Name	Predicted Value
1	Total Clearance	1.054 ml/Kg
2	Renal OCT2 substrate	No

The predicted values of excretion of the reference drug are given in Table 4.57. Total clearance expressed as log (CL tot) value is 0.316 ml/min/kg which indicates the hepatic and renal clearance of mifepristone. Mifepristone predicts Renal OCT2 substrate 'No' which means it is not interfering in the functioning of OCT2 in the cell.

TABLE 4.57: The Excretion Properties of Mifepristone.

Sr. No	Model Name	Predicted Value
1	Total Clearance	0.316 ml/Kg
2	Renal OCT2 substrate	No

4.10 Mechanism of Actions of Standard drugs

4.10.1 Tamoxifen Mechanism of Action

Tamoxifen (C07108) is a nonsteroidal antiestrogen that suppresses the growth of estrogen receptor-positive cancers and causes apoptosis [125]. Figure 4.58 depicts the competitive binding of estrogen hormone and tamoxifen medication to the ER receptor. Insulin-like growth factor 1 and tumor growth factor are both reduced by tamoxifen. It also induces an increase in sex hormone-binding globulin 1, which reduces the quantity of estradiol that is freely available. The amounts of substances that promote tumor growth are reduced as a result of these alterations [126].

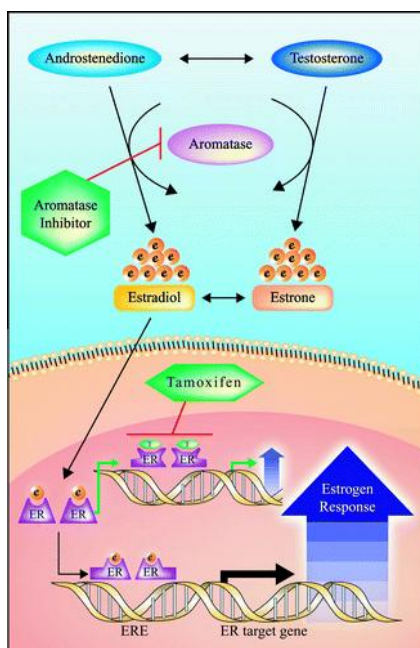


FIGURE 4.58: Mechanism of Action of Tamoxifen [131].

Tamoxifen has a limited affinity for the estrogen receptor on its own. It is converted in the liver into the active forms of afimoxifene (4-hydroxy tamoxifen) and endoxifen (N-desmethyl-4-hydroxy tamoxifen), which bind to target proteins more competitively. Afimoxifene inhibits the transcription of estrogen-sensitive genes by acting as an estrogen receptor antagonist [127]. The binding of 4-hydroxy tamoxifen with ER brings NCoR and SMRT protein which act as co-repressor thus

regulate several other proteins [128]. NcoR and SMRT bind directly to transcription factors and cause their deregulation by forming stable complexes with histone deacetylase 3, and G protein pathway receptor, transducin b like protein1/TBL1 related protein 1. Tamoxifen requires protein PAX2 to help in the suppression of pro-proliferative protein ERBB [129]. Tamoxifen also causes apoptosis by preventing DNA synthesis by inhibiting protein kinase C. This apoptotic effect can also result due to a 3-fold increase level of calcium in the cytoplasm and mitochondria after the induction of tumor growth factor β [130].

4.10.2 Capecitabine Mechanism of Action

Capecitabine is a prodrug that is converted to fluorouracil by the enzyme thymidine phosphorylase, which is abundant in tumor cells. Fluorouracil is a cytotoxic moiety that is converted into two active metabolites in tumor and normal cells, 5-fluoro-2'-deoxyuridine 5'-monophosphate (FdUMP) and 5-fluorouridine triphosphate (FUTP). Fluorouracil has two mechanisms for cell killing. By attaching to thymidylate synthase, FdUMP and N5-10-methylenetetrahydrofolate (the folate cofactor) form a covalently bonded ternary complex (TS). By blocking the synthesis of thymidylate, this complex hinders DNA synthesis (precursor of thymidine triphosphate). Second, during the synthesis of RNA by transcriptional enzyme, FUTP is incorrectly substituted for uridine triphosphate (UTP), resulting in the creation of fraudulent RNA [132].

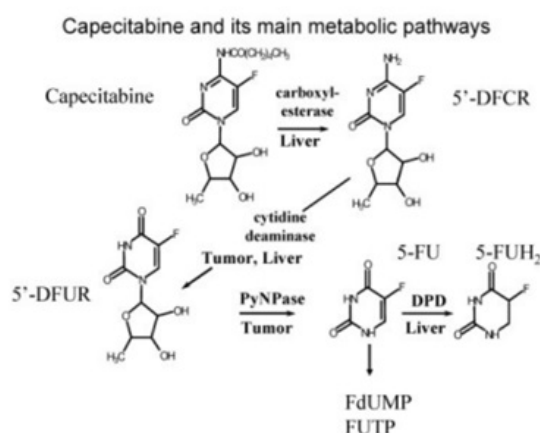


FIGURE 4.59: Capecitabine and its main metabolic pathway [133].

4.10.3 Mifepristone Mechanism of Action

Mifepristone (MF, RU486) has a strong antagonist activity against the progesterone receptor. It acts as a progesterone receptor modulator [134]. At the molecular level, MF can bind the receptor with high binding affinity, its phenylamino dimethyl group in the 11β -position binds to receptor binding pocket at a specific position and cause Trans conformation changes in the ligand-binding domain. Mifepristone can cause dose and time-dependent cytotoxicity by inducing apoptosis (DNA fragmentation), downregulating bcl 2, and inducing protein TGF beta1 [135].

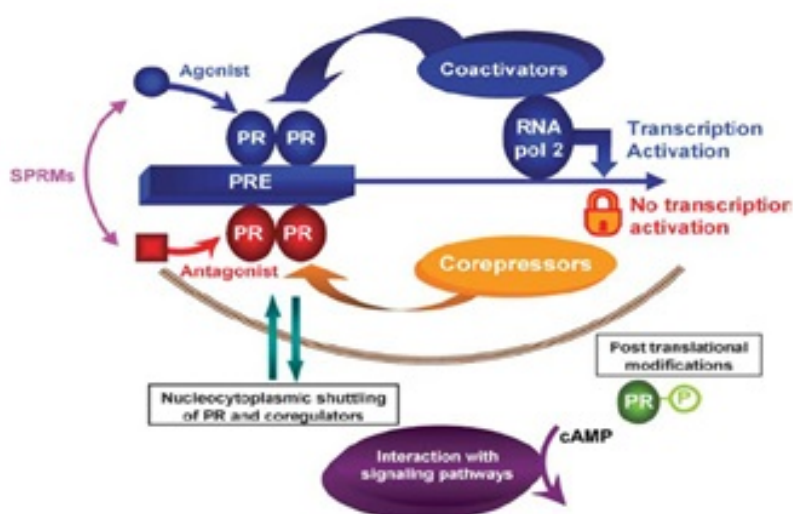


FIGURE 4.60: Mechanism of Action of Mifepristone [138].

MF can cause inhibition in cell growth by arresting the cell in the G1 phase of the cell cycle. Increase MF exposure to cancer cells increases the concentration of inhibitor of cell cycle p21cip1 and p27kip1 and cause a decline in abundance of Cdk 2 and cyclin E. It can also reduce the activity of Cdk2 [136]. Mifepristone prevents cancer cells from adhesion and metastasis by interacting with key signaling proteins FAK which is involved in carcinogenesis and tumor metastasis. FAK is the key protein that interacts with other adapter proteins Src and paxillin and is involved in the assembly of focal adhesion and integrin engagement. Thus, mifepristone prevents metastasis by decreasing FAK expression at both protein level and mRNA level as shown in figure 4.58 [137].

4.11 Effects on Body of Standard drugs

4.11.1 Tamoxifen Effects on Body

In breast and mammary tissue, tamoxifen is anti-estrogenic. Tamoxifen, which works like estrogen in bone and decreases circulating cholesterol in the body, has been used to treat hypercholesterolemia [139].

Tamoxifen may lower the levels of serum cholesterol, low-density lipoprotein cholesterol, and fibrinogen, which may minimize the risk of cardiovascular disease [140]. Tremor, hyperreflexia, unsteady gait, and dizziness are signs of acute neurotoxicity caused by high doses of tamoxifen [141].

Menopause-like symptoms such as hot flashes, night sweats, and vaginal dryness, weight gain and edema, unpredictability or disappearance of feminine periods, leg swelling, nausea, vaginal release, skin rash, erectile dysfunction, exhaustion, and migraines are all possible side effects of tamoxifen. Tamoxifen use has been linked to birth abnormalities, blood clots, cataracts, uterine cancer, and the risk of stroke.

4.11.2 Capecitabine Effects on Body

Cardiotoxicity occurs in 3% of capecitabine-treated people and can be deadly [142]. Diarrhea is reported commonly in many patients and can get severe in some cases [143]. Hand-foot skin reactions often appear in a patient undergoing treatment.

In this condition, the palm of hand and sole of feet become numb, dry, red, and blister making it difficult and painful for the patient to do routine activities [144]. Adermatoglyphia (fingerprint loss) has been seen in capecitabine-treated patients [145].

Severe hyperbilirubinemia has also been observed in a patient undergoing capecitabine therapy. Other side effects include nausea, stomatitis, vomiting, dizziness, insomnia, and headache.

4.11.3 Mifepristone Effects on Body

This drug has been used to control hyperglycemia and to treat hypercortisolism. More intense bleeding than a heavy menstrual cycle, uterine cramping, nausea, abdominal pain, diarrhea, and vomiting are some of the drug's side effects. Patients taking mifepristone may report symptoms of back pain, indigestion, anemia, abdominal cramping, viral infection, vaginal discharge, weakness, and pelvic pain. It can slow down the removal of other drugs from your body thus affecting the normal working of drugs [146].

4.12 Docking Results of Standard drugs

4.12.1 Tamoxifen Docking

Tamoxifen as a ligand was docked by an online automatic docking tool that is CB dock. The drug target was the estrogen receptor in this research work. The best docking score was -9.2. Molecular docking interactions of the docked drug with the target are listed below in Table 4.58.

TABLE 4.58: Tamoxifen Docking Score via CB Dock.

Sr. No	Docking Score	Values
1	Binding scores	-9.2
2	Cavity size	1905
3	HBD	0
4	HBA	2
5	Log P	5.9961
6	Molecular weight g/mol	371.524 g/mol
7	Rotatable bond	8
8	Grid map	42
9	Min energy kcal/mol	0
10	Max energy kcal/mol	1.60E+00

4.12.2 Capecitabine Docking

Capecitabine as a ligand was docked by an online automatic docking tool that is CB dock. The drug target was HER2 in this research work. The best docking score was -7.5. Molecular docking interactions of the docked drug with the target are listed below in Table 4.59.

TABLE 4.59: Capecitabine Docking Score via CB Dock.

Sr. No	Docking Score	Values
1	Binding scores	-7.5
2	Cavity size	665
3	HBD	3
4	HBA	8
5	Log P	0.7602
6	Molecular weight g/mol	359.3501 g/mol
7	Rotatable bond	6
8	Grid map	1
9	Min energy kcal/mol	0
10	Max energy kcal/mol	1.60E+00

4.12.3 Mifepristone Docking

Mifepristone as a ligand was docked by an online automatic docking tool that is CB dock. The drug target was the progesterone receptor in this research work. The best docking score was -7.7. Molecular docking interactions of the docked drug with the target are listed below in Table 4.60.

TABLE 4.60: Mifepristone Docking Score via CB Dock.

Sr. No	Docking Score	Values
1	Binding scores	-7.7
2	Cavity size	206

3	HBD	1
4	HBA	3
5	Log P	5.4065
6	Molecular weight g/mol	429.5937 g/mol
7	Rotatable bond	2
8	Grid map	22
9	Min energy kcal/mol	0
10	Max energy kcal/mol	1.60E+00

4.13 Standard Drugs and Lead Compounds Comparison

The standard drugs and lead compounds were compared for their physicochemical and pharmacokinetic properties to assess their bioavailability, drug-likeness, efficacy, and safety.

All these compounds passed the drug-likeness criteria (Lipinski's rule of five). However, luteolin has low molecular weight and log P value than tamoxifen and shows 4 H-BD and 6 H-BA whereas tamoxifen shows 0 H-BD and 2 H-BA (Table 4.61).

TABLE 4.61: Luteolin - Tamoxifen Lipinski Rule of Five.

Sr. No	Name of compound	Log P-value	Molecular Weight	H-bond donor	H-bond acceptor
1	Luteolin	2.2824	286.24 g/mol	4	6
2	Tamoxifen	5.9961	371.524 g/mol	0	2

Artemisone has high molecular weight and log P value than capecitabine and shows 0 H-BD and 7 H-BA whereas capecitabine shows 3 H-BD and 8 H-BA (Table 4.62).

TABLE 4.62: Artemisone- Capecitabine Lipinski Rule of Five.

Sr. No	Name of compound	Log P-value	Molecular Weight	H-bond donor	H-bond acceptor
1	Artemisone	1.9248	401.5 g/mol	0	7
2	Capecitabine	0.7602	359.3501 g/mol	3	8

Kaempferol has low molecular weight and log P value than mifepristone and shows 4 H-BD and 6 H-BA whereas mifepristone shows 1 H-BD and 3 H-BA (Table 4.63).

TABLE 4.63: Kaempferol - Mifepristone Lipinski Rule of Five.

Sr. No	Name of compound	Log P-value	Molecular Weight	H-bond donor	H-bond acceptor
1	Kaempferol	2.2824	152.237 g/-mol	4	6
2	Mifepristone	5.4065	429.5937 g/mol	1	3

4.13.1 ADMET Properties Comparison

Pharmacokinetics properties play a critical role in the screening of compounds as drug candidates. ADMET properties were compared by using Byju's 'Greater Than Calculator' learning app. Pharmacokinetic properties of reference drug and lead compound are listed in Table 4.65 to 4.78.

4.13.1.1 Toxicity Comparison

Toxicity is the most important parameter of pharmacokinetic (ADMET) properties which consists of 10 models. Model 1 of AMES toxicity shows that both standard drug and lead compound are not mutagenic.

Maximum tolerated dose helps to set maximum recommended tolerated dose if the value is equal or less than 0.477 log mg/kg/day then considered low and greater

values are considered high table shows 0.313 log mg/Kg/day value for tamoxifen and log mg/kg/day=0.499 for luteolin which shows bio compound is ahead in safety than reference drug. The models h ERG I/II inhibitors predict either analyzed compounds are inhibitors of potassium channels or not. If the answer is 'yes' then the compound may not be fit for the drug. From table 4.64, it is evident that tamoxifen shows itself as an h ERG II inhibitor. Mostly h ERG I/II inhibitors are withdrawal from the pharmaceutical market. The model named oral rat acute toxicity (LD₅₀) expressed as mol/kg is the amount of drug that can cause the death of 50% of rats (test animals).

The LD₅₀ value of tamoxifen is slightly lower than luteolin. Oral rat chronic toxicity (LOAEL) determines the lowest dose of a drug which can produce adverse effects over long duration usage (chronic use) of a drug. LOAEL predicted value of tamoxifen is less than luteolin which shows its potency to be less toxic than bio compound. Hepatotoxicity simply indicates the injury to the liver which shows result in two categories yes/no. Tamoxifen predicted result shows it as non-hepatotoxic also luteolin is not a hepatotoxic compound (Table 4.64).

Both compounds do not cause any allergic reactions. *T. pyriformis* toxicity value >- 0.5 is considered toxic according to which both tamoxifen and luteolin are considered toxic to *T. pyriformis*. For minnow toxicity values below 0.5mM are considered toxic. Tamoxifen's predicted value is 0.6mM, whereas 3.169 m M is the predicted value of luteolin. Both compounds pass this toxicity test. Overall, the models of toxicity show luteolin as a safe compound than tamoxifen.

TABLE 4.64: Toxicity Values of Tamoxifen & Luteolin.

Sr. No	Model Name	Predicted Values	
		Tamoxifen	Luteolin
1	AMES toxicity	No	No
2	Max.tolerated dose(human)	0.313 mg/Kg	0.499 mg/Kg
3	hERG I inhibitor	Yes	No
4	hERG II inhibitor	Yes	No

5	Oral rat acute toxicity	2.285 mg/Kg	2.455 mol/Kg
6	Oral rat chronic toxicity	0.41 mg/Kg	2.409 mg/Kg
7	Hepatotoxicity	No	No
8	Skin sensitization	No	No
9	<i>T. pyriformis</i> toxicity	0.316 log ug/L	0.326 log ug/L
10	Minnow toxicity	0.6 log mM	3.169 log mM

Model 1 of AMES toxicity shows that both standard drug and lead compound are not mutagenic. Maximum tolerated dose helps to set maximum recommended tolerated dose if the value is equal or less than 0.477 log mg/kg/day then considered low and greater values are considered high table shows 1.051 log mg/Kg/day value for capecitabine and log mg/kg/day=-0.475 for artemisone. From Table 4.64, it is evident that both capecitabine and artemisone do not show themselves as h ERG II inhibitors. The LD₅₀ value of capecitabine is slightly lower than artemisone. LOAEL predicted value of capecitabine is more than artemisone which shows its potency to be more toxic than bio compound. Both compounds predicted results show them as hepatotoxic (Table 4.64). Both compounds do not cause any allergic reactions. *T. pyriformis* toxicity value > -0.5 is considered toxic according to which both tamoxifen and luteolin are considered toxic to *T. pyriformis*. For minnow toxicity values below 0.5mM are considered toxic. Capecitabine predicted value is 2.893mM, whereas 2.089mM is the predicted value of artemisone. Both compounds pass this toxicity test. Overall, the models of toxicity show artemisone as a safe compound than capecitabine.

TABLE 4.65: Toxicity Values of Capecitabine & Artemisone

Sr. No	Model Name	Predicted Values	
		Capecitabine	Artemisone
1	AMES Toxicity	No	No
2	Max.tolerated dose(human)	1.051 mg/Kg	-0.475 mg/Kg
3	hERG I inhibitor	No	No
4	hERG II inhibitor	No	No

TABLE 4.65: Toxicity Values of Capecitabine & Artemisone

Sr. No	Model Name	Predicted Values	
		Capecitabine	Artemisone
5	Oral rat acute toxicity	2.459 mg/Kg	2.98 mol/Kg
6	Oral rat chronic toxicity	2.401 mg/Kg	1.066 mg/Kg
7	Hepatotoxicity	Yes	Yes
8	Skin sensitization	No	No
9	<i>T. pyriformis</i> toxicity	0.288 log ug/L	0.285 log ug/L
10	Minnow toxicity	2.893 log mM	2.089 log mM

Model 1 of AMES toxicity shows that both standard drug and lead compound are not mutagenic. Maximum tolerated dose helps to set maximum recommended tolerated dose if the value is equal or less than 0.477 log mg/kg/day then considered low and greater values are considered high table shows log -0.342 mg/Kg/day value for mifepristone and log mg/kg/day=0.531 for kaempferol which shows bio compound is ahead in safety than reference drug. From Table 4.65, it is evident that mifepristone shows itself as h ERG II inhibitor and kaempferol does not show itself as h ERG II inhibitor.

The LD₅₀ value of mifepristone is slightly more than kaempferol. LOAEL predicted value of mifepristone is less than kaempferol which shows its potency to be less toxic than bio compound. The predicted result shows mifepristone and kaempferol as non-hepatotoxic (Table 4.66). Both compounds do not cause any allergic reactions.

T. pyriformis toxicity value > -0.5 is considered toxic according to which both mifepristone and kaempferol are considered toxic to *T. pyriformis*. For minnow toxicity values below 0.5 mM are considered toxic. The predicted value is -0.659m M, whereas 2.885 log m M is the predicted value of kaempferol. According to which mifepristone is toxic and kaempferol is considered nontoxic Overall, the models of toxicity show kaempferol as a safe compound than mifepristone.

TABLE 4.66: Toxicity Values of Mifepristone & Kaempferol.

Sr. No	Model Name	Predicted Values	
		Mifepristone	Kaempferol
1	AMES Toxicity	No	No
2	Max.tolerated dose(human)	-0.342 mg/Kg	0.531 mg/Kg
3	hERG I inhibitor	No	No
4	hERG II inhibitor	Yes	No
5	Oral rat acute toxicity	2.61mg/Kg	2.449 mol/Kg
6	Oral rat chronic toxicity	1.212mg/Kg	2.505 mg/Kg
7	Hepatotoxicity	No	No
8	Skin sensitization	No	No
9	<i>T. pyriformis</i> toxicity	0.62 log ug/L	0.312 log ug/L
10	Minnow toxicity	-0.659 log mM	2.885 log mM

4.13.1.2 Absorption Properties Comparison

From Table 4.67 it is evident that water solubility of the standard drug is less than the lead compound. CaCo₂ permeability model is within a safe range for both compounds but luteolin shows less value than tamoxifen. Model intestinal absorption in humans predicts 81.13% & 96.885% values for luteolin and tamoxifen respectively. Both compounds predict low skin permeability. Tamoxifen falls in the 'Yes' category for P-gp substrate and P-gp I/II inhibitors' while luteolin stands in the 'Yes' category for P-gp substrate and 'No' category for P-gp I/II inhibitors' models. This means tamoxifen and luteolin as P-gp substrate shows low oral absorption and as P-gp I/II inhibitor reduce the pumping out of xenobiotics and toxins activity of P-gp from cell and may have high absorption.

TABLE 4.67: Absorption Properties of Tamoxifen & Luteolin.

Sr. No	Absorption Properties	Tamoxifen	Luteolin
1	Water solubility	-5.929 mol/L	-3.094 mol/L

2	CaCo ₂ permeability	1.065 cm/S	0.096 cm/S
3	Intestinal absorption (human)	96.885%	81.13 %
4	Skin Permeability	-2.737 log Kp	-2.735 log Kp
5	P-glycoprotein substrate	Yes	Yes
6	P-glycoprotein I inhibitor	Yes	No
7	P-glycoprotein II inhibitor	Yes	No

From Table 4.68 it is evident that water solubility of the lead compound is less than the standard drug. CaCo₂ permeability model is within a safe range for both compounds but capecitabine shows less value than artemisone. Model intestinal absorption in humans predicts 68% & 95.812% values for capecitabine and artemisone respectively. Both compounds predict low skin permeability. Artemisone and capecitabine stand-in 'No' category for all these three models.

TABLE 4.68: Absorption Properties of Capecitabine & Artemisone.

Sr. No	Absorption Properties	Capecitabine	Artemisone
1	Water solubility	-3.135 mol/L	-3.788 mol/L
2	CaCo ₂ permeability	0.255 cm/S	1.124 cm/S
3	Intestinal absorption (human)	68.027 %	95.812%
4	Skin Permeability	-2.755 log Kp	-2.74 log Kp
5	P-glycoprotein substrate	No	No
6	P-glycoprotein I inhibitor	No	No
7	P-glycoprotein II inhibitor	No	No

From Table 4.69 it is evident that water solubility of the standard drug is less than the lead compound. CaCo₂ permeability model is within a safe range for both compounds but mifepristone shows more value than kaempferol.

Model intestinal absorption in humans predicts 98% & 74.29% values for mifepristone and kaempferol respectively. Both compounds predict low skin permeability. Kaempferol falls in the 'Yes' category for P-gp substrate and 'No' for P-gp I/II

inhibitors while mifepristone stands in the 'No' category for P-gp substrate and 'No' for P-gp I/II inhibitors.

TABLE 4.69: Absorption Properties of Mifepristone & Kaempferol.

Sr. No	Absorption Properties	Mifepristone	Kaempferol
1	Water solubility	-5.97 mol/L	-3.04 mol/L
2	CaCo ₂ permeability	1.297 cm/S	0.032 cm/S
3	Intestinal absorption (human)	98.023%	74.29 %
4	Skin Permeability	-2.9 log Kp	-2.735 log Kp
5	P-glycoprotein substrate	No	Yes
6	P-glycoprotein I inhibitor	Yes	No
7	P-glycoprotein II inhibitor	Yes	No

4.13.1.3 Distribution Properties Comparison

The first model of distribution properties VD_{ss} (human) is the uniform distribution of the drug in the blood plasma and if the value is above 2.81 L/ kg then the drug is more distributed in the tissue rather than blood plasma. Both tamoxifen and luteolin have reasonable VD_{ss} values. Fu value of luteolin is more than tamoxifen which shows luteolin is more effective than reference drug in case of unbounded friction present in plasma. For BBB permeability if the value is greater than 0.3 then the drug is easily cross the blood-brain barriers and if <-1 then the drug is not or poorly distributed to the brain. Luteolin has a value > -1 but less than 0.3 whereas tamoxifen has a value greater than 0.3 thus considered permeable to the brain. CNS permeability if > -2 then the drug can easily penetrate the central nervous system and if <-3 then it is considered poorly permeable. Luteolin and tamoxifen has value > -3 as shown in Table 4.70.

TABLE 4.70: Distribution Properties of Tamoxifen & Luteolin.

Sr. No	Distribution Properties	Tamoxifen	Luteolin
1	VD _{ss} (human)	0.83 L/Kg	1.153 L/Kg

2	Fraction unbound (human)	0.093 Fu	0.168 Fu
3	BBB permeability	1.329 log BB	-0.907 log BB
4	CNS permeability	-1.473 log PS	-2.251 log PS

The first model of distribution properties VD_{ss} (human) is the uniform distribution of the drug in the blood plasma and if the value is above 2.81 L/ kg then the drug is more distributed in the tissue rather than blood plasma. Both capecitabine and artemisone have reasonable VD_{ss} values. Fu value of artemisone is more than capecitabine.

For BBB permeability if the value is greater than 0.3 then the drug easily crosses the blood-brain barriers and if <-1 then the drug is not or poorly distributed to the brain. Capecitabine has a value <-1 which indicates it is poorly permeable to the brain whereas artemisone has a value > -1 but less than 0.3. CNS permeability <-3 is considered poorly permeable. Both capecitabine and artemisone have values <-3 thus poorly permeable to CNS as shown in Table 4.71.

TABLE 4.71: Distribution Properties of Capecitabine & Artemisone.

Sr. No	Distribution Properties	Capecitabine	Artemisone
1	VD_{ss} (human)	-0.396 L/Kg	0.075 L/Kg
2	Fraction unbound (human)	0.394 Fu	0.493 Fu
3	BBB permeability	-1.448 log BB	-0.331 log BB
4	CNS permeability	-3.315 log PS	-3.081 log PS

The first model of distribution properties VD_{ss} (human) is the uniform distribution of the drug in the blood plasma and if the value is above 2.81 L/ kg then the drug is more distributed in the tissue rather than blood plasma. Both mifepristone and kaempferol have reasonable VD_{ss} values. Fu value of kaempferol is more than mifepristone which shows kaempferol is more effective than reference drug in case of unbounded friction present in plasma. For BBB permeability if the value is greater than 0.3 then the drug easily crosses the blood-brain barriers and if <-1

then the drug is not or poorly distributed to the brain. Both compounds have values > -1 but less than 0.3 . CNS permeability if > -2 then the drug can easily penetrate the central nervous system and if < -3 then it is poorly permeable. Both compounds have values > -3 but < -2 as shown in Table 4.72.

TABLE 4.72: Distribution Properties of Mifepristone & Kaempferol.

Sr. No	Distribution Properties	Mifepristone	Kaempferol
1	VD _{ss} (human)	0.585 L/Kg	1.274 L/Kg
2	Fraction unbound (human)	0 Fu	0.178 Fu
3	BBB permeability	-0.042 log BB	-0.939 log BB
4	CNS permeability	-2.266 log PS	-2.228 log PS

4.13.1.4 Metabolic Properties Comparison

Metabolic properties are predicted based on isoforms of cytochrome P450 which are CYP2D6, CYP3A4, CYP1A2, CYP2C19, and CYP2C9. Table 4.73 shows tamoxifen as a substrate of CYP3A4 isoforms whereas luteolin is not predicted as a substrate of these isoforms. Tamoxifen predicts itself as an inhibitor of CYP1A2 and CYP2D6 which are the main isoforms for drug metabolism while luteolin shows itself as inhibiting CYP1A2 and CYP2C9 isoforms.

TABLE 4.73: Metabolic Properties of Tamoxifen & Luteolin.

Sr. No	Metabolic Properties	Tamoxifen	Luteolin
1	CYP2D6 substrate	No	No
2	CYP3A4 substrate	Yes	No
3	CYP1A2 inhibitor	Yes	Yes
4	CYP2C19 inhibitor	No	No
5	CYP2C9 inhibitor	No	Yes
6	CYP2D6 inhibitor	Yes	No
7	CYP3A4 inhibitor	No	No

Metabolic properties are predicted based on isoforms of cytochrome P450 which are CYP2D6, CYP3A4, CYP1A2, CYP2C19, and CYP2C9. Artemisone and capecitabine are not predicted as a substrate of these isoforms. Both compounds are not inhibitors of any isoform as shown in Table 4.74.

TABLE 4.74: Metabolic Properties of Capecitabine & Artemisone

Sr. No	Metabolic Properties	Capecitabine	Artemisone
1	CYP2D6 substrate	No	No
2	CYP3A4 substrate	No	No
3	CYP1A2 inhibitor	No	No
4	CYP2C19 inhibitor	No	No
5	CYP2C9 inhibitor	No	No
6	CYP2D6 inhibitor	No	No
7	CYP3A4 inhibitor	No	No

Metabolic properties are predicted based on isoforms of cytochrome P450 which are CYP2D6, CYP3A4, CYP1A2, CYP2C19, and CYP2C9. Table 4.75 shows mifepristone as a substrate of CYP3A4 isoform whereas kaempferol is not predicted as a substrate of these isoforms. Mifepristone predicts itself as an inhibitor of CYP1A2 and CYP2C19 which are the main isoforms for drug metabolism while kaempferol shows itself as inhibiting CYP1A2 isoform.

TABLE 4.75: Metabolic Properties of Mifepristone & Kaempferol.

Sr. No	Metabolic Properties	Mifepristone	Kaempferol
1	CYP2D6 substrate	No	No
2	CYP3A4 substrate	Yes	No
3	CYP1A2 inhibitor	Yes	Yes
4	CYP2C19 inhibitor	Yes	No
5	CYP2C9 inhibitor	No	No
6	CYP2D6 inhibitor	No	No
7	CYP3A4 inhibitor	No	No

4.13.1.5 Excretion Properties Comparison

Excretion properties consist of two models with predicted values are displayed in Table 4.76. The predicted value of drug clearance as total clearance of tamoxifen is high as compared to luteolin.

Both compounds stand in the 'No' category for the Renal OCT2 substrate model, which means that they do not interfere in the normal functioning of organic cation transporter 2 who plays role in renal clearance of drugs.

TABLE 4.76: Excretion Properties of Tamoxifen & Luteolin.

Sr. No	Excretion Properties	Tamoxifen	Luteolin
1	Total Clearance	0.556 ml/Kg	0.495 ml/Kg
2	Renal OCT2 substrate	No	No

Excretion properties consist of two models with predicted values are displayed in Table 4.77.

The predicted value of drug clearance as total clearance of capecitabine is high as compared to artemisone. Both compounds stand in the 'No' category for the Renal OCT2 substrate model.

TABLE 4.77: Excretion Properties of Capecitabine & Artemisone.

Sr. No.	Excretion Properties	Capecitabine	Artemisone
1	Total Clearance	1.054 ml/Kg	0.377 ml/Kg
2	Renal OCT2 substrate	No	No

The predicted value of drug clearance as total clearance of kaempferol is high as compared to mifepristone. Both compounds stand in the 'No' category for the Renal OCT2 substrate model as shown in Table 4.78.

TABLE 4.78: Excretion Properties of Mifepristone & Kaempferol.

Sr. No	Excretion Properties	Mifepristone	Kaempferol
1	Total Clearance	0.316 ml/Kg	0.477 ml/Kg
2	Renal OCT2 substrate	No	No

4.13.2 Physiochemical Properties Comparison

Physiochemical properties describe the fundamental properties of compounds which also act as primary screeners to sort out compounds with desirable properties. Tamoxifen consists of 57 atoms of carbon, hydrogen, oxygen, and nitrogen whereas luteolin consists of 31 atoms of carbon, hydrogen, and oxygen which shows its simplicity as a bio-compound.

The molecular weight and log P value of tamoxifen are also high than luteolin. Luteolin donates 4 more hydrogen than tamoxifen which shows its oxidation power. Rotatable bonds if more than 10 show decreased oral bioavailability and tamoxifen has 8 rotatable bonds as compares to luteolin which has only 1 rotatable bond as shown in Table 4.79.

TABLE 4.79: Physiochemical Properties of Tamoxifen & Luteolin.

Sr. No	Drug	logP Value	Rotatable Bonds	H-bond Acceptor	H-bond Donor	Mol. Formula	Mol. Weight
1	Luteolin	2.2824	1	6	4	C ₁₅ H ₁₀ O ₆	286.24 g/mol
2	Tamoxifen	5.9961	8	2	0	C ₂₆ H ₂₉ NO	371.524

Capecitabine consists of 47 atoms of carbon, hydrogen, oxygen, fluorine, and nitrogen whereas artemisone consists of 112 atoms of carbon, hydrogen, nitrogen, sulphur, and oxygen. The molecular weight and log P value of artemisone are high

than capecitabine. Capecitabine donates 2 more hydrogens than artemisone. Rotatable bonds if more than 10 show decreased oral bioavailability and capecitabine has 6 rotatable bonds as compares to artemisone which has only 1 rotatable bond as shown in Table 4.80.

TABLE 4.80: Physiochemical Properties of Capecitabine & Artemisone.

Sr. No	Drug	logP Value	Rotatable Bonds	H-bond Acceptor	H-bond Donor	Mol. Formula	Mol. Weight
1	Artemisone	1.9248	1	7	0	C ₁₉ H ₃₁ NO ₆ S	401.5 g/mol
2	Capecitabine	0.7602	6	8	3	C ₁₅ H ₂₂ FN ₃ O ₆	359. 3501 g/mol

Mifepristone consists of 67 atoms of carbon, hydrogen, oxygen, and nitrogen whereas kaempferol consists of 31 atoms of carbon, hydrogen, and oxygen which shows its simplicity as a bio-compound. The molecular weight and log P value of mifepristone are also high than kaempferol. Kaempferol donates 2 more hydrogen than mifepristone which shows its oxidation power. Rotatable bonds if more than 10 show decreased oral bioavailability and mifepristone has 2 rotatable bonds as compares to kaempferol which has only 1 rotatable bond as shown in Table 4.81.

TABLE 4.81: Physiochemical Properties of Mifepristone & Kaempferol.

Sr. No	Drug	logP Value	Rotatable Bonds	H-bond Acceptor	H-bond Donor	Mol. Formula	Mol. Weight
1	Kaempferol	2.2824	1	6	4	C ₁₅ H ₁₀ O ₆	286.24 g/mol
2	Mifepristone	5.4065	2	3	1	C ₂₉ H ₃₅ NO ₂	429.5937 g/mol

4.13.3 Docking Score Comparison

In drug development, finding protein-ligand binding sites and conformations is critical. CB-dock, which predicts the cavities of the protein and calculates the centers and sizes of the top 5 cavities for all three proteins individually, was used to dock a conventional medication as a ligand against specified receptors. Results of docking of standard drugs and lead compounds against selected three receptors namely estrogen receptor, HER2 receptor, progesterone receptor is shown in table 4.82. The highest binding score shown by luteolin is -9.0 against estrogen receptor which is less than tamoxifen which shows -9.2 against the same protein.

Among the top 5 cavities (n=5 by default), the first one for both ligands is displayed in Figures 4.61 & 4.66. The highest binding score shown by artemisone is -8.8 against HER2 receptor which is higher than capecitabine who shows -7.5 against the same protein. The highest binding score shown by kaempferol is -9.2 against progesterone receptor which is higher than mifepristone who shows -7.7 against the same protein. Among the top 5 cavities (n=5 by default), the first one for both ligands is displayed in Figures 4.61 -4.66. All the interaction visualization analysis studies are performed by PyMol molecular visualization tool and LIGPLOT+ (V.1.4.5).



FIGURE 4.61: Best Pose Interaction of Luteolin as Ligand with ER.



FIGURE 4.62: Best Pose Interaction of Tamoxifen as Ligand with ER.

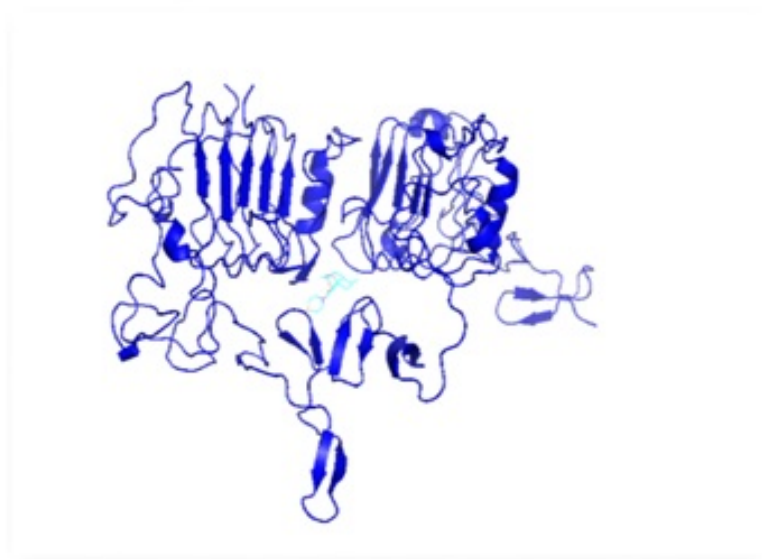


FIGURE 4.63: Best Pose Interaction of Artesmisone as Ligand with HER2.

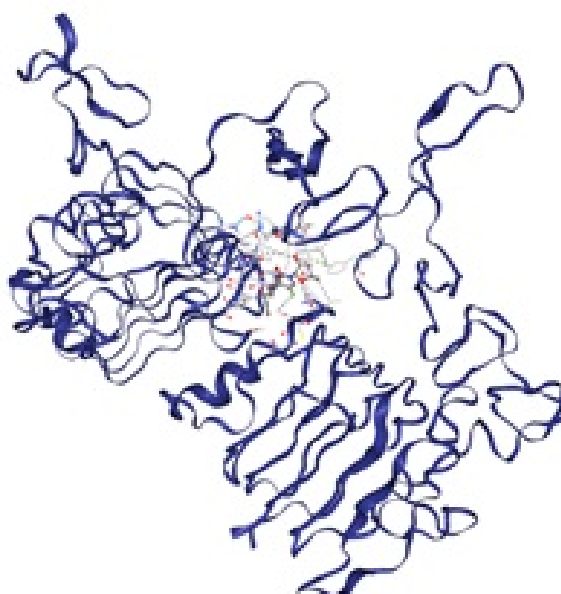


FIGURE 4.64: Best Pose Interaction of Capecitabine as Ligand with HER2.

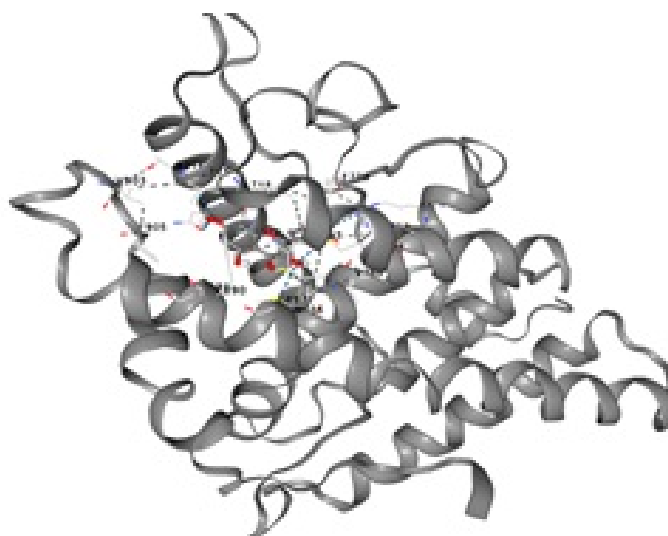


FIGURE 4.65: Best Pose Interaction of Kaempferol as Ligand with PR.

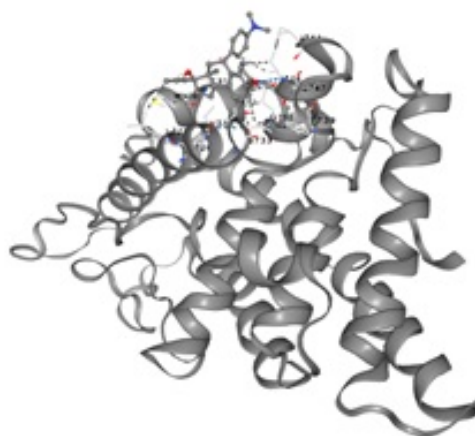


FIGURE 4.66: Best Pose Interaction of Mifepristone as Ligand with PR.

4.13.3.1 Docking Analysis Comparison

Best docking scores of reference drug and lead compound are analyzed by LIG-PLOT+ (V.1.4.5), and shown in Figure 4.67 & 4.72. Docking results are analyzed based on;

1. No. of hydrogen bonds.
2. No. of steric interactions.
3. No. of interacting amino acids.

TABLE 4.82: Hydrogen Bonds and Interactions Comparison of Tamoxifen & Luteolin.

Sr. No	Ligands	Binding Energy	No of H. B	Hydrogen Bonding		Hydrophobic Interaction
				Amino acids	Distance	
1	Luteolin	-9.0	5	O: Met: O4	3.03	Phe 454
				ND1: His: O2	3.02	Ile 424
				OE2: Glu: O6	2.86,	Phe 404
				OE2: Glu: O5	2.73	Leu 391
				NH2: Arg: O6	3.29	Ala 350
						Leu 387
						Leu 525
						Leu 428
						Ile424
						Gly521
2	Tamoxifen	-9.2	1	OD1:Asp351: N	3.20	His 524
						Leu 384
						Leu 525
						Trp 383
						Thr 347
						Leu 536
						Ala350
						Glu 353
						Leu 346
						Phe 404
		Leu 387				
		Leu 391				
		Met 388				

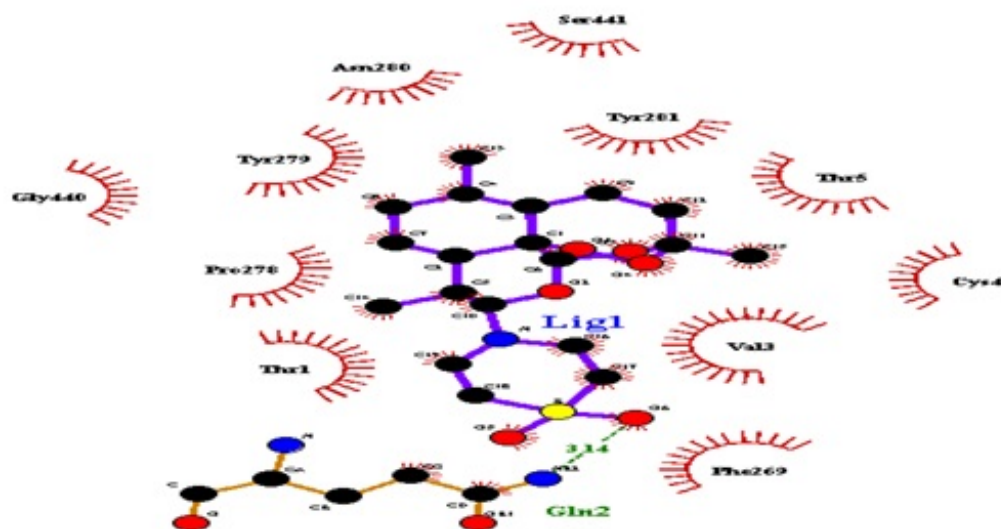


FIGURE 4.69: Hydrogen Bonds and Interactions of Artemisone (ligand) with HER2.

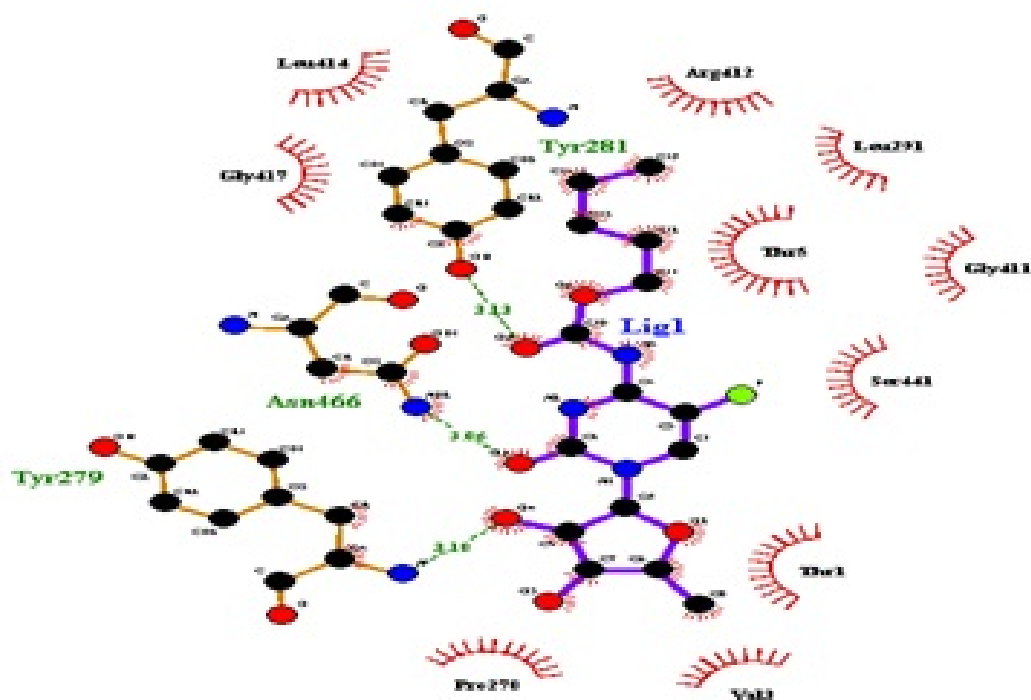


FIGURE 4.70: Hydrogen Bonds and Interactions of Capecitabine (ligand) with HER2

Artemisone makes 1 hydrogen bond with residue Gln and capecitabine makes 3 hydrogen bonds with residues Tyr and Asn. Furthermore, hydrophobic interactions are more in number for artemisone than capecitabine as shown in Table 4.83.

TABLE 4.83: Hydrogen Bonds and Interactions Comparison of Capecitabine & Artemisone

Sr. No	Ligands	Binding Energy	No of H. B	Hydrogen Bonding		Hydrophobic Interaction
				Amino acids	Distance	
1	Artemisone	-8.8	1	NE2: Gln: O6	3.14	Ser 441
						Tyr 281
						Thr 5
						Cys 4
						Val 3
						Phe 269
						Thr 1
						Pro 278
						Tyr 279
						Asn 280
						Gly 440
						Arg412
						Leu291
						Thr 5
Gly 411						
2	Capecitabine	-7.5	3	N: Tyr279:O4	3.18	Ser 441
				ND2: Asn: O1	3.06	Thr 1
				OH: Tyr: O5	3.13	Val3
						Pro 278
						Gly 417
						Leu 414

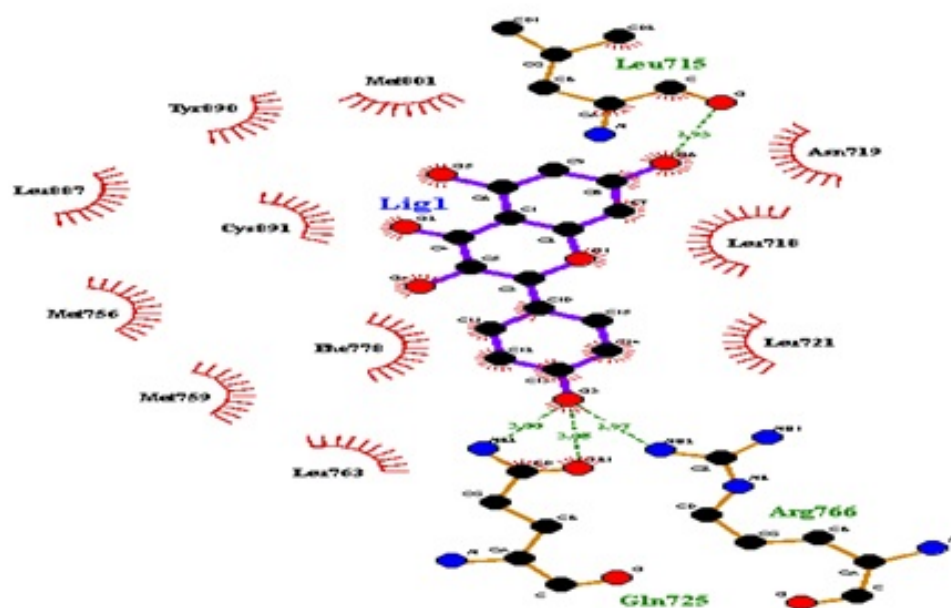


FIGURE 4.71: Hydrogen Bonds and Interactions of Kaempferol (ligand) with PR.

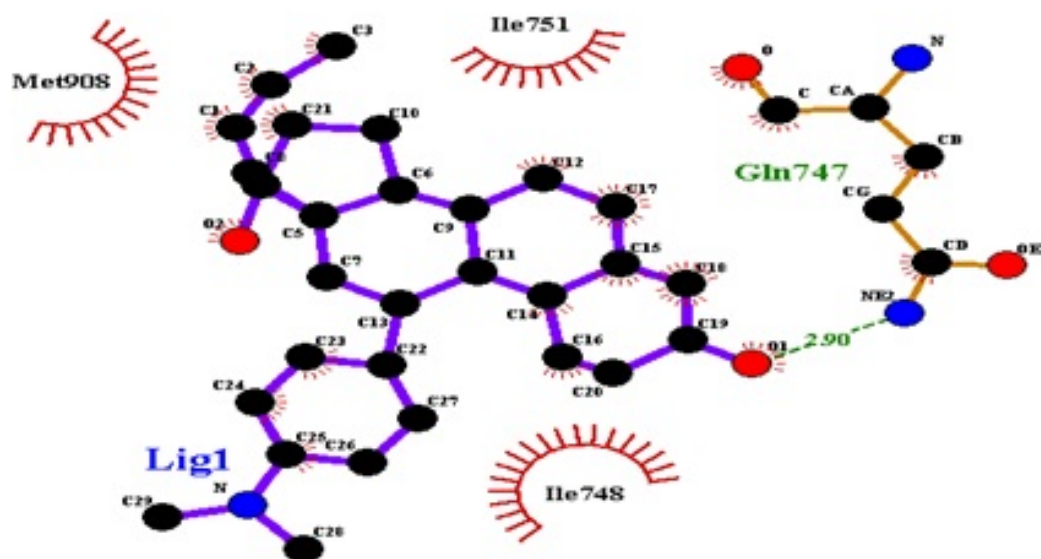


FIGURE 4.72: Hydrogen Bonds and Interactions of Mifepristone (ligand) with PR.

The detail of hydrogen bonds and hydrophobic interactions are displayed in Table 4.84. Kaempferol makes 4 hydrogen bonds with residues leu, Arg, and Gln due to having oxygen electronegative atoms whereas mifepristone makes only 1 hydrogen bond with Gln. Furthermore, hydrophobic interactions are more in number in kaempferol than mifepristone.

TABLE 4.84: Hydrogen Bonds and Interactions Comparison of Mifepristone & Kaempferol.

Sr. No.	Ligands	Binding Energy	No of H.B	Hydrogen Bonding		Hydrophobic Interaction
				Amino acids	Distance	
1	Kaempferol	-9.2	4	O: Leu: O6	2.95	Asn 719
				NH2: Arg: O3	2.97	Leu 718
				NE2: Gln: O3	3.00	Leu 721
				OE1: Gln: O3	3.08	Leu 763
						Met 759
						Phe 778
						Met 756
						Leu 887
						Cys891
						Tyr 890
2	Mifepristone	-7.7	1	NE2:Gln747: O1	2.90	Met 801
						Ile751
						Ile748
						Met 908

Chapter 5

Conclusion and Future Prospects

The motive of the present research was to discover active constituents from *Artemisia carvifolia* which could act as anticancer agents in Breast cancer. For this purpose, 15 ligands were selected after performing data mining studies on literature databases and docked against receptor proteins involved in the majority of Breast cancer namely estrogen, progesterone, and HER 2. The structures of all the 15 ligands were easily available in PubChem and proteins structures were also available in PDB. Drug likeliness of compounds was studied and reported by using primary and secondary filters (Lipinski rule of 5 as primary and Pharmacokinetics properties as a secondary filter). The docking procedures were performed using CB -dock automated version of auto Dock vina. The results were visualized using PyMol and were analyzed through ligPlot version v.1.4.5. After detailed analysis of their bonding score, physicochemical properties, and ADMET properties, luteolin was selected as lead compound against estrogen receptor, artemisone as lead compound against HER2, kaempferol against progesterone receptor. Virtual screening results, Physiochemical properties & Pharmacokinetics properties of these compounds were compared with FDA approved drugs namely tamoxifen, capecitabine, and mifepristone. Based on results it was found that selected lead compounds show better binding affinity to respective protein targets and show less toxicity than standard drugs.

5.1 Recommendations

Lead compounds luteolin, artemisone, and kaempferol as per this research results should be explored as a drug candidate for the treatment of Breast cancer in further *in-vitro* and *in-vivo* experiments and should be tested in clinical trials.

Bibliography

- [1] Aghabarari, M., Ahmadi, F., Mohammadi, I., Hajizadeh, E., & Varvant, F. A. (2007). Physical, emotional and social dimension of quality of life among breast cancer women under chemotherapy. *Iranian journal of nursing research*, 1(3), 55-65.
- [2] Hasanpoor Dehkordi, A., & Azari, S. (2006). Quality of life and related factor in cancer patients. *Behbood*, 10(2), 110-19.
- [3] Torre, L. A., Bray, F., Siegel, R. L., Ferlay, J., Lortet-Tieulent, J., & Jemal, A. (2015). Global cancer statistics, 2012. *CA: a cancer journal for clinicians*, 65(2), 87-108.
- [4] Lynch, H. T., Watson, P., Conway, T. A., & Lynch, J. F. (1990). Clinical/genetic features in hereditary breast cancer. *Breast cancer research and treatment*, 15(2), 63-71.
- [5] Jemal, A., Center, M. M., DeSantis, C., & Ward, E. M. (2010). Global patterns of cancer incidence and mortality rates and trends. *Cancer Epidemiology and Prevention Biomarkers*, 19(8), 1893-1907.
- [6] Akram, M., & Siddiqui, S. A. (2012). Breast cancer management: past, present and evolving. *Indian journal of cancer*, 49(3), 277-282.
- [7] Papavramidou, N., Papavramidis, T., & Demetriou, T. (2010). Ancient Greek and Greco-Roman methods in the modern surgical treatment of cancer. *Annals of surgical oncology*, 17(3), 665-667.

- [8] Kamińska, M., Ciszewski, T., Łopacka-Szatan, K., Miotła, P., & Starosławska, E. (2015). Breast cancer risk factors. *Przegląd menopauzalny= Menopause review*, 14(3), 196-202.
- [9] Brenton, J. D., Carey, L. A., Ahmed, A. A., & Caldas, C. (2005). Molecular classification and molecular forecasting of breast cancer: ready for clinical application? *Journal of clinical oncology*, 23(29), 7350-7360.
- [10] Levin, E. R. (2005). Integration of the extranuclear and nuclear actions of estrogen. *Molecular endocrinology*, 19(8), 1951-1959.
- [11] Allred, D. C. (2010). Issues and updates: evaluating estrogen receptor- α , progesterone receptor, and HER2 in breast cancer. *Modern Pathology*, 23(2), S52-S59.
- [12] Alanazi, I. O., & Khan, Z. (2016). Understanding EGFR signaling in breast cancer and breast cancer stem cells: overexpression and therapeutic implications. *Asian pacific journal of cancer prevention*, 17(2), 445-453.
- [13] Hayes, E. L., & Lewis-Wambi, J. S. (2015). Mechanisms of endocrine resistance in breast cancer: an overview of the proposed roles of non-coding RNA. *Breast Cancer Research*, 17(1), 1-13.
- [14] Simpson, E. R., Mahendroo, M. S., Means, G. D., Kilgore, M. W., Hinshelwood, M. M., Graham-Lorence, S., ... & Bulun, S. E. (1994). Aromatase cytochrome P450, the enzyme responsible for estrogen biosynthesis. *Endocrine Reviews*, 15(3), 342-355.
- [15] Iqbal, N., & Iqbal, N. (2014). Human epidermal growth factor receptor 2 (HER2) in cancers: overexpression and therapeutic implications. *Molecular biology international*, 2014, 852748-852748.
- [16] Segovia-Mendoza, M., González-González, M. E., Barrera, D., Díaz, L., & García-Becerra, R. (2015). Efficacy and mechanism of action of the tyrosine

- kinase inhibitors gefitinib, lapatinib and neratinib in the treatment of HER2-positive breast cancer: preclinical and clinical evidence. *American journal of cancer research*, 5(9), 2531-2561.
- [17] De Santos Galíndez, J., Díaz Lanza, A., & Fernandez Matellano, L. (2002). Biologically active substances from the genus *Scrophularia*. *Pharmaceutical biology*, 40(1), 45-59.
- [18] Adams Jr, J. D. (2014). What can traditional healing do for modern medicine? *CELLMED*, 4(2), 9-1.
- [19] Abad, M. J., Bedoya, L. M., Apaza, L., & Bermejo, P. (2012). The *Artemisia* L. genus: a review of bioactive essential oils. *Molecules*, 17(3), 2542-2566.
- [20] Ferreira, L. G., Dos Santos, R. N., Oliva, G., & Andricopulo, A. D. (2015). Molecular docking and structure-based drug design strategies. *Molecules*, 20(7), 13384-13421.
- [21] Shanmugaraj, K., Anandakumar, S., & Ilanchelian, M. (2015). Probing the binding interaction of thionine with lysozyme: A spectroscopic and molecular docking investigation. *Dyes and Pigments*, 112, 210-219.
- [22] Friesner, R. A., Banks, J. L., Murphy, R. B., Halgren, T. A., Klicic, J. J., Mainz, D. T., ... & Shenkin, P. S. (2004). Glide: a new approach for rapid, accurate docking and scoring. 1. Method and assessment of docking accuracy. *Journal of medicinal chemistry*, 47(7), 1739-1749.
- [23] Rodríguez, D., Gao, Z. G., Moss, S. M., Jacobson, K. A., & Carlsson, J. (2015). Molecular docking screening using agonist-bound GPCR structures: probing the A2A adenosine receptor. *Journal of chemical information and modeling*, 55(3), 550-563.
- [24] Bray, F., Ferlay, J., Soerjomataram, I., Siegel, R. L., Torre, L. A., & Jemal, A. (2018). Global cancer statistics 2018: Globocan estimates of incidence and mortality worldwide for 36 cancers in 185 countries. *CA: a cancer journal for clinicians*, 68(6), 394-424.

- [25] Bjerkgvig, R., Tysnes, B. B., Aboody, K. S., Najbauer, J., & Terzis, A. J. A. (2005). The origin of the cancer stem cell: current controversies and new insights. *Nature Reviews Cancer*, 5(11), 899-904.
- [26] Regitha, R. N., Parthasarathy, V., & Balakrishnan, N. (2021). Cancer Protective effect of Brassica nigra and Role of its Chemical Constituents. *Research Journal of Pharmacy and Technology*, 14(2), 1115-1121.
- [27] Sainsbury, J. R. C., Anderson, T. J., & Morgan, D. A. L. (2000). Breast cancer. *Bmj*, 321(7263), 745-750.
- [28] Boyd, N. F., Guo, H., Martin, L. J., Sun, L., Stone, J., Fishell, E., & Yaffe, M. J. (2007). Mammographic density and the risk and detection of breast cancer. *New England journal of medicine*, 356(3), 227-236.
- [29] Montazeri, A., Vahdaninia, M., Harirchi, I., Harirchi, A. M., Sajadian, A., Khaleghi, F., ... & Jarvandi, S. (2008). Breast cancer in Iran: need for greater women awareness of warning signs and effective screening methods. *Asia Pacific family medicine*, 7(1), 1-7.
- [30] Hayes, J., Richardson, A., & Frampton, C. (2013). Population attributable risks for modifiable lifestyle factors and breast cancer in New Zealand women. *Internal medicine journal*, 43(11), 1198-1204.
- [31] Reeder, J. G., & Vogel, V. G. (2008). Breast cancer prevention. *Advances in Breast Cancer Management, Cancer treatment, and research*, 141, 149-164.
- [32] Sharma, G. N., Dave, R., Sanadya, J., Sharma, P., & Sharma, K. K. (2010). Various types and management of breast cancer: an overview. *Journal of advanced pharmaceutical technology & research*, 1(2), 109-126.
- [33] Khuwaja, G. A., & Abu-Rezq, A. N. (2004). Bimodal breast cancer classification system. *Pattern analysis and applications*, 7(3), 235-242
- [34] Kerlikowske, K., Hubbard, R. A., Miglioretti, D. L., Geller, B. M., Yankaskas, B. C., Lehman, C. D., ... & Sickles, E. A. (2011). Comparative effectiveness of

- digital versus film-screen mammography in community practice in the United States: a cohort study. *Annals of internal medicine*, 155(8), 493-502.
- [35] Palmer, M. L., & Tsangaris, T. N. (1993). A breast biopsy in women 30 years old or less. *The American journal of surgery*, 165(6), 708-712.
- [36] Mustafa, M., Nornazirah, A., Salih, F., Illzam, E., Suleiman, M., & Sharifa, A. (2016). Breast cancer: Detection markers, prognosis, and prevention. *IOSR Journal of Dental and Medical Sciences*, 15(08), 73-80.
- [37] Samadi, P., Saki, S., Dermani, F. K., Pourjafar, M., & Saidijam, M. (2018). Emerging ways to treat breast cancer: will promises be met?. *Cellular Oncology*, 41(6), 605-621.
- [38] Murthy, N. S., Chaudhry, K., & Rath, G. K. (2008). Burden of cancer and projections for 2016, Indian scenario: gaps in the availability of radiotherapy treatment facilities. *Asian Pac J Cancer Prev*, 9(4), 671-7.
- [39] Shah, R., Rosso, K., & Nathanson, S. D. (2014). Pathogenesis, prevention, diagnosis and treatment of breast cancer. *World journal of clinical oncology*, 5(3), 283-298.
- [40] Leite, A. D. M., Macedo, A. V. S., Jorge, A. J. L., & Martins, W. D. A. (2018). Antiplatelet Therapy in Breast Cancer Patients Using Hormonal Therapy: Myths, Evidence and Potentialities–Systematic Review. *Arquivos brasileiros de cardiologia*, 111(2), 205-212.
- [41] Ullah, N. (2017). Medicinal plants of Pakistan: challenges and opportunities. *Journal of Complementary & Alternative Medici*, 6(4), 00193.
- [42] Shinwari, Z. K., Salima, M., Faisal, R., Huda, S., & Asrar, M. (2013). Biological screening of indigenous knowledge-based plants used in diarrheal treatment. *Pak. J. Bot*, 45(4), 1375-1382.
- [43] Girach, R. D., Khan, H., & Ahmad, M. (2003). Botanical identification of *Thuhar* is seldom used as Unani medicine. *Hamdard Med*, 46(1), 27-33.

- [44] Marchowsky, K. (2002). The Psychopharmacology of Herbal Medicine: Plant Drugs That Affect Mind, Brain, and Behavior. *Northeastern Naturalist*, 9(1), 122.
- [45] Abdel-Sattar, E., Ahmed, A. A., Hegazy, M. E. F., Farag, M. A., & Al-Yahya, M. A. A. (2007). Acylated pregnane glycosides from *Caralluma russeliana*. *Phytochemistry*, 68(10), 1459-1463.
- [46] Phillipson, J. D. (2001). Phytochemistry and medicinal plants. *Phytochemistry*, 56(3), 237-243.
- [47] Dewick, P. M. (2002). Medicinal natural products: a biosynthetic approach. John Wiley & Sons, 507-510.
- [48] Grabley, S., & Sattler, I. (2003). Natural products for lead identification: nature is a valuable resource for providing tools. *Modern methods of drug discovery*, 93, 87-107.
- [49] Ali-Shtayeh, M. S., Yaniv, Z., & Mahajna, J. (2000). Ethnobotanical survey in the Palestinian area: a classification of the healing potential of medicinal plants. *Journal of Ethnopharmacology*, 73(1-2), 221-232.
- [50] Robertshawe, P. (2007). Yaniv Z, Bachrach U (eds). Handbook of Medicinal Plants. *Journal of the Australian Traditional-Medicine Society*, 13(4), 242-243.
- [51] Singh, R. (2015). Medicinal plants: A review. *Journal of plant sciences*, 3(1), 50-55.
- [52] Kang, Y. J., Park, H. J., Chung, H. J., Min, H. Y., Park, E. J., Lee, M. A., ... & Lee, S. K. (2012). Wnt/ β -catenin signaling mediates the antitumor activity of magnolol in colorectal cancer cells. *Molecular Pharmacology*, 82(2), 168-177.
- [53] Verhoeven, D. T., Goldbohm, R. A., van Poppel, G., Verhagen, H., & van den Brandt, P. A. (1996). Epidemiological studies on brassica vegetables and cancer risk. *Cancer Epidemiology and Prevention Biomarkers*, 5(9), 733-748.

- [54] Ranganathan, S., Halagowder, D., & Sivasithambaram, N. D. (2015). Quercetin suppresses twists to induce apoptosis in MCF-7 breast cancer cells. *PloS one*, 10(10), e0141370.
- [55] Kumar, J., Dhar, P., Tayade, A. B., Gupta, D., Chaurasia, O. P., Upreti, D. K., ... & Srivastava, R. B. (2015). Chemical composition and biological activities of trans-Himalayan alga *Spirogyra porticalis* (Muell.) Cleve. *PloS One*, 10(2), e0118255.h
- [56] Čavar, S., Maksimović, M., Vidic, D., & Parić, A. (2012). Chemical composition and antioxidant and antimicrobial activity of essential oil of *Artemisia annua* L. from Bosnia. *Industrial Crops and Products*, 37(1), 479-485.
- [57] Adams, J. D. (2012). The use of California sagebrush (*Artemisia californica*) liniment to control pain. *Pharmaceuticals*, 5(10), 1045-1053.
- [58] Vallès, J., Garcia, S., Hidalgo, O., Martín, J., Pellicer, J., Sanz, M., & Garnatje, T. (2011). Biology, genome evolution, biotechnological issues, and research including applied perspectives in *Artemisia* (Asteraceae). *Advances in botanical research*, 60, 349-419.
- [59] Dilshad, E., Ismail, H., Khan, M. A., Cusido, R. M., & Mirza, B. (2020). Metabolite profiling of *Artemisia carvifolia* Buch transgenic plants and estimation of their anticancer and antidiabetic potential. *Biocatalysis and Agricultural Biotechnology*, 24, 101539.
- [60] Nath, S., & Mukherjee, P. (2014). MUC1: a multifaceted oncoprotein with a key role in cancer progression. *Trends in molecular medicine*, 20(6), 332-342.
- [61] Greenshields, A. L., Fernando, W., & Hoskin, D. W. (2019). The anti-malarial drug artesunate causes cell cycle arrest and apoptosis of triple-negative MDA-MB-468 and HER2-enriched SK-BR-3 breast cancer cells. *Experimental and molecular pathology*, 107, 10-22.
- [62] Tin, A. S., Sundar, S. N., Tran, K. Q., Park, A. H., Poindexter, K. M., & Firestone, G. L. (2012). Antiproliferative effects of artemisinin on human

- breast cancer cells require the downregulated expression of the E2F1 transcription factor and loss of E2F1-target cell cycle genes. *Anti-cancer drugs*, 23(4), 370-379.
- [63] Hilakivi-Clarke, L., Cabanes, A., Olivo, S., Kerr, L., Bouker, K. B., & Clarke, R. (2002). Do estrogens always increase breast cancer risk?. *The Journal of steroid biochemistry and molecular biology*, 80(2), 163-174.
- [64] Hilakivi-Clarke, L., Onojafe, I., Raygada, M., Cho, E., Skaar, T., Russo, I., & Clarke, R. (1999). Prepubertal exposure to zearalenone or genistein reduces mammary tumorigenesis. *British journal of cancer*, 80(11), 1682-1688.
- [65] Warner, M., Nilsson, S., & Gustafsson, J. Å. (1999). The estrogen receptor family. *Current Opinion in Obstetrics and Gynecology*, 11(3), 249-254.
- [66] Kumar, V., Green, S., Stack, G., Berry, M., Jin, J. R., & Chambon, P. (1987). Functional domains of the human estrogen receptor. *Cell*, 51(6), 941-951.
- [67] McKenna, N. J., Lanz, R. B., & O'Malley, B. W. (1999). Nuclear receptor coregulators: cellular and molecular biology. *Endocrine Reviews*, 20(3), 321-344.
- [68] Tsai, M. J., & O'Malley, B. W. (1994). Molecular mechanisms of action of steroid/thyroid receptor superfamily members. *Annual review of biochemistry*, 63(1), 451-486.
- [69] Onate, S. A., Tsai, S. Y., Tsai, M. J., & O'Malley, B. W. (1995). Sequence and characterization of a coactivator for the steroid hormone receptor superfamily. *Science*, 270(5240), 1354-1357.
- [70] Mazumdar, A., Wang, R. A., Mishra, S. K., Adam, L., Bagheri-Yarmand, R., Mandal, M., ... & Kumar, R. (2001). Transcriptional repression of estrogen receptor by metastasis-associated protein 1 corepressor. *Nature cell biology*, 3(1), 30-37.
- [71] Chakravarty, D., Nair, S. S., Santhamma, B., Nair, B. C., Wang, L., Bandyopadhyay, A., ... & Vadlamudi, R. K. (2010). Extranuclear functions of

- ER impact invasive migration and metastasis by breast cancer cells. *Cancer Research*, 70(10), 4092-4101.
- [72] Gassmann, M., Casagrande, F., Orioli, D., Simon, H., Lai, C., Klein, R., & Lemke, G. (1995). Aberrant neural and cardiac development in mice lacking the ErbB4 neuregulin receptor. *Nature*, 378(6555), 390-394.
- [73] Muthuswamy, S. K., Li, D., Lelievre, S., Bissell, M. J., & Brugge, J. S. (2001). ErbB2, but not ErbB1, reinitiates proliferation and induces luminal repopulation in epithelial acini. *Nature cell biology*, 3(9), 785-792.
- [74] O-charoenrat, P., & Rhys-Evans, P. (1999). Court WJ, Box GM, Eccles SA. Differential modulation of proliferation, matrix metalloproteinase expression and invasion of human head and neck squamous carcinoma cells by c-erbB ligands. *Clin Exp Metastasis*, 17(63), 1-639.
- [75] Campiglio, M., Tagliabue, E., Srinivas, U., Pellegrini, R., Martignone, S., Ménard, S., ... & Marchisio, P. C. (1994). Colocalization of the p185HER2 oncoprotein and integrin $\alpha 6\beta 4$ in Calu-3 lung carcinoma cells. *Journal of cellular biochemistry*, 55(4), 409-418.
- [76] Ménard, S., Tagliabue, E., Campiglio, M., & Pupa, S. M. (2000). Role of HER2 gene overexpression in breast carcinoma. *Journal of cellular physiology*, 182(2), 150-162.
- [77] Hewitt, S. C., & Korach, K. S. (2000). Progesterone action and responses in the α ERKO mouse. *Steroids*, 65(10-11), 551-557.
- [78] Morris, G. M., & Lim-Wilby, M. (2008). Molecular docking. In *Molecular modeling of proteins. Methods in Molecular Biology*, 443, 365-382.
- [79] Shoichet, B. K., McGovern, S. L., Wei, B., & Irwin, J. J. (2002). Lead discovery using molecular docking. *Current opinion in chemical biology*, 6(4), 439-446.

- [80] Yuriev, E., & Ramsland, P. A. (2013). Latest developments in molecular docking: 2010–2011 in review. *Journal of Molecular Recognition*, 26(5), 215-239.
- [81] Carey, L. A., Dees, E. C., Sawyer, L., Gatti, L., Moore, D. T., Collichio, F., ... & Perou, C. M. (2007). The triple-negative paradox: primary tumor chemosensitivity of breast cancer subtypes. *Clinical cancer research*, 13(8), 2329-2334.
- [82] Sussman, J. L., Lin, D., Jiang, J., Manning, N. O., Prilusky, J., Ritter, O., & Abola, E. E. (1998). Protein Data Bank (PDB): the database of three-dimensional structural information of biological macromolecules. *Acta Crystallographica Section D: Biological Crystallography*, 54(6), 1078-1084.
- [83] UniProt Consortium. (2015). UniProt: a hub for protein information. *Nucleic acids research*, 43(D1), D204-D212.
- [84] Garg, V. K., Avashthi, H., Tiwari, A., Jain, P. A., Ramkete, P. W., Kayastha, A. M., & Singh, V. K. (2016). MFPPI–multi FASTA ProtParam interface. *Bioinformatics*, 12(2), 74.
- [85] Yuan, S., Chan, H. S., & Hu, Z. (2017). Using PyMOL as a platform for computational drug design. *Wiley Interdisciplinary Reviews: Computational Molecular Science*, 7(2), e1298.
- [86] Hunter, S., Jones, P., Mitchell, A., Apweiler, R., Attwood, T. K., Bateman, A., ... & Yong, S. Y. (2012). InterPro in 2011: new developments in the family and domain prediction database. *Nucleic acids research*, 40(D1), D306-D312.
- [87] Septembre-Malaterre, A., Lalarizo Rakoto, M., Marodon, C., Bedoui, Y., Nakab, J., Simon, E., ... & Gasque, P. (2020). *Artemisia annua*, a Traditional Plant Brought to Light. *International Journal of Molecular Sciences*, 21(14), 4986.

- [88] Bolton, E. E., Wang, Y., Thiessen, P. A., & Bryant, S. H. (2008). PubChem: integrated platform of small molecules and biological activities. In *Annual reports in computational chemistry*, Elsevier, 4, 217-241.
- [89] Dias, R., de Azevedo, J., & Walter, F. (2008). Molecular docking algorithms. *Current drug targets*, 9(12), 1040-1047.
- [90] DeLano, W. L. (2002). Pymol: An open-source molecular graphics tool. *CCP4 Newsletter on protein crystallography*, 40(1), 82-92.
- [91] Mostafa, S. I. (2007). Mixed ligand complexes with 2-piperidine-carboxylic acid as primary ligand and ethylenediamine, 2, 2'-bipyridyl, 1, 10-phenanthroline, and 2 (2'-pyridyl) quinoxaline as secondary ligands: preparation, characterization and biological activity. *Transition Metal Chemistry*, 32(6), 769-775.
- [92] Pires, D. E., Blundell, T. L., & Ascher, D. B. (2015). pkCSM: predicting small-molecule pharmacokinetic and toxicity properties using graph-based signatures. *Journal of medicinal chemistry*, 58(9), 4066-4072.
- [93] Ntie-Kang, F. (2013). An in silico evaluation of the ADMET profile of the StreptomeDB database. *Springerplus*, 2(1), 1-11.
- [94] Morya, V. K., Yadav, S., Kim, E. K., & Yadav, D. (2012). In silico characterization of alkaline proteases from different species of *Aspergillus*. *Applied biochemistry and biotechnology*, 166(1), 243-257.
- [95] Yang, J., & Zhang, Y. (2015). I-TASSER server: new development for protein structure and function predictions. *Nucleic acids research*, 43(W1), W174-W181.
- [96] Beato, M. (1993). Gene regulation by steroid hormones. *Cell*, 56(3), 335-344.
- [97] Tanenbaum, D. M., Wang, Y., Williams, S. P., & Sigler, P. B. (1998). Crystallographic comparison of the estrogen and progesterone receptor's ligand-binding domains. *Proceedings of the National Academy of Sciences*, 95(11), 5998-6003.

- [98] Elizalde, P. V., Russo, R. I. C., Chervo, M. F., & Schillaci, R. (2016). ErbB-2 nuclear function in breast cancer growth, metastasis, and resistance to therapy. *Endocrine-related cancer*, 23(12), T243-T257.
- [99] Hill, K. K., Roemer, S. C., Churchill, M. E., & Edwards, D. P. (2012). Structural and functional analysis of domains of the progesterone receptor. *Molecular and cellular endocrinology*, 348(2), 418-429.
- [100] Kim, S., Thiessen, P. A., Bolton, E. E., Chen, J., Fu, G., Gindulyte, A., ... & Bryant, S. H. (2016). PubChem substance and compound databases. *Nucleic acids research*, 44(D1), D1202-D1213.
- [101] Kumar, N., Tomar, R., Pandey, A., Tomar, V., Singh, V. K., & Chandra, R. (2018). Preclinical evaluation and molecular docking of 1, 3-benzodioxole propargyl ether derivatives as a novel inhibitor for combating the histone deacetylase enzyme in cancer. *Artificial cells, nanomedicine, and biotechnology*, 46(6), 1288-1299.
- [102] Lipinski, C. A. (2004). Lead-and drug-like compounds: the rule-of-five revolution. *Drug Discovery Today: Technologies*, 1(4), 337-341.
- [103] Daina, A., Michielin, O., & Zoete, V. (2017). SwissADME: a free web tool to evaluate pharmacokinetics, drug-likeness, and medicinal chemistry friendliness of small molecules. *Scientific reports*, 7(1), 1-13.
- [104] Pires, D. E., Kaminskas, L. M., & Ascher, D. B. (2018). Prediction and Optimization of Pharmacokinetic and Toxicity Properties of the Ligand. *Methods in molecular biology* (Clifton, NJ), 1762, 271-284.
- [105] Khurshid, Z. (2021). Determination of Potential Antioxidants of *Artemisia annua* by Computational Approaches (Doctoral dissertation, Capital University).
- [106] Qidwai, T. (2017). QSAR modeling, docking, and ADMET study for the exploration of potential anti-malarial compounds against *Plasmodium falciparum*. *In silico pharmacology*, 5(1), 1-13.

- [107] Al-Nour, M. Y., Ibrahim, M. M., & Elsaman, T. (2019). Ellagic acid, Kaempferol, and Quercetin from *Acacia nilotica*: Promising combined drug with multiple mechanisms of action. *Current pharmacology reports*, 5(4), 255-280.
- [108] Kiran, G., Karthik, L., Devi, M. S., Sathiyarajeswaran, P., Kanakavalli, K., Kumar, K. M., & Kumar, D. R. (2020). In silico computational screening of Kabasura Kudineer-official Siddha formulation and JACOM against SARS-CoV-2 spike protein. *Journal of Ayurveda and integrative medicine*, 20, 0975-9476.
- [109] Maharani, M. G., Lestari, S. R., & Lukiati, B. (2020, April). Molecular docking studies flavonoid (quercetin, isoquercetin, and kaempferol) of single bulb garlic (*Allium sativum*) to inhibit lanosterol synthase as anti-hyper cholesterol therapeutic strategies. In *AIP Conference Proceedings*. AIP Publishing LLC, 2231(1), 040021.
- [110] Morris, G. M., Huey, R., Lindstrom, W., Sanner, M. F., Belew, R. K., Goodsell, D. S., & Olson, A. J. (2009). AutoDock4 and AutoDockTools4: Automated docking with selective receptor flexibility. *Journal of computational chemistry*, 30(16), 2785-2791.
- [111] Shivanika, C., Kumar, D., Ragnathan, V., Tiwari, P., & Sumitha, A. (2020). Molecular docking, validation, dynamics simulations, and pharmacokinetic prediction of natural compounds against the SARS-CoV-2 main-protease. *Journal of biomolecular structure & dynamics*, 1,27.
- [112] Puranik, N. V., Srivastava, P., Bhatt, G., Mary, D. J. S. J., Limaye, A. M., & Sivaraman, J. (2019). Determination and analysis of agonist and antagonist potential of naturally occurring flavonoids for estrogen receptor (ER α) by various parameters and molecular modelling approach. *Scientific reports*, 9(1), 1-11.

- [113] Pratama, M. R. F. (2015, December). Molecular docking of anticancer agents: Artemisinin and derivatives as HER2 inhibitor. In Proceeding of 1st Sari Mulia International Conference on Health and Sciences.
- [114] Zarezade, V., Abolghasemi, M., Rahim, F., Veisi, A., & Behbahani, M. (2018). In silico assessment of new progesterone receptor inhibitors using molecular dynamics: a new insight into breast cancer treatment. *Journal of molecular modeling*, 24(12), 1-19.
- [115] Laskowski, R. A., & Swindells, M. B. (2011). LigPlot+: multiple ligand-protein interaction diagrams for drug discovery. *Journal of chemical information and modeling*, 51(10), 2778-2786.
- [116] Umar, A. B., Uzairu, A., Shallangwa, G. A., & Uba, S. (2020). Docking-based strategy to design novel flavone-based aryl amides as potent V600E-BRAF inhibitors with prediction of their drug-likeness and ADMET properties. *Bulletin of the National Research Centre*, 44(1), 1-11.
- [117] Wang, P. H., Tu, Y. S., & Tseng, Y. J. (2019). PgpRules: a decision tree-based prediction server for P-glycoprotein substrates and inhibitors. *Bioinformatics*, 35(20), 4193-4195.
- [118] Han, Y., Zhang, J., Hu, C. Q., Zhang, X., Ma, B., & Zhang, P. (2019). In silico ADME and toxicity prediction of ceftazidime and its impurities. *Frontiers in pharmacology*, 10, 434.
- [119] Ujan, R., Saeed, A., Channar, P. A., Larik, F. A., Abbas, Q., Alajmi, M. F., ... & Seo, S. Y. (2019). Drug-1, 3, 4-thiadiazole conjugates as novel mixed-type inhibitors of acetylcholinesterase: synthesis, molecular docking, pharmacokinetics, and ADMET evaluation. *Molecules*, 24(5), 860.
- [120] Ambrose, G. O., Afees, O. J., Nwamaka, N. C., Simon, N., Oluwaseun, A. A., Soyinka, T., ... & Bankole, S. (2018). Selection of Luteolin as a potential antagonist from molecular docking analysis of EGFR mutant. *Bioinformatics*, 14(5), 241-247.

- [121] Siniprasad, P., Nair, B., Balasubramaniam, V., Sadanandan, P., Namboori, P. K., & Nath, L. R. (2020). Evaluation of kaempferol as AKT dependent mTOR regulator via targeting FKBP-12 in hepatocellular carcinoma: An in silico approach. *Letters in Drug Design & Discovery*, 17(11), 1401-1408.
- [122] Yu, F., & Bender, W. (2001, May). The mechanism of tamoxifen in breast cancer prevention. In *Breast Cancer Research*. BioMed Central, 3(1), 1.
- [123] Pronk, L. C., Vasey, P., Sparreboom, A., Reigner, B., Planting, A. T., Gordon, R. J., ... & Twelves, C. (2000). A phase I and pharmacokinetic study of the combination of capecitabine and docetaxel in patients with advanced solid tumors. *British journal of cancer*, 83(1), 22-29.
- [124] Tieszen, C. R., Goyeneche, A. A., Brandhagen, B. N., Ortbahn, C. T., & Telleria, C. M. (2011). Antiprogestin mifepristone inhibits the growth of cancer cells of reproductive and non-reproductive origin regardless of progesterone receptor expression. *BMC Cancer*, 11(1), 1-12.
- [125] Howell, A., Cuzick, J., Baum, M., Buzdar, A., Dowsett, M., Forbes, J. F., ... & Tobias, J. S. (2005). Results of the ATAC (Arimidex, Tamoxifen, Alone or in Combination) trial after completion of 5 years' adjuvant treatment for breast cancer. *Lancet*, 365(9453), 60-62.
- [126] Jordan, V. C. (1993). A current view of tamoxifen for the treatment and prevention of breast cancer. *British journal of pharmacology*, 110(2), 507-517.
- [127] Lazzeroni, M., Serrano, D., Dunn, B. K., Heckman-Stoddard, B. M., Lee, O., Khan, S., & Decensi, A. (2012). Oral low dose and topical tamoxifen for breast cancer prevention: modern approaches for an old drug. *Breast Cancer Research*, 14(5), 1-11.
- [128] Wong, M. M., Guo, C., & Zhang, J. (2014). Nuclear receptor corepressor complexes in cancer: mechanism, function, and regulation. *American journal of clinical and experimental urology*, 2(3), 169-187.

- [129] Hurtado, A., Holmes, K. A., Geistlinger, T. R., Hutcheson, I. R., Nicholson, R. I., Brown, M., ... & Carroll, J. S. (2008). Regulation of ERBB2 by estrogen receptor–PAX2 determines response to tamoxifen. *Nature*, 456(7222), 663-666.
- [130] Radin, D. P., & Patel, P. (2016). Delineating the molecular mechanisms of tamoxifen's oncolytic actions in estrogen receptor-negative cancers. *European journal of pharmacology*, 781, 173-180.
- [131] Ali, S., Rasool, M., Chaoudhry, H., Pushparaj, P. N., Jha, P., Hafiz, A., ... & Jamal, M. S. (2016). Molecular mechanisms and mode of tamoxifen resistance in breast cancer. *Bioinformation*, 12(3), 135-139.
- [132] Eliason, J. F., & Megyeri, A. (2004). Potential for predicting toxicity and response of fluoropyrimidines in patients. *Current drug targets*, 5(4), 383-388.
- [133] Schellens, J. H. (2007). Capecitabine. *The oncologist*, 12(2), 152-155.
- [134] Rocereto, T. F., Saul, H. M., Aikins Jr, J. A., & Paulson, J. (2000). Phase II study of mifepristone (RU486) in refractory ovarian cancer. *Gynecologic oncology*, 77(3), 429-432.
- [135] El Etreby, M. F., Liang, Y., Wrenn, R. W., & Schoenlein, P. V. (1998). Additive effect of mifepristone and tamoxifen on apoptotic pathways in MCF-7 human breast cancer cells. *Breast cancer research and treatment*, 51(2), 149-168.
- [136] Goyeneche, A. A., Carón, R. W., & Telleria, C. M. (2007). Mifepristone inhibits ovarian cancer cell growth in vitro and in vivo. *Clinical Cancer Research*, 13(11), 3370-3379.
- [137] Parri, M., & Chiarugi, P. (2010). Rac and Rho GTPases in cancer cell motility control. *Cell communication and signaling*, 8(1), 1-14.

- [138] Chabbert-Buffet, N., Meduri, G., Bouchard, P., & Spitz, I. M. (2005). Selective progesterone receptor modulators and progesterone antagonists: mechanisms of action and clinical applications. *Human Reproduction Update*, 11(3), 293-307.
- [139] Esteva, F. J., & Hortobagyi, G. N. (2006). Comparative assessment of lipid effects of endocrine therapy for breast cancer: implications for cardiovascular disease prevention in postmenopausal women. *The Breast*, 15(3), 301-312.
- [140] Grey, A. B., Stapleton, J. P., Evans, M. C., & Reid, I. R. (1995). The effect of the anti-estrogen tamoxifen on cardiovascular risk factors in normal postmenopausal women. *The Journal of Clinical Endocrinology & Metabolism*, 80(11), 3191-3195.
- [141] Cohen, M. H., Hirschfeld, S., Honig, S. F., Ibrahim, A., Johnson, J. R., O'Leary, J. J., ... & Pazdur, R. (2001). Drug approval summaries: arsenic trioxide, tamoxifen citrate, anastrozole, paclitaxel, bexarotene. *The oncologist*, 6(1), 4-11.
- [142] Van Cutsem, E., Hoff, P. M., Blum, J. L., Abt, M., & Osterwalder, B. (2002). Incidence of cardiotoxicity with the oral fluoropyrimidine capecitabine is typical of that reported with 5-fluorouracil. *Annals of Oncology*, 13(3), 484-485.
- [143] Reigner, B., Blesch, K., & Weidekamm, E. (2001). Clinical pharmacokinetics of capecitabine. *Clinical pharmacokinetics*, 40(2), 85-104.
- [144] Mrozek-Orlowski, M. E., Frye, D. K., & Sanborn, H. M. (1999, May). Capecitabine: nursing implications of a new oral chemotherapeutic agent. In *Oncology nursing forum*, 26(4), 753-762.
- [145] Cohen, P. R. (2017). Capecitabine-associated loss of fingerprints: report of capecitabine-induced dermatoglyphics in two women with breast cancer and review of acquired dermatoglyphic absence in oncology patients treated with capecitabine. *Cureus*, 9(1), e969-e969.

- [146] Sarkar, N. N. (2002). Mifepristone: bioavailability, pharmacokinetics, and use-effectiveness. *European Journal of Obstetrics & Gynecology and Reproductive Biology*, 101(2), 113-120.

An Appendix

TABLE 5.1: Active Ligand Showing Hydrogen and Hydrophobic Interactions with ER

Sr. No.	Ligands	Binding Energy	No of H.B	Hydrogen Bonding		Hydrophobic interaction
				Amino acids	Distance	
1	Artemisinin	-8.9	0			Met 343
						Leu 525
						Leu 346
						Thr 347
						Ala 350
						Leu 349
						Leu 387
						Glu 353
						Phe 404
						Leu 391
		Met 388				
		Leu 384				

						Ala 350
						Phe404
						Leu 391
						Ile 424
						Gly 521
2	Artem- ether	-8.3	0			Met 421
						Met 388
						Leu 525
						Leu 346
						Met 343
						Thr 347
						Leu 384
						Leu 346
						Ala 350
						Met 343
						Leu 525
						Gly 521
						Met 421
3	Artesu- nate	-8.3	1	ND1: His: O7	3.01	Ile 424
						Met 388
						Leu 428
						Leu 391
						Phe 404
						Leu 384
						Leu 387
						Glu 353

				Ala 350
				Thr 347
				Leu 346
				Met 343
	Dihy-			Leu 525
4	droar-	-8.8	0	Met 421
	temi-			Ile 424
	sinin			Leu 428
				Leu 391
				Met 388
				Leu 384
				Leu 387
				Met 388
				Leu 428
				Leu 384
5	Artean-	-8.4	0	Leu 387
	nuin B			Glu 353
				Leu 349
				Phe 404
				Leu 346
				Leu 525

						Leu 387
						Leu 391
						Met 388
						Leu 384
						Leu 428
6	Artemimol	-8.8	0			Ile 424
						Leu 525
						Met 421
						Met 343
						Leu 346
						Ala 350
						Thr347
						Val 446
						Trp 393
						Glu 323
7	Artem- isone	-7.3	2	NZ: Lys: O5	2.80	Phe 445
				NH1: Arg: O6	3.06	Pro324
						Gly 390
						Ile 326
						Leu 525
						Leu 384
						Ala 350
				ND1: His: O6	3.04	Leu 387
				O: Met: O7	3.18	Leu 391
8	Quercetin	-9.2	4	NH2: Arg: O4	3.30	Phe 404
				OE2: Glu: O4	2.88	Ile 424
						Leu 428
						Phe 425

					Ala 350	
					Met 343	
					Trp 383	
				OE2: Glu: O9	3.04	Leu 384
				OE2: Glu: O10	2.85	Leu 391
				NH2: Arg: O10	3.12	Leu 346
9	Isoquercetin	-9.2	7	OG1: Thr: O7	2.78	Leu 525
				OG1: Thr: O6	2.70	Ile 424
				ND1: His: O11	3.16	Leu 428
				O: Met: O12	3.12	Phe 425
						Phe 404
						Leu 349
						Leu 387
						Leu 525
						Trp 383
						Leu 346
				OD1: Asp: O12	3.06	Leu 384
				OD2: Asp: O12	2.96	Leu 387
10	Rutin	-7.2	5	O: Met: O16	2.96	Ala 350
				OG1: Thr: O9	3.03,	Met 343
				OG1: Thr: O4	2.70	Leu 536
						Asn 532
						Val 534
						Pro 324
				NZ: Lys: O3	2.98	Ile 326
11	Gallic acid	-6.2	4	NH1: Arg: O1	3.25	Gly 390
				O: Pro: O2	2.89	Leu 387
				O: Glu: O4	2.96	Met 357
						His 356

						Leu 525
						Leu 384
				O: Met: O6	3.21	Leu 387
12	Kaempferol	-9.0	4	ND1: His: O5	3.06	Leu 391
				OE2: Glu: O3	3.88	Phe 404
				NH2: Arg: O3	3.30	Ile 424
						Phe 425
						Leu 428
						Met 343
						Leu 346
						Phe 404
						Met 388
13	Chryso-splenol D	-7.4	3	OG1: Thr: O6	2.72	Leu 391
				O: Leu: O4	2.82	Glu 353
				NH2: Arg: O4	3.21	Asp 351
						Trp 383
						Leu 525
						Ala 350
						Phe 454
						Ile 424
				O: Met: O4	3.03	Phe 404
				ND1: His: O2	3.02	Leu 391
14	Luteolin	-8.9	5	OE2: Glu: O6	2.86,	Ala 350
				OE2: Glu: O	2.73	Leu 387
				NH2: Arg: O6	3.29	Leu 525
						Leu 428

						Phe 404
						Glu353
15	Caffeic acid	-6.4	3	O: leu: O4	2.99	Leu346
				NH2: Arg: O4	3.07	Met 343
				OG1: Thr: O2	3.22	Met 388
						Leu 391

TABLE 5.2: Active Ligand Showing Hydrogen and Hydrophobic Interactions with HER 2.

Sr. No.	Ligands	Binding energy	No of H.B	Hydrogen Bonding		Hydrophobic interaction
				Amino acids	Distance	
						Pro278
						Arg 465
						Asn 466
						Set 441
1	Artemisinin	-8.0	0			Thr 5
						Tyr 281
						Phe 269
						Val 3
						Thr 1
						Tyr 279

						Arg 465
						Asn 466
						Tyr 279
						Gly 440
						Ser 441
2	Arteme- ther	-8.2	1	OG1: Thr: O2	3.11	Tyr 281
						Thr 5
						Cys 4
						Val 3
						Pro 278
						Phe 269
						Tyr 279
						Gly 440
						Asn 466
						Arg 465
3	Artesu- nate	-9.1	3	OH: Tyr: O5	2.94	Leu 291
				OG1: Thr: O8	3.12	Leu 414
				OG: Ser: O7	3.06	Cys 4
						Val 5
						Phe 269
						Pro 278
						Arg 465
						Ser 441
						Pro 278
4	Dihyd- roartem- isinin	-8.4	2	N: Tyr: O4	3.15	Phe 269
				ND2: Asn: O5	2.95	Tyr 281
						Val 3
						Thr 1

						Ser 441
				OH: Tyr: O1	3.03	Thr 5
5	Artean- nuin B	-8.7	3	N: Gly: O3	3.20	His 468
				ND2: Asn: O2	2.98	Val 3
						Tyr 279
						Arg 465
						Ser 441
						Val 3
6	Arteni- mol	-8.4	2	N: Tyr: O4	3.14	Tyr 281
				ND2: Asn: O5	2.96	Thr 1
						Pro 278
						Phe 269
						Ser 441
						Tyr 281
						Thr 5
						Cys 4
						Val 3
7	Artemi- sone	-8.8	1	NE2: Gln: O6	3.14	Phe 269
						Thr 1
						Pro 278
						Tyr 279
						Asn 280
						Gly 440
				O: Val: O7	2.95	Tyr 281
				N: Leu: O3	3.11	Arg 412
8	Querc- etin	-8.5	5	O: Gly: O5	3.22	Ile 413
				OG; Ser: O2	3.19	Leu 291
				ND2: Asn: O2	2.97	Thr 5

				N: Cys: O8	3.01	Val 33
				NE2: Gln: O9	3.03	Val 3
				O: Cys: O7	3.12,	Gln 2
9	Isoque- rceetin	-8.0	7	O: Cys: O6	3.30	Ala 271
				NH2: Arg: O11	3.26	Asn 237
				OE2: Glu: O11	2.83	Leu 231
				OG: Ser: O12	3.04	Ala 232
						Gln 32
				NH2: Arg: O12	2.88,	
				NH1: Arg: O12	3.18,	Ala 276
				NH1: Arg: O13	2.80	Cys 277
				OH: Tyr: O13	3.09	Thr 306
10	Rutin	-8.8	10	OE2: Glu: O13	2.97	Tyr 281
				OE1: Glu: O13	2.96	Asn 280
				OE1: Glu: O14	3.17	Gly 305
				OG: Ser: O8	2.79	Thr 301
				OE1: Gln: O6	2.87	
				NH2: Arg: O6	3.03	
				N: Ala: O4	2.86	
				NE2: Gln: O5	3.05	
				ND2: Asn: O2	3.19	Val 3
11	Gallic acid	-5.8	7	ND2: Asn: O1	3.03	Gly 270
				NH2: Arg: O3	3.00	Val 33
				OE2: Glu: O3	2.90	
				OG: Ser: O4	2.98	

						Asn 466
						Tyr 279
				O: Val: O6	2.88	Asn 280
12	Kaempferol	-8.3	4	OG1: Thr: O6	3.06	Leu 291
				O: Gly: O4	2.98	Arg 412
				O: Gly: O3	2.95	Thr 5
						Tyr 281
						Ser 441
						Val 274
						Gln 2
						Thr 1
						Asn 466
13	Chryso-splenol D	-7.4	0			Cys 4
						Tyr 281
						Thr 5
						Gln 35
						Val 3
						Pro 278
						Phe 269
						Tyr 279
						Ser 441
						Gly 411
14	Luteolin	-8.1	3	O: Val: O4	2.89	Arg412
				ND2: Asn: O3	3.03	Ile 413
				N: Leu: O5	3.17	Leu 291
						Thr 5
						Tyr 281

				O: Pro: O3	3.18	Glu299
				O: Pro: O4	3.13	Phe349
15	Caffeic acid	-6.4	5	N: Asn: O4	3.09	Met 325
				O: Asn: O4	2.93	Val 292
				OG1: Thr: O2	3.15	Cys 293

TABLE 5.3: Active Ligand Showing Hydrogen and Hydrophobic Interactions with PR.

Sr. No	Ligands	Binding Energy	No of H.B	Hydrogen Bonding		Hydrophobic interaction
				Amino acids	Distance	
						Asn 719
						Met 909
						Phe 778
						Met 759
						Val 760
1	Artemisinin	-8.5	0			Met 756
						Met 801
						Leu 887
						Tyr 890
						Leu 797
						Leu 718

						Leu 797
						Leu 887
						Met 909
						Phe 778
						Met 759
2	Artem- ether	-7.3	0			Trp 755
						Leu 718
						Gly 722
						Asn 719
						Leu 715
						Tyr 890
						Met 692
						Glu 695
						Pro 696
3	Artesunate	-7.8	2	NE2: Gln: O8	3.10	Asp 697
				N: Ile: O7	2.95	Arg 766
						Val 698
						Trp 765
						His 778
						Gln 725
						Asp 697
						Trp 765
						Glu 695
						Phe 818
4	Dihydro- artemisinin	-7.8	2	NZ: Lys: O3	3.31	Gly 762
				NH1: Arg: O1	2.83	Leu 758
						Val 729
						Ser 728
						Ile 699
						Pro 696

						Met 801
						Leu 887
						Leu 797
						Leu 715
						Leu 718
5	Artean- nuin B	-8.1	1	SG: Cys: O3	3.20	Phe 794
						Asn 719
						Phe 905
						Met 909
						Gly 722
						Met 759
						Met 756
						Gln725
						Trp 765
						Glu 695
						Phe 818
						Gly 762
6	Arteni- mol	-7.8	2	NZ: Lys: O3	3.31	Val 729
				NH1: Arg: O1	2.86	Leu 758
						Ser 728
						Asp 697
						Pro 696
						Ile 699

						Glu 695
						Val 698
						Arg 766
						Asp 697
7	Artem- isone	-8.5	1	O: Pro: N	3.31	Ile 699
						Gln 725
						Phe 818
						Gln 815
						Trp 765
						Gln 725
						Leu 721
						Phe 778
						Leu 718
						Leu 715
8	Quercetin	-8.5	0			Cys 891
						Asn 719
						Phe 905
						Met 801
						Leu 887
						Val 760
						Met 759
						Pro 696
						Met 692
				O: Ile: O12	3.17	Phe 818
9	Isoquer- cetin	-7.4	4	NE2: Gln: O12	2.81	Trp 765
				NE2: Gln: O6	2.66,	Glu 695
				OE1: Gln: O7	2.70	His 770
						Arg 766
						Val 698

					Ile 920
					Thr 829
				ND1: His: O14 3.17	Asn 879
				O: His: O13 2.69	Asp 878
10	Rutin	-7.9	6	NZ: Lys: O8 3.21	Val 925
				OD1: Asp: O9 2.90,	Leu 929
				NZ: Lys: O15 3.05	Pro 927
				NZ: Lys: O16 2.09	Val 884
					Leu 921
					Leu 721
					Leu 718
					Val 760
					Leu 887
11	Gallic acid	-6.2	1	OE1: Gln: O4 2.95	Met 801
					Met 759
					Phe 778
					Leu 763
					Arg 766
					Asn 719
					Leu 718
					Leu 721
					Leu 763
				O: Leu: O6 2.95	Met 759
12	Kaempferol	-9.2	4	NH2: Arg: O3 2.97	Phe 778
				NE2: Gln: O3 3.00,	Met 756
				OE1: Gln: O3 3.08	Leu 887
					Cys891
					Tyr 890
					Met 801

						Val 729
						Lys 822
						Glu 695
13	Chryso-	-8.0	2	O: Leu: O4	2.99	Gly 762
	plenol D			NE1: Trp: O7	3.11	Arg 766
						Val 698
						Pro 696
						Ile 699
						Asn 719
						Leu 718
						Leu 721
				O: Met: O6	3.16	Leu 763
14	Luteolin	-9.0	4	NH2: Arg: O6	3.18	Phe 778
				NE2: Gln: O6	3.35	Met 756
				O: Leu: O4	3.01	Leu 887
						Tyr 890
						Cys 891
						Leu 763
						Val 760
15	Caffeic	-6.6	2	OE1: Gln: O4	3.08	Phe 778
	acid			O: Met: O4	2.90	Phe 794
						Leu 718
						Leu 721
